ABSTRACT

Title of Dissertation: CONSERVED ROLE OF EMX2 IN ESTABLISHING POLARITY OF SENSORY HAIR CELLS

Tao Jiang, Doctor of Philosophy, 2016

Dissertation directed by: Professor Dr. Catherine E. Carr, Department of Biology, University of Maryland, College Park

Senior Investigator Dr. Doris K. Wu, Laboratory of Molecular Biology, National Institute on Deafness and Other Communication Disorders, National Institutes of Health

Sensory hair cells in the inner ear are responsible for relaying information such as sounds and head positions to the brain. Stereocilia, which are specialized microvilli, are arranged in a staircase-pattern with the longest row sitting adjacent to the kinocilium. These two structures together form the stereociliary bundle (hair bundle), which are polarized asymmetrically at the apical surface of the hair cell. Deflection of the stereocilia towards the kinocilium opens the mechanotransduction channels at the tip of the stereocilia, which enables ion influx to depolarize the hair cell and activates action potentials in the postsynaptic neurons. Deflection towards the opposite direction results in hyperpolarization. Thus, the stereociliary bundle polarity defines the directional sensitivity of a given hair cell.

Each sensory hair cell organ displays a specific pattern of stereocilia polarity. In the maculae, which detect linear acceleration in all directions, HCs can be divided into two regions with opposite polarity by a line of polarity reversal (LPR). Similar LPR is also present in the neuromast of the zebrafish lateral line system that detect pressure change of surrounding water.

My results show that the homeodomain transcription factor Emx2 is essential for establishing the LPR. Expression of *Emx2* in the maculae and neuromasts determines the stereocilia polarity pattern in a cell-autonomous fashion. Gain- and loss-of *Emx2* function in the sensory hair cell organs of mouse and zebrafish indicate that the role of *Emx2* in polarity reversal is both necessary and sufficient. In addition, my results demonstrated that Emx2 mediates this polarity reversal via one of the heterotrimer G-proteins, Gαi. Take together, my results show that Emx2 has a conserved role in dictating stereociliary bundle polarity.

CONSERVED ROLE OF EMX2 IN ESTABLISHING POLARITY OF SENSORY HAIR CELLS

by

Tao Jiang

Dissertation submitted to the Faculty of the Graduate School of the
University of Maryland, College Park, in partial fulfillment
of the requirements for the degree of
Doctor of Philosophy
2016

Advisory Committee:
Dr. Catherine E. Carr, Chair
Dr. Doris K. Wu, Co-Chair
Dr. Leslie Pick
Dr. Lisa A. Taneyhill
Dr. Sandra Gordon-Salant

Dedication

I dedicate this dissertation to my parents, my family, and my friends for their consistent and sincere support.

Veni Vidi Vici

Acknowledgements

I would like to start off by thanking my mentor Dr. Doris Wu for her continuous support and guidance. Her motivation and encouragement has transformed me from a naïve medical student to a diligent Ph.D. graduate. She is always there for me when I need her, but she also pushes me to work harder to achieve my goals in life. Her immense knowledge has inspired my project in many ways. She constantly reminds me that I am held accountable for not wasting taxpayers' money.

I would like to thank my advisor Dr. Catherine Carr for her generous support throughout the years, like how she encouraged me to survive the first year when I almost failed on the courses I took by telling me that "you look like a smart guy".

I really appreciate that my committee members are very understandable and they are always available whenever I needed them. They provided constructive criticisms and excellent suggestions for my projects, and they are set a great example for me during my training.

I would like to thank Pamela Komarek at NACS for her helpful suggestions, her impeccable organizational skills, and for looking after me so I did not get kick out of my program.

I would like to express my deepest gratitude to Dr. Katie Kindt from NIDCD. Without her unreserved help, I would never be able to step into the wonderful zebrafish field. And, I will never forget how supportive and great her lab members are, particularly their incomparable baking skills.

I would give my sincere appreciation to the members of the Wu lab. Michael Mulheisen, the "God" in the lab. He taught me everything that I need to know to survive

in our lab. My friend Dr. Lok Sum Wong has always been there for me and has generously provided very helpful information to me even when she was sick. Dr. Kazuya Ono and Dr. YoungRae Ji have always provided insightful suggestions and critical thinking for my projects, plus their great taste in Japanese and Korean food. Thanks to our former lab members Dr. Xiaohong Deng and Dr. James Keller for their guidance to this naïve young graduate student. Thanks to our lovely post-bacs, Andrew Lin, Kaya Matson, Yanghan Huang, Charles Reener, Andrew Yatteau, and Colleen Zenczak, who have all help me throughout the years and being good friends. Also, I would like to thank all the high school students we had for the past six years: Nicole, Eric, Nathan, Tiffany, Claire, and Tim. They have assisted me in many ways, especially on cell counting.

I also want to thank all the great scientists that have generously shared with us their antibodies, mice, and zebrafish lines. Without those reagents and animals, my *Emx2* project would not ever reach this stage.

I would like to thank Yi, Dashu, Wenhui, Zhifan, and all my friends, for supporting me, encouraging me, and walking along this incredibly difficult path with me when I tried to pursue my Ph.D. goal, in daily life or online chat. You guys spent hours driving over to meet me, and picked me up from the airport when my plane was forced to detour to another city. I truly value your friendships.

Last but not least, I must thank my Mom and Dad, who have never given up on me and support me in every aspect. They are always there for me and listen to my frustrations and concerns; but most importantly, telling me that my figures look as pretty as “fireworks” even though they do not have a clue what polarity means.

Table of Contents

List of Figures

Chapter 1: Introduction

Chapter 2:

Chapter 3: Discussion

Appendix

List of Tables

Chapter 1: Introduction

List of Abbreviations

A: anterior
AC: anterior crista
aPKC: atypical protein kinase C
Celsr: Cadherin EGF LAG seven-pass G-type receptors
cPCP: core planar cell polarity
D: dorsal
Dgo: Diego
Dlg: Discs-large
dpf: day-post fertilization
Ds: Dachsous
Dsh: Disheveled
E: embryonic day
Eve: even-skipped
Fj: four-jointed
Fmi: flamingo
Ft: Fat
Fz: Frizzled
GMC: ganglion mother cell
GOF: gain of function
HC: hair cell
hpf: hours-post fertilization
Ift: intraflagellar transport
Insc: Inscutable
IR: inner region
LC: lateral crista
LES: lateral extrastriola
Lfng: Lunatic fringe
Lgl: Lethal giant larvae
LPR: line of polarity reversal
MES: medial extrastriola
MTOC: microtubule-organizing center
NB: neuroblast
NuMA: nuclear and mitotic apparatus
oC: organ of Corti
OR: outer region
P: posterior
Par: partition-defective gene
PC: posterior crista
PCP: planar cell polarity
Pins: partner of Inscutable
pLL: posterior lateral line
PAK: p21-activated kinase
Pk: Prickle-like
PTK: Protein tyrosine kinase

Ptx: Pertussis Toxin
S: saccule
SC: supporting cell
Scrb: Scribble
SOP: sensory organ precursor
Sple: spiny-leg
Stbm: strabismus
U: utricle
V: ventral
Vangl: Van Gogh-like
VPC: vulva progenitor cells
VZ: ventricular zone
Wg: Wingless

Chapter 1: Introduction

I. Sensory hair cell organs

A. The inner ear

1. Development of the inner ear

It is hard to imagine how life would be without our ears to detect sound, speech, and music. Sounds collected by the pinna cause vibrations of the tympanic membrane. These vibrations are amplified by the three ossicles of the middle ear, which lead to fluid displacements in the cochlea. Depending on the frequency of the sound, different hair cells (HCs) along the cochlear duct will be activated. In addition to the cochlea, there are five vestibular sensory organs responsible for maintaining balance. The three cristae, anterior, posterior, and lateral crista, are responsible for detecting angular head movements in three dimensions, whereas the two maculae, utricle and saccule, are responsible for detecting linear accelerations (Fig. 1.1).

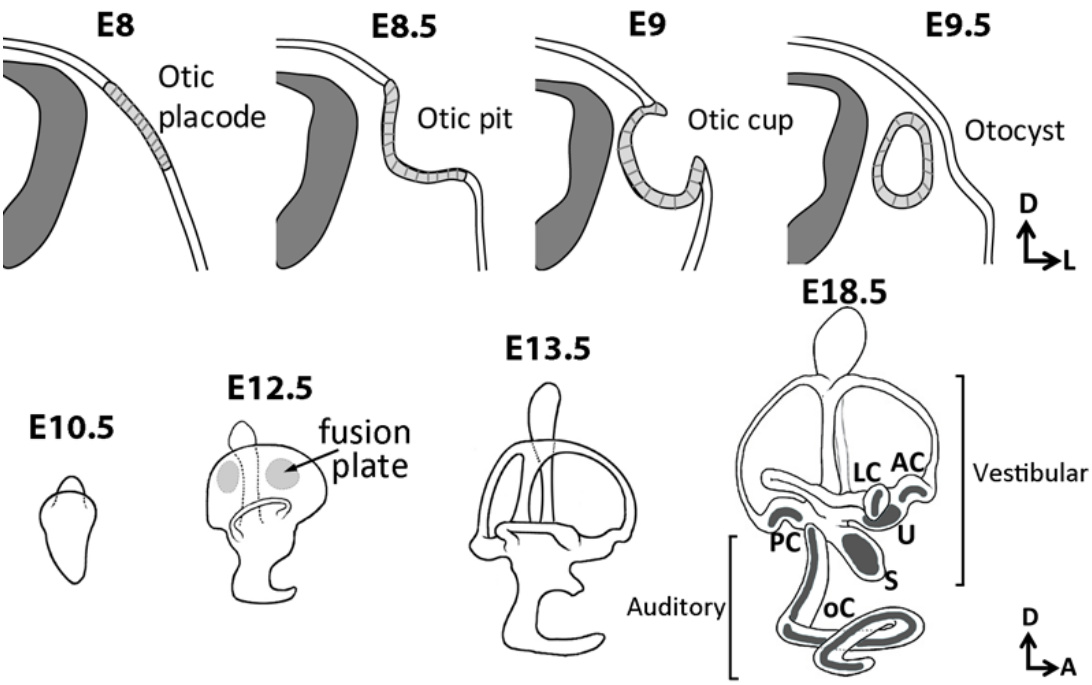

Figure 1.1. Development of the mouse inner ear. Upper: Coronal sections of the developing inner ear from E8 to E10.5. The formation of inner ear initiates from a thickening of the ectoderm known as the otic placode around E8. Then, the placode invaginates to form the otic pit (E8.5), otic cup (E9), and otocyst (E9.5) sequentially. Bottom: Lateral views of the developing inner ear from E10.5 to E18.5. After otocyst formation at E10.5, the inner ear undergoes remarkable morphogenesis to reach its mature pattern by E18.5. All the sensory organs are labeled in grey. AC, LC, and PC: anterior, lateral, and posterior crista; oC: organ of Corti; S: saccule; U: utricle. Figures are adapted from published work (Bok, Chang, & Wu, 2007; Kiernan, Steel, & Fekete, 2002; D. K. Wu & Kelley, 2012).

The inner ear undergoes a complicated morphogenesis during development. In the mouse, the otic placode is evident starting around embryonic day (E) 8, as a thickening of the ectoderm next to the hindbrain. The placode then invaginates and deepens to form the otic pit, then otic cup, and closes to form the otocyst by E9.5. Then the otocyst elongates and divides to form the dorsal vestibular and ventral auditory components. Starting from E12.5, the opposing epithelia of each prospective canal merge towards each other, fuse

and disappear, leaving behind the tube-like canal. At the same time, the sensory epithelia within the inner ear start to differentiate forming HCs and supporting cells. The gross structure of the mouse inner ear is complete around E16.5 (Fig. 1.1; (Kiernan et al., 2002; D. K. Wu & Kelley, 2012)).

2. Sensory hair cells

Within each sensory organ, there is a sensory epithelium comprised of sensory HCs and supporting cells. Each mechanosensitive HC is surrounded by several supporting cells, which provide protection for the HC (May et al., 2013; D. K. Wu & Kelley, 2012). On the apical surface of the HC, the kinocilium, the only true cilium, together with specialized microvilli, stereocilia, arranged in a staircase pattern, form the hair bundle that is asymmetrically localized at the lateral edge. When hair bundle is deflected towards the kinocilium, mechanotransduction channels at the tip of stereocilia are opened, which allow potassium and calcium entry into the HC, leading to depolarization and release of the neurotransmitter, glutamate, which may activate action potentials in the post-synaptic neuron (Fig. 1.2; (Hudspeth & Corey, 1977)). These excitatory signals are propagated and relayed to other nuclei in the central nervous system. In contrast, deflection of the stereocilia towards the opposite direction hyperpolarizes the HCs and reduces glutamate release (Fig. 1.2; (Hudspeth & Corey, 1977; Lopez-Schier, Starr, Kappler, Kollmar, & Hudspeth, 2004; Shotwell, Jacobs, & Hudspeth, 1981)). Thus, the polarity of the stereocilia bundle defines directional sensitivity of a given HC (H. May-Simera & Kelley, 2012).

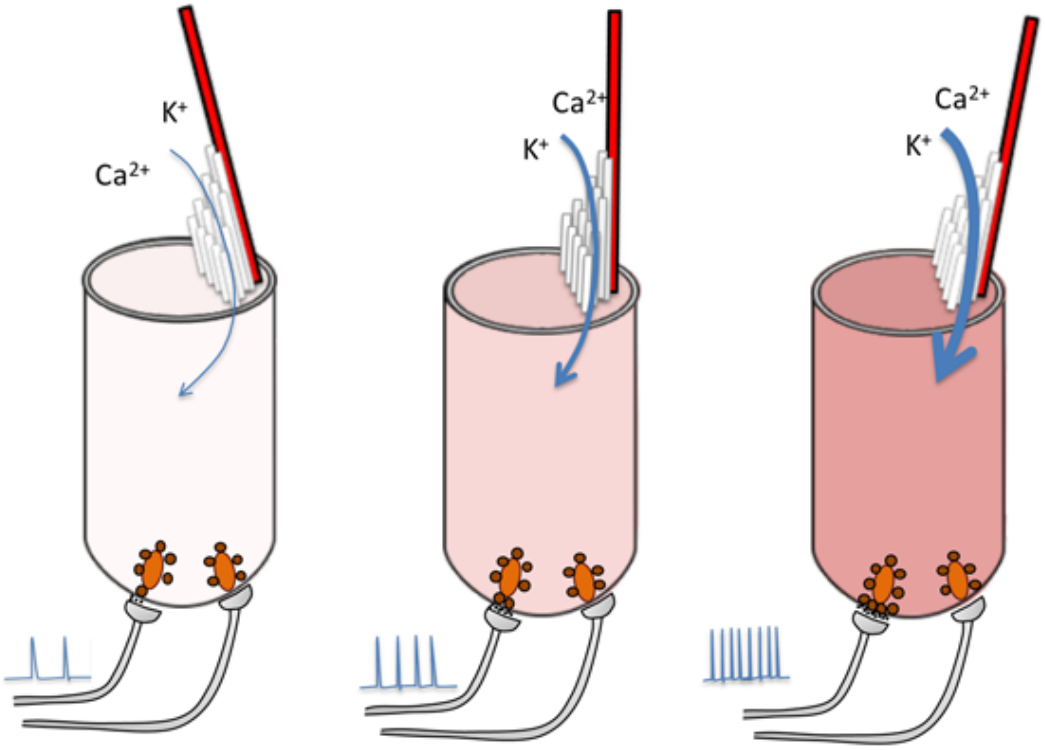

Figure 1.2. Polarity of stereocilia dictates HC sensitivity. Under steady state (pink cell in the center), some mechanosensory channels in a HC are open (blue arrow) to maintain the resting potential and release certain amount of neurotransmitters (black dots) from ribbon synapses (orange ovals) to the post-synaptic afferents (grey). When stereocilia are deflected towards the kinocilium position, the influx of potassium ions increases significantly (thick blue arrow) causing HC depolarization (dark pink cell on the right). The released neurotransmitters generate more action potentials in the innervating neurons. When stereociliary bundle deflect away from the kinocilium, the mechanotransduction channels are closed, leading to a reduction in potassium ion entry (thin blue line), hyperpolarization of HC (light pink cell on the left), and reduction of activity in the innervated neurons.

HCs within each sensory organ are continuously being generated during development until E14.5 in the cochlea and postnatal ages for the utricle (Burns, On, Baker, Collado, & Corwin, 2012; Denman-Johnson & Forge, 1999; Tilney, Tilney, & DeRosier, 1992). In the mouse maculae, first HCs could be identified after E12.5. By E13.5, differentiated HCs and supporting cells can be observed, at which time, the kinocilium emerges from

the apical surface and starts to migrate from the center to the periphery (Fig. 1.3). By E15.5-E16.5, mature hair bundles can be observed (Denman-Johnson & Forge, 1999). The staircase stereocilia are built after the kinocilium reaches its final position (Fig. 1.3). Evidence suggests that the stereocilia will go through a refinement process after they reach the lateral edge. in coordination with neighboring HCs (Copley, Duncan, Liu, Cheng, & Deans, 2013; Duckert & Rubel, 1993). As a result, stereocilia of HCs across each sensory organ are aligned in a defined pattern.

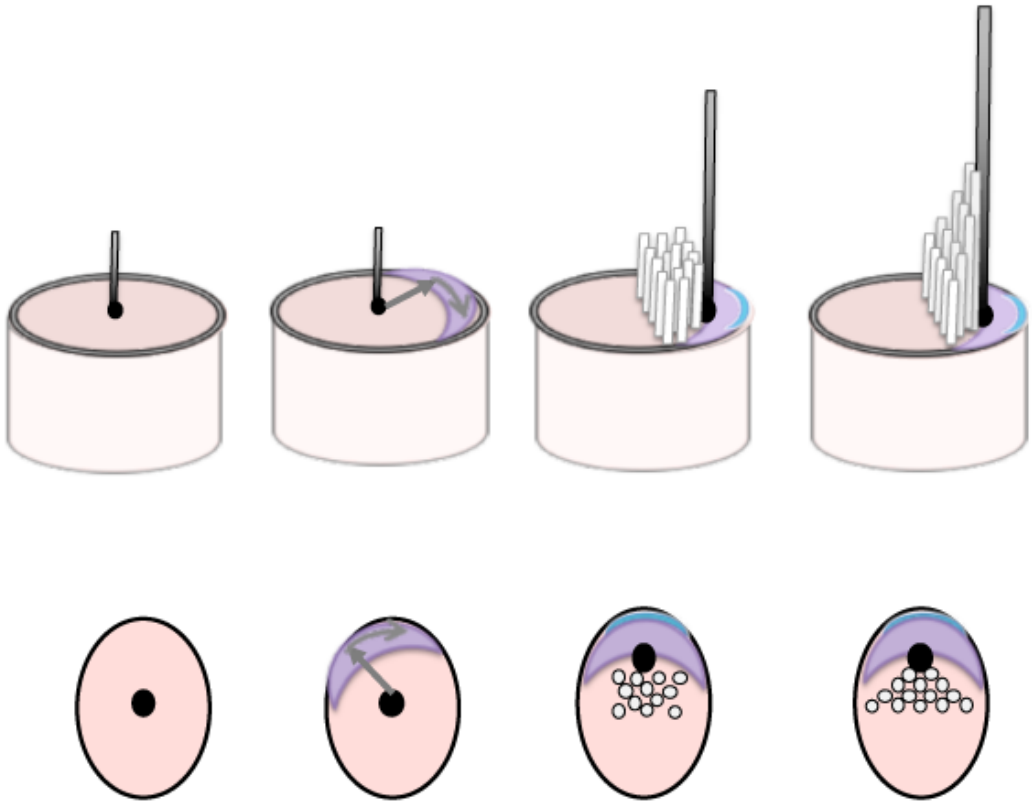

Figure 1.3. The establishment of stereocilia orientation. Stereociliary bundle formation in a HC from a side view (top panel) and apical view (bottom panel). A nascent kinocilium (dark gray) is first erected from the basal body located in the center of apical HC surface. Guided by intracellular polarity proteins (purple), the nascent kinocilium migrates towards the lateral edge of the HC. Then, collaborations between intra- and intercellular polarity signaling (blue) refine the kinocilium position. After the kinocilium reaches its final position, a staircase pattern of stereocilia (light gray) is built next to it.

3. The maculae

The maculae of the utricle and saccule are responsible for detecting linear acceleration in all directions, including gravity. The two maculae are at right angles to each other with the utricle positioned horizontally and the saccule placed vertical to the ground. Stereocilia of macular HCs are embedded in otoconia, which are crystallites consisting of calcium crystals and specialized proteins (Lundberg, Zhao, & Yamoah, 2006). During head movements and postural changes, inertia of the otoconia helps to deflect the hair bundles toward the direction of acceleration, leading to HC depolarization (Deans, 2013; Denman-Johnson & Forge, 1999; Li, Xue, & Peterson, 2008).

a. Hair cell types and striola

Macular HCs are classified as Type I and Type II. Type I HCs have a pear-shape cell body that is innervated by calyx synapse, whereas Type II cell bodies are columnar-shaped and innervated by bouton synapses (Fig. 1.4). Although these two types of HCs are broadly distributed in the maculae, the types of nerve endings that innervate these HCs are different regionally. For example, within the striola, a specialized region in the middle of the maculae, pure calyx synapses innervating Type I HCs are the most prevalent. Outside this region, the extrastriolar region contains dimorphic synapses and pure bouton synapses (Fig. 1.4). Striolar neurons have an irregular firing pattern, which is more suited to coding temporal information, whereas neurons innervating extrastriola HCs show regular firing pattern responsible for detecting spatial information (Eatock & Songer, 2011; Lysakowski et al., 2011). In addition, a number of region-specific markers are expressed in the striola, such as oncomodulin and *β-tectorin*, in HCs and supporting

cells, respectively (Goodyear, Killick, Legan, & Richardson, 1996; Simmons, Tong, Schrader, & Hornak, 2010). In contrast, genes such as *Lunatic fringe (Lfng)*, are only expressed in the extrastriola regions and excluded from the striola (Morsli, Choo, Ryan, Johnson, & Wu, 1998). Thus, the striola is a cellular and functional distinct region of the macula.

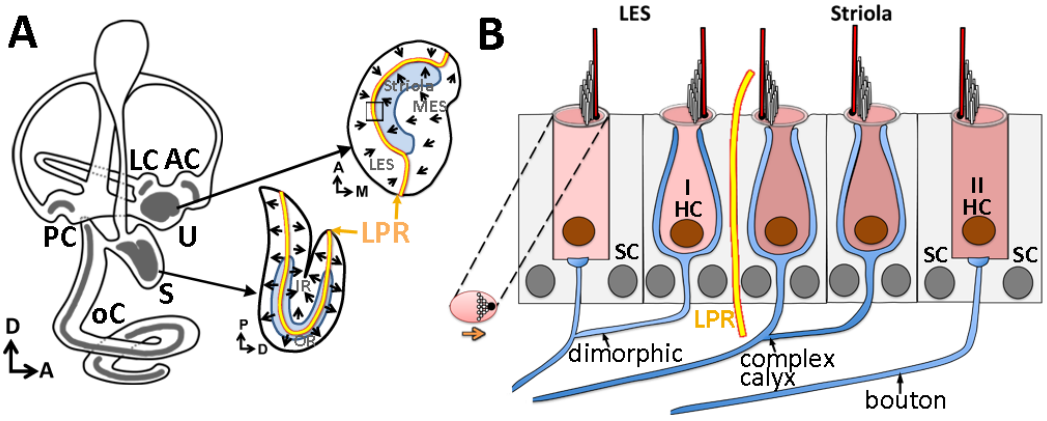

Figure 1.4. Schematics of the maculae and the LPR. (A) Left mouse inner ear (medial-view) with its six sensory organs (grey). LPR (yellow line), HC polarity, and striola (blue) in the two maculae are shown. (B) Cellular architecture across the LPR in the utricle representing the bracket area in A. HCs facing towards the LPR in the utricle. Pure calyx synapses (blue) are found in striolar Type I HCs only, whereas dimorphic synapses are found in extrastriola HCs. Bouton synapses are present in the entire utricle.

b. The line of polarity reversal (LPR)

The stereocilia within each sensory HC organ forms a unique and well-defined pattern that is coupled to its function. HCs in the cochlea and cristae uniformly point in one direction. In contrast, stereocilia are aligned in a mirror image across the line of polarity reversal (LPR) in the maculae. The position of the LPR and striola divide the maculae into different regions. In the utricle, the LPR is located by the lateral edge of striola, both of which together divide the macula into the extrastriola (LES), striola, and

medial extrastriola regions (MES; Fig. 1.4). Stereocilia of HCs in the LES are pointing towards the medial direction, whereas stereocilia within striola and MES are oriented towards the lateral edge (Fig. 1.4; (Deans, 2013; Li et al., 2008)). In contrast to the utricle, the LPR bisects the striola in the saccule, across which stereocilia are pointing away from each other. Thus, along the anterior-posterior axis, the saccule is separated into the inner region (IR) and outer region (OR) by the LPR (Fig. 1.4; (Deans, 2013; Desai, Zeh, & Lysakowski, 2005)). These polarity patterns presumably allow better assessment of spatial orientation of head movements but the precise functional significance and formation of the LPR is unknown. Notably, lipophilic dye tracing results in mice indicate that neurons that innervate the lateral region of the utricle and inner region of the saccule project to a different part of the brain than the rest of the maculae (Maklad & Fritzsch, 2003; Maklad, Kamel, Wong, & Fritzsch, 2010). These segregated central projections further support the notion that these HC polarity reversal patterns enhance the sensitivity for detecting spatial orientation of the head.

B. Lateral line system

HCs are not only present in the inner ears of all vertebrates, but they are also present in lateral line system of aquatic vertebrates. The lateral line system in the aquatic vertebrates detects water movements that provide a "touch-at-a-distance" sense, which is required for schooling behavior, food detection, and predator avoidance. The ability of these sensory receptors to transduce mechanical force to chemical signals enables HCs in the lateral line system to sense surrounding water pressure changes, which is essential for the survival of aquatic vertebrates (Chitnis, Nogare, & Matsuda, 2012).

1. Organization of neuromast

In zebrafish, the lateral line is comprised of neuromasts distributed over the surface of the body from head to tail (Ghysen & Dambly-Chaudiere, 2007; Rouse & Pickles, 1991). Within each neuromast is a cluster of ten to twenty mechanosensitive HCs with a similar stereociliary bundle as described for inner ear sensory organs. The stereociliary bundles, each with an exceptional long kinocilium, are embedded in a gelatinous cupula and respond to a change in water pressure. Similar to the inner ear, each sensory HC is surrounded by supporting cells. At the edge of the neuromast is a ring of mantle cells, which produce the gelatinous cupula. These cells can also replenish supporting cells after severe injury (Fig. 1.5; (Romero-Carvajal et al., 2015)).

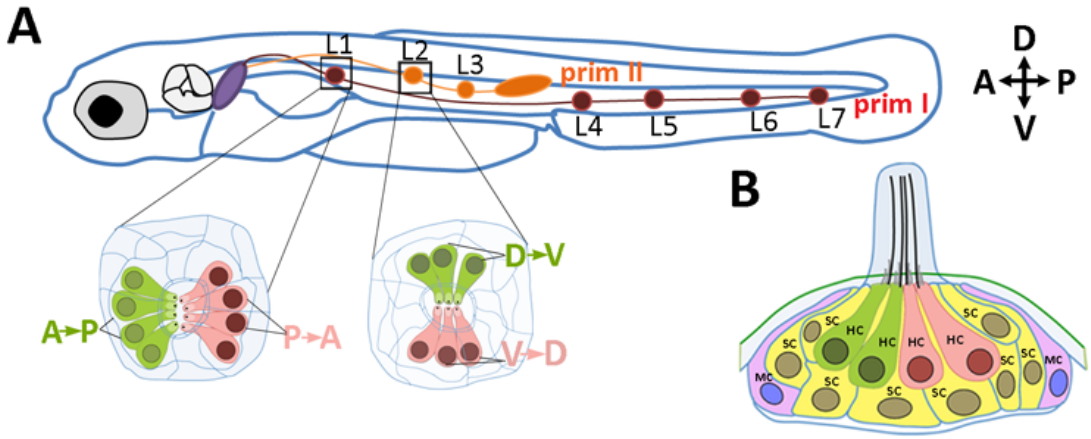

Figure 1.5. Surface and side views of oriented neuromasts in the lateral line of zebrafish. (A) A 3-day post fertilization (dpf) zebrafish is shown. The pLL placode (purple) is located posterior to the inner ear (grey circled). The first pLL primordium (red) migrates towards the tail and drops the anterior-posterior oriented neuromasts (red dots). Orange line and dots represent the second primordium migration giving rise to the dorsal-ventral neuromasts. HCs oriented towards the posterior or ventral are labeled in green and the ones in opposite orientation are labeled in pink. (B) A sagittal-section of a neuromast is shown on the right. HCs are surrounded by supporting cells (yellow) and the mantle cells (purple) that are located at the periphery of the neuromast. Figures are adapted from published work (Haffter et al., 1996; Nagiel, Andor-Ardo, & Hudspeth, 2008; Pujol-Marti & Lopez-Schier, 2013; Romero-Carvajal et al., 2015).

Although the presence of the gelatinous cupula in the neuromast resembles that of an inner ear crista, the stereocilia arrangement of HCs is similar to the utricle, a mirror image pattern with HCs facing each other. Neuromasts are separated into two groups of anterior-posterior and dorsal-ventral orientation along the body axes. Thus, water movement will deflect the kinocilia towards one direction: exciting half of the HCs and inhibiting the other half (Fig. 1.5). Interestingly, in addition to the polarity pattern, the neuromasts also present a mutually segregated pattern of afferent innervation, similar to the maculae. HCs sharing the same polarity are innervated by the same afferents. This organization of afferents is suggested to provide the functional compartmentalization of the lateral line system and maculae (Faucherre, Baudoin, Pujol-Marti, & Lopez-Schier, 2010; Faucherre, Pujol-Marti, Kawakami, & Lopez-Schier, 2009; Lopez-Schier et al., 2004; Nagiel et al., 2008).

2. Development of the lateral line system

The lateral line system can be divided into two groups: anterior and posterior lateral lines, which are located in the head and trunk, respectively. Most studies of the neuromast are mainly focused on the posterior lateral line system (pLL). The pLL is derived from the pLL placode, which is an epidermal thickening behind the otocyst around 18 hours post fertilization (hpf). The placode is further divided into two groups of cells, anterior cells form the ganglion that innervate the pLL, and the posterior cluster of about eighty cells forms the primordium that starts to migrate along the horizontal myoseptum along the anterior-posterior body axis (Fig. 1.5, (Chitnis et al., 2012; Ghysen & Dambly-Chaudiere, 2007; Piotrowski & Baker, 2014)). During this migration, groups

of cells transition from mesenchymal to epithelial-like morphology to form a rosette, which will be periodically deposited and develop into a neuromast (Chitnis et al., 2012; Piotrowski & Baker, 2014). The first pLL primordium migration starts at 22 hpf and it takes about 20 hours for it to migrate from the placode to the tail and deposit the neuromasts marked as L1 and L4-7 at 3 day-post fertilization (dpf). After the first pLL primordium finished migrating, another primordium will start to migrate along the same tract as the first primordium and deposit L2-3 (Fig. 1.5, (Chitnis et al., 2012; Ghysen & Dambly-Chaudiere, 2007; Pujol-Marti & Lopez-Schier, 2013)). The HCs within neuromasts from these two different primordia will adapt different orientations: HCs from first PLL primordium are oriented along the anterior-posterior axis, whereas HCs in L2-3 are oriented along the dorsal-ventral axis (Fig. 1.5, (Chitnis et al., 2012)). The HC progenitor marker, Atoh1a, starts to express in the center cell of the rosette in the trailing region of primordium during deposition. Then, this center cell undergoes the last cell division and generates two HCs with opposite polarity along the given axis of the neuromast as mentioned above. After deposition, pairs of HCs with the opposite polarity are continuously being generated until they reach the final number of about twenty HCs. During HC differentiation, the bipolar neurons from the pLL ganglion will innervate the mature HCs (Chitnis et al., 2012; Ghysen & Dambly-Chaudiere, 2007; Pujol-Marti & Lopez-Schier, 2013). Even though the times of origin and development are different from neuromast to neuromast, the polarity pattern, HC function, and innervation pattern are similar, suggesting that there are common factors that regulate HC polarity and neuronal innervation among neuromasts (Chitnis et al., 2012; Faucherre et al., 2010; Faucherre et al., 2009; Ghysen & Dambly-Chaudiere, 2007; Lopez-Schier et al., 2004;

Maklad & Fritzsch, 2003; Maklad et al., 2010; Nagiel et al., 2008; Piotrowski & Baker, 2014; Pujol-Marti & Lopez-Schier, 2013).

II. Planar cell polarity

Breaking symmetry in a cell is defined as cell polarization. The manifestation of cell polarity within a two-dimensional surface is defined as planar cell polarity (PCP). From global tissue organization to subcellular organelle polarization, the establishment and maintenance of cell polarity are required for various development processes (Fig. 1.6). For example, body axial formation and patterning require convergent and extension of cells during gastrulation. During this process, neighboring cells intercalate and align along the anterior-posterior axis of the body (Fig. 1.6D). At the organ level such as the ommatidia of *Drosophila,* the eight photoreceptors are arranged in a specific trapezoid pattern and are polarized towards the equator of the eye. At the single cell level such as the neuroblasts of *Drosophila*, the apical-basal axis is important for asymmetric cell division, which ensures a balance of stem cell pool maintenance and neuronal differentiation (Fig. 1.6B, E; (Goodrich & Strutt, 2011; Gray, Roszko, & Solnica-Krezel, 2011)).

In addition to normal development, planar polarity pathways also play an important role during pathological conditions. During wound healing, the cytoskeleton of epidermal cells is polarized towards the wounded site, which requires planar polarity mechanisms (Fig. 1.6C; (Etienne-Manneville, 2004; Lamouille, Xu, & Derynck, 2014)). Metastasis of tumor cells is one of the major targets of cancer therapy development. In order for tumor cells to metastasize and exit from the basement membrane, tumor cells

undergo epithelial-mesenchymal transition and loss their normal apical-basal polarity. Thus, maintaining polarity for tumor cells is a potential therapeutics for treating cancer (Gray et al., 2011; Grifoni, Froldi, & Pession, 2013).

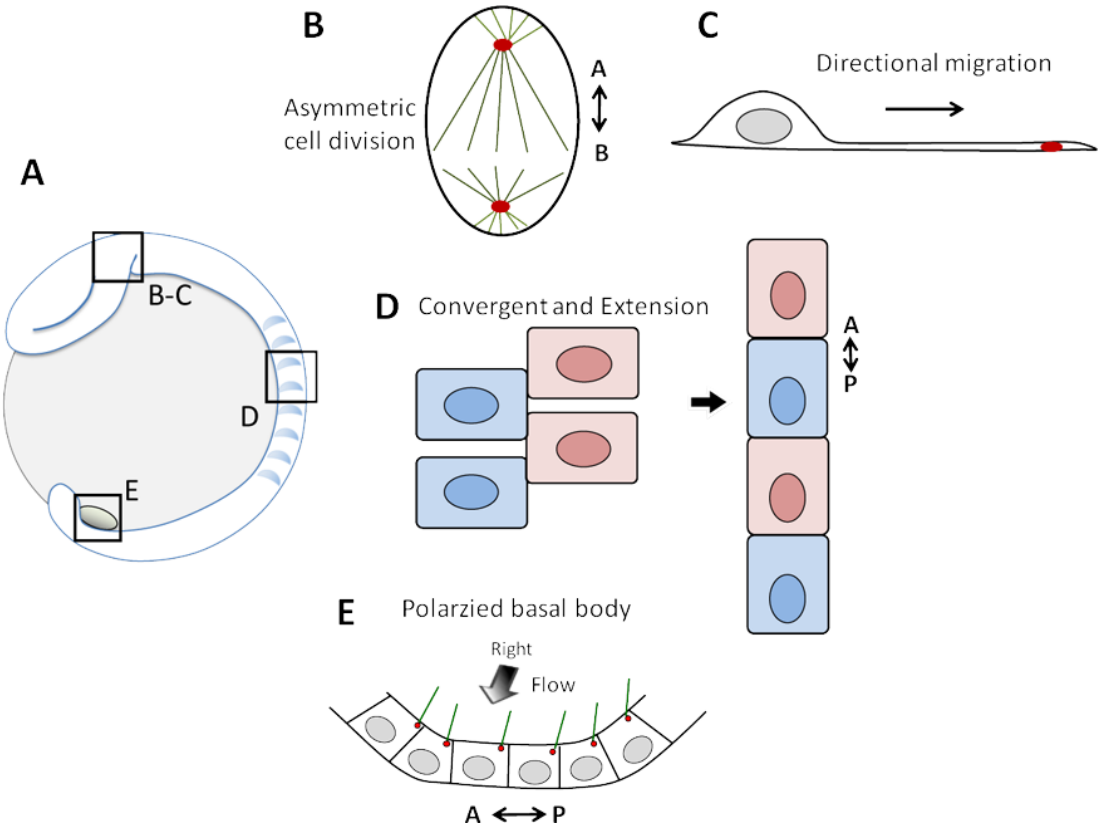

Figure 1.6. Planar cell polarity. (A) A developing zebrafish embryo around 30 hpf. Squares indicate the locations where planar polarity mechanisms are required. (B) Asymmetric cell division that two daughter cells adopt different fates and possibly different sizes. Green lines represent the spindle, and the red dots mark the centrosomes. (C) Neurons need to go through directional migration to reach their designations. The centrioles (red) migrate towards the pre-determined direction and the soma follows subsequently. (D) During gastrulation, mesodermal cells go through convergent and extension. Cells are reorganized and intercalated with each other along the anterior-posterior axis. (E) In the Kupffer's vesicles, the cilium is polarized posteriorly at the apical surface of a given epithelial cell. The beating of these polarized cilia generate a left-ward flow, which determines the left-right body asymmetry. Red: basal body. Green: cilia. Figures are adapted from published work (Gray et al., 2011; Hirokawa, Tanaka, Okada, & Takeda, 2006).

A. Three levels of planar polarity regulation

Regulation of planar polarity can be categorized into global, intercellular, and intracellular pathways (Fig. 1.7; (Deans, 2013; Matis & Axelrod, 2013)). The global polarity signaling can be mediated by transcription factors and morphogens that regulate large-scale polarity, such as body axis and tissue polarity. The intercellular polarity pathways such as Ds/Ft/Fj and core planar cell polarity (cPCP) proteins form complexes across the cell boundary. These pathways serve a conserved role in PCP regulation, and are responsible for establishing polarity within a group of cells. In order to polarize the subcellular organelles, intracellular polarity proteins, like spindle orientation and ciliogenesis proteins are critical. Coordination of these polarity signals is needed for the tissue polarization and establishment, like vulva in *c.elegans,* ommatidia of *Drosophila* and polarized ciliated cells. Each level of planar polarity regulation will be described in more detail in the following sections.

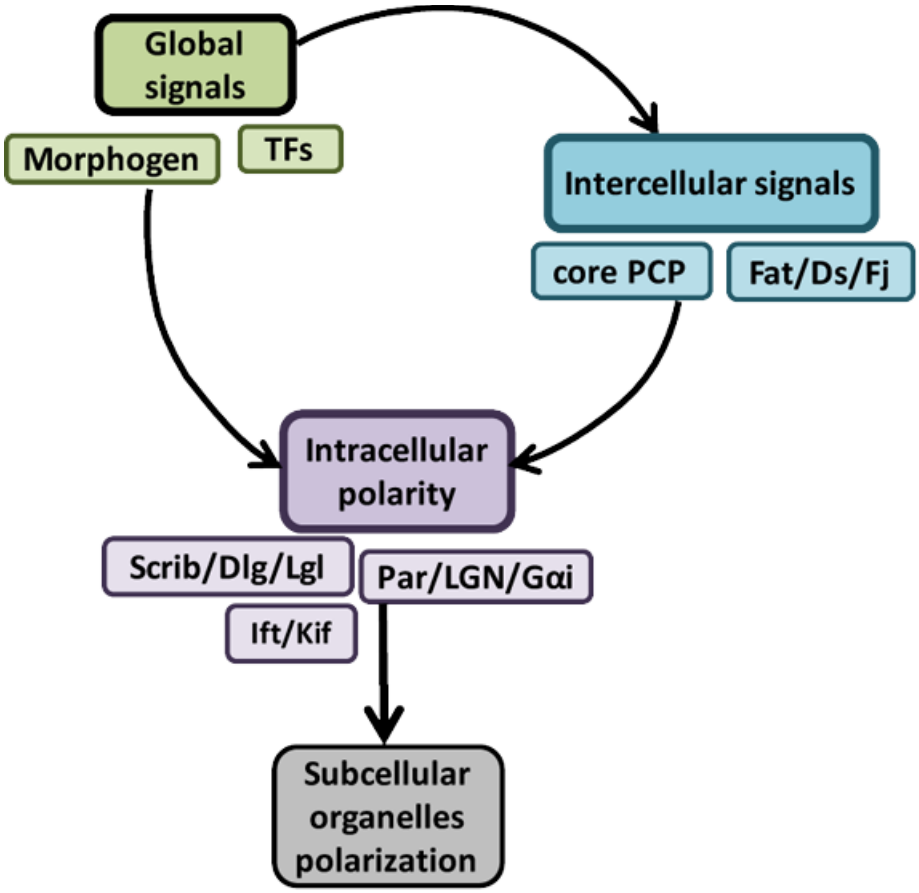

Figure 1.7. Regulation of PCP at three levels. Global signals (green) could regulate the intercellular (cyan) and intracellular (magenta) independently. The intracellular polarity proteins could receive and amplify polarity cues from global and intercellular signaling. Together, they regulate the polarization of subcellular organelles within individual cells.

1. Global polarity signaling pathways

Global polarity signaling is responsible for conferring body axial information to specific tissues. These signals provide polarity formation within whole organs or even organisms (Deans, 2013; Matis & Axelrod, 2013). Thus, global signals, such as morphogens, provide long-distance information for the asymmetrical distribution of inter- or intracellular polarity proteins, which further establish polarity at the cellular level (Fig. 1.7).

a. Transcription factors

During *Drosophila* germband elongation, cells double their length along the anterior-posterior axis, while narrow down on dorsal-ventral axis. Thus, the establishment of the axes is required for cells to intercalate cells during convergent and extension. A transcriptional cascade controls the anterior-posterior axis patterning in *Drosophila* embryo: maternal genes, gap genes and pair rule genes. Pair rule genes are expressed in stripes along the anterior-posterior axis of *Drosophila* embryo, within which, *even-skipped* (*eve*) and *runt* are believed to be the main regulators in germband elongation by regulating the PCP (Bertet & Lecuit, 2009). *Eve* and *runt* express in stripes, induce and control the intracellular distribution of the Bazooka and Myosin II (Fig. 1.8). The Myosin II is asymmetric distributed on the anterior-posterior boundary and responsible for extending the intercalated cells along this axis. In contrast, Bazooka is expressed at the dorsal-ventral boundary and it mediates contraction of the cells along this axis (Fig. 1.8B). Overexpression of *eve* and *runt* generate severe polarity defects that perturb the axial information and orientation of cell elongation, whereas double knockout mutant resulted in loss of polarity and failure of germband elongation. Thus, *eve* and *runt* provide the polarizing information for germband cells to undergo elongation (Zallen & Wieschaus, 2004).

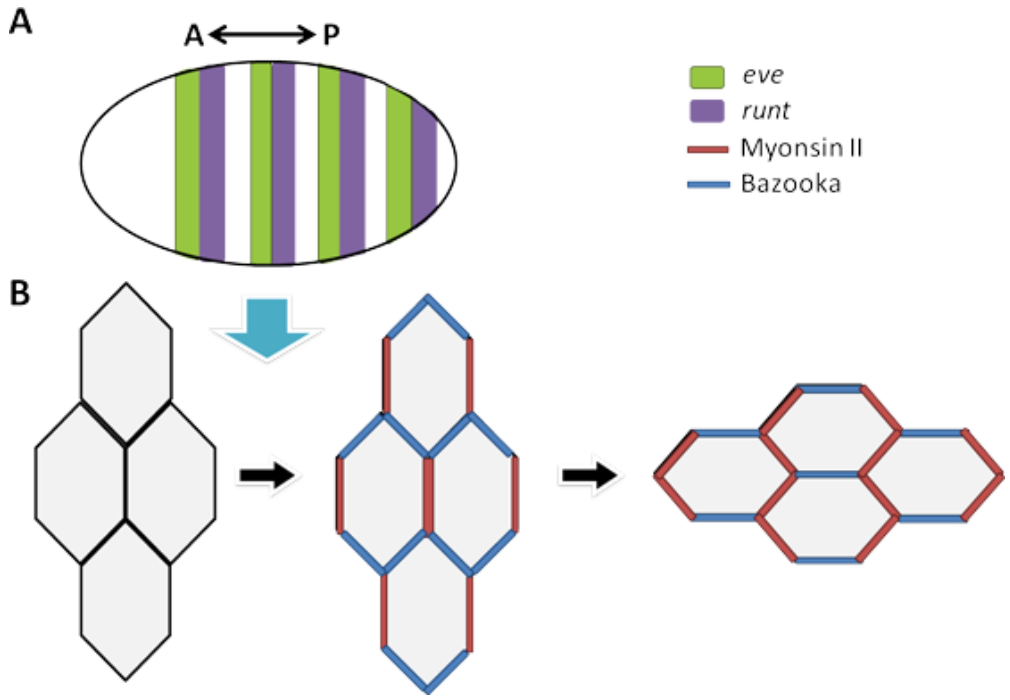

Figure 1.8. Transcription factors eve and runt establish the anterior-posterior polarity during *Drosophila* germband elongation. (A) *Eve* (green) and *runt* (purple) are expressed in a striped-pattern along the embryo and establishes the anterior-posterior axis. (B) Before the *eve* and *runt* establish the anterior-posterior axis within the cell, intracellular proteins are not asymmetrically distributed. In the presence of *eve* and *runt,* Myosin II (red) and Bazooka (blue) are asymmetrically distributed in germband cells (grey) along anterior-posterior and dorsal-ventral axis, respectively. These polarity proteins are able to reshape the intercalated cells and elongate the cells along the anterior-posterior axis, while reduces the width along the dorsal-ventral axis. Figures are adapted from published work (Bertet & Lecuit, 2009; Zallen, 2007).

How do *eve* and *runt* regulate the germband convergence and extension? First of all, the intercellular polarity pathway is not required for germband elongation, suggesting that *eve* and *runt* do not regulate the cPCP pathway (Zallen & Wieschaus, 2004). One hypothesis is that the morphogen, wingless (wg), is the target of *eve* and *runt*. The striped-expression pattern of eve and runt might provide the polarizing information to

express wg in a gradient, which sets up the asymmetric information within the embryo (Bertet & Lecuit, 2009). Thus, transcription factors, such as *eve* and *runt* could also regulate PCP by activation of a morphogen.

b. Morphogens

In *Drosophila*, secreted proteins such as hedgehog, decapentaplegic (dpp) and wingless (wg) act as morphogens to specify the polarity of monolayer epithelium in wing disc. The expression of hedgehog in posterior wing disc initiates the expression of DPP that establishes the border of anterior-posterior axis. In a similar manner, expression of wingless establishes the dorsal-ventral border of the wing disc (Strigini & Cohen, 1999). The gradient concentration of morphogens establishes the polarity of the intercellular polarity proteins (Fig. 1.9-1.10). Wingless is a good example to illustrate how a morphogen regulates PCP. During the wing disc formation, the gradient of wingless concentration in the tissue regulates the asymmetric distribution of the intercellular polarity proteins, such as the cPCP components. Wingless generates the fz 'activity' gradient that is referred as the binding affinity of fz to vang (Fig. 1.10; (J. Wu, Roman, Carvajal-Gonzalez, & Mlodzik, 2013)). This 'activity' gradient allows the local wing cells respond differently along the tissue axis that orients the trichomes towards the distal ends. Thus, the gradient of morphogen wingless provides directional information for the local cells to polarize within a specific tissue.

In addition to *Drosophila*, the gradient of Wnt5a is important for the direction of mouse limb bud elongation during development. Wnt5a establishes the proximal-distal axis via cPCP pathway: Wnt5a recruits Ror2/Vangl2 to form a complex at one end of the

cell along the axis. This distal to proximal gradient of Wnt5a provides the directional information for the establishment of Vangl2 activity axis within the limb. Knockout of Wnt5a causes the morphogenetic defects and limb elongation defects along the proximal-distal axis (Gao et al., 2011). Based on these results, globally-expressed morphogens could form a concentration gradient within the tissue to regulate the polarity of each cell, mainly through cPCP pathway. These concentration gradients establish the asymmetry of cPCP proteins and link the polarity within the tissue to the body axis.

2. Intercellular polarity signaling pathway

Whereas global polarity signaling establishes polarity within a given tissue, intercellular polarity signals are responsible to amplify the polarity and coordinate alignment with neighboring cells. There are two well-known signaling pathways: Ds/Ft/Fj and cPCP pathway (Fig. 1.7; (Deans, 2013; Matis & Axelrod, 2013)).

a. Ds/Ft/Fj pathways

The atypical cadherin Dachsous (Ds) and Fat (Ft), together with the Golgi kinase Four-jointed (Fj), comprised the Ds/Ft/Fj system (Bayly & Axelrod, 2011; Goodrich & Strutt, 2011; Matis & Axelrod, 2013). In between two cells, the extracellular domain of Ds and Ft interact with each other at the cell-cell boundaries. The Fj kinase, on the other hand, phosphorylates the cadherin repeats of Ft and Ds. As a result, phosphorylation of Ft increases its ability to bind Ds, but phosphorylated Ds decreases its ability to bind Ft. Thus, cells with higher levels of Fj will have higher ability for Ft to bind Ds (Fig. 1.9; (Hale, Brittle, Fisher, Monk, & Strutt, 2015)). In the *Drosophila* wing, Ds/Ft/Fj system

establishes the polarity axes of wing disc and regulates the wing growth through feed-forward circuit to enable the cells to growth in response to wingless. Higher concentration of wingless at the distal edge of the wing promotes the Fj expression, where the Ds expression is higher at the wing hinge with lowest wingless expression (Fig. 1.9; (A. Brittle, Thomas, & Strutt, 2012; Zecca & Struhl, 2010)). This imbalance between gradients of Fj and Ds established the subcellular asymmetries of Ds/Ft in adjacent cells and propagate the polarity signals across tissue (Fig 1.9; (Ambegaonkar, Pan, Mani, Feng, & Irvine, 2012; Ayukawa et al., 2014; A. L. Brittle, Repiso, Casal, Lawrence, & Strutt, 2010)).

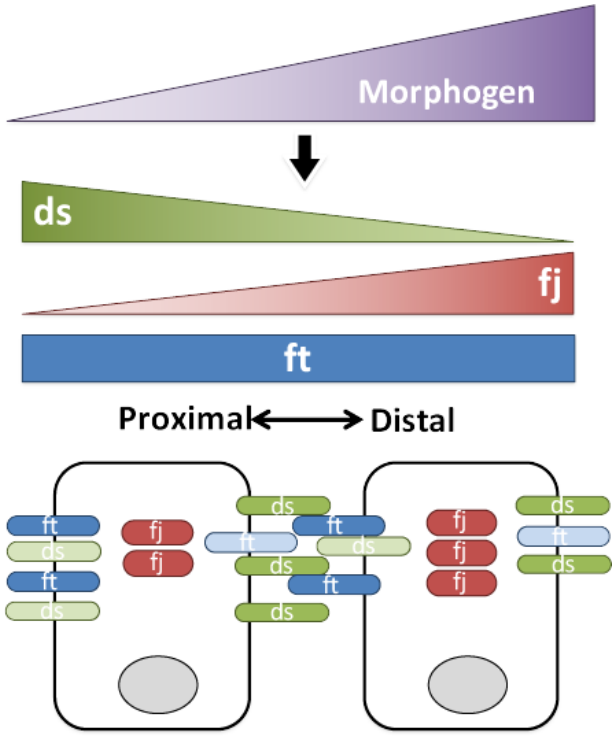

Figure 1.9. Gradient distribution of Ds/Ft/Fj system. In the *Drosophila* wing disc, a gradient of morphogen establishes the opposite gradient of ds and fj. Although ft is uniformly expressed across the tissue during development, the higher concentration of fj increases the phosphorylation of ft and ds, which resulted in an increased binding affinity of ft to ds but at the same time decreased the binding affinity of ds to ft. As a result, ds is asymmetrical distributed at the distal end of the cell to interact with the proximal ft from the adjacent cell. This pattern of ds/ft interaction orient the PCP towards distal. Figure is adapted from published work (Goodrich & Strutt, 2011; Hale et al., 2015).

Homologs of *Drosophila* Ds/Ft/Fj system, Fat1-4, Ds1-2 and Fjx1, have been identified in the vertebrates. Knockout analyses of these genes in mice resulted in different extent of PCP defects (Saburi et al., 2008; Saburi, Hester, Goodrich, & McNeill, 2012). Fat4 is most similar to the *Drosophila* ft in sequence and it is proposed to be the most important gene of the Ds/Ft/Fj system in mammals. *Fat4* knockouts show conversion and extension defects in the cochlea, and the HCs are slightly disoriented. The kidneys are smaller in these mutants, suggesting that Ds/Ft/Fj system may contribute to polycystic kidney disease in the mouse (Saburi et al., 2008; Saburi et al., 2012). Thus, the interaction between neighboring cells via this system of cadherins establishes their polarization and propagation across tissues.

b. Core PCP pathway

The cPCP pathway participates in majority planar polarity processes in flies and this pathway is highly conserved among other species (Goodrich & Strutt, 2011; D. Strutt, 2003). This pathway is comprised of six proteins forming the complex between cell boundaries: seven-pass transmembrane Wnt receptor Frizzled (Fz); four-pass transmembrane protein Strabismus (Stbm), which is also known as Van Gogh (Vang, and Vangl in mammals); seven-pass transmembrane cadherin Flamingo (Fmi, also known as Starry Night, or Celsr in vertebrates); and cytoplasmic component Dishevelled (Dsh/Dvl), Diego (Dgo), and Prickle (Pk) (Fig. 1.10; (Goodrich & Strutt, 2011; Matis & Axelrod, 2013; Y. Yang & Mlodzik, 2015)).

In *Drosophila*, cPCP proteins functions to establish the posterior polarization of trichomes in the wing (Goodrich & Strutt, 2011; D. Strutt, 2003). During the wing disc

development, the Wnt signal receptor, fz, is asymmetrically polarized at distal end of the cell under the instruction of the wnt gradient. Polarized fz form a complex with cadherin fmi, extracellular domain of which assembled homodimers with fmi of the adjacent cells. Then, vang in the adjacent cell is recruited to the proximal end with interaction to fmi. After the cross-cell boundary complex is established, cytoplasmic components of cPCP pathway are being recruited such that dsh and dgo are distributed at distal ends with fz, whereas pk is polarized at proximal end with vang (Fig. 1.10). Failure of this complex to form properly will affect hair polarization and may lead to formation of multiple hairs (Goodrich & Strutt, 2011; Gray et al., 2011; D. Strutt, 2003).

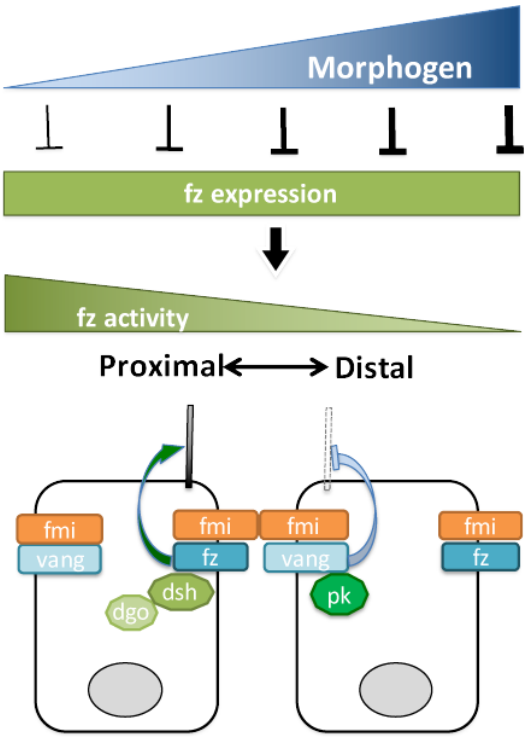

Figure 1.10. Gradient of morphogen establish the cPCP direction and orientation of trichomes in the *Drosophila* wing disc. Higher concentration of morphogen inhibits the activity of fz to interact with vang and establishes the PCP direction in *Drosophila* wing disc. Across the cell boundary, fz is concentrated at the distal end of the cell that interacts with the proximal distributed vang from the neighboring cell. Trichome formation is promoted by fz at the distal end of the cell but inhibited by vang at the proximal side. Figure is adapted from published work (Goodrich & Strutt, 2011; J. Wu et al., 2013).

Ten Frizzled (Fzd1-10), two Vangl (Vangl1-2), three Celsr (elsr1-3), three Dsh (Dsh1-3), and four Pk (Pk1-4) genes have been identified in vertebrates (Goodrich & Strutt, 2011; Matis & Axelrod, 2013; Y. Yang & Mlodzik, 2015). In zebrafish, the mutant of vangl2 (Stbm homologs) shows disrupted posterior polarization of cilia in cells of Kupffer's vesicles (Fig. 1.6D), floor plate, and pronephric duct (Borovina, Superina, Voskas, & Ciruna, 2010). As a result, significant increase the bilateral or right expression of left-side marker *lefty2,* indicating the left-right asymmetry is interrupted. Some of the cPCP genes have also been implicated in neural migration and axonal guidance in zebrafish and mammals. For example, mutation in fmi and its verterbrate homologs, Celsr, are suggested to have profound defects in facial branchiomotor neurons migration in zebrafish and major neuronal tract formation in mice (Fig. 1.6C, (Boutin et al., 2014; Tissir & Goffinet, 2013)). Core PCP regulates the convergent and extension movements during gastrulation (Goodrich & Strutt, 2011; Matis & Axelrod, 2013; Y. Yang & Mlodzik, 2015). In the *looptail* mouse mutant, which encodes a missense mutation on the C-terminal cytoplasmic domain of Vangl2 ($Vangl2^{lp/lp}$), the neural tube is not closed properly during development due to disrupted convergent and extension problem (Kibar et al., 2001). Thus, conserved role of the cPCP pathway is observed in various process of planar polarity establishment.

For the downstream effect, it is possible that the cPCP pathway, signaling at the intercellular level, acts to orient subcellular organelles within individual cells. It has been shown that cPCP signaling orients the microtubules and locate the basal body at one end of the apical surface (Borovina et al., 2010; Gray et al., 2011). How cPCP pathway organizes subcellular organelles remains unclear. Recent studies revealed that the ratio

between the two isoforms of prickle, pk and sple, can change the orientation of plus-minus ends of microtubules in *Drosophila* (Ayukawa et al., 2014; Olofsson, Sharp, Matis, Cho, & Axelrod, 2014). However, the mechanisms involved are still under investigation.

c. The relationship between intercellular polarity pathways

The relationship between Ds/Ft/Fj and cPCP pathways has been a subject of debate. The Ds/Ft/Fj pathway is thought to be upstream of cPCP pathway since Ds/Ft/Fj regulates the distribution of cPCP proteins. For example, during ommatidia development, higher activity of ft in the photoreceptors, which is established by gradients of ds and fj, results in a biased fz expression and polarized trapezoid establishment (C. H. Yang, Axelrod, & Simon, 2002). In addition, the Ds/Ft asymmetry leads to biased growth of microtubules, which is thought to contribute to cPCP proteins asymmetric distribution in *Drosophila* wing discs (Harumoto et al., 2010). These results suggest that Ds/Ft/Fj is upstream of cPCP. However, recent studies suggest that the relationship between the two pathways may be more parallel in other organs. First, both groups of proteins are regulated by global signals, like morphogens wingless, which provide the directional information of their polarization establishment, and both pathways require cell-cell interactions to polarize groups of cells locally (J. Wu et al., 2013). In the *Drosophila* wing, the Ds/Ft/Fj pathway can act to orient the trichomes in the absence of cPCP systems suggesting that Ds/Ft/Fj can function independently from cPCP. The trichomes and bristles are more randomized when both pathways are disrupted, compared to single system mutation. Furthermore, mutations in a single pathway could not be rescued by the other (Lawrence, Struhl, & Casal, 2007). In contrast to the ommatidia, these results in

wing disc suggest that these two intercellular polarity signals function parallel to each other. Thus, the relationship of these two pathways are complicated and may have different inputs and effects in different tissues. Nevertheless, both function at the intercellular level to mediate polarity (Fig. 1.7; (Bayly & Axelrod, 2011; Lawrence et al., 2007; Y. Yang & Mlodzik, 2015)).

3. Intracellular polarity pathway

Within individual cells, the global and intercellular polarity signaling are interpreted and amplified by intracellular polarity proteins. These proteins function to polarize subcellular organelles and establish the intrinsic polarity (Deans, 2013; Matis & Axelrod, 2013).

a. Insc/LGN/Gαi complex and Par complex: Spindle orientation

To mediate cell division, mitotic spindles pull the chromosomes apart from the center. What dictates the position of the spindles and the size of the daughter cells during asymmetric cell division are interesting questions. A conserved protein complex, Par/Insc/LGN/Gαi has been implicated in mediating cell divisions of embryonic blastomeres of *c.elegans*, sensory organ precursor (SOP) and neuroblasts of *Drosophila*, as well as mammalian neuronal progenitors (Lancaster & Knoblich, 2012; Morin & Bellaiche, 2011; Siller & Doe, 2009). Gαi, an α subunit of the heterotrimeric G-protein, is attached to the plasma membrane with lipid modification. It is generated in a receptor-independent manner and binds, Partner of Inscutable (Pins). Pins, also known as mPins, LGN or GPSM2 in mammals, contains a tetratricopeptide (TPR)-GoLoco domain that

binds Gαi and interacts with Inscutable (Insc). The presence of Insc, the scaffold protein, links the Pins/Gαi complex to Par complex (Lancaster & Knoblich, 2012; Morin & Bellaiche, 2011; Siller & Doe, 2009). The Par family of proteins is named for causing partition defects during asymmetrical division in *c.elegans* zygotes when the genes that encode these proteins are mutated. Among the six Par proteins that have been identified so far, Par3 (also known as Bazooka in *Drosophila)* and Par6 belong to PDZ-domain-containing scaffold proteins. Par6 combined with aPKC (atypical protein kinase C) interact with Par3 through kinase domain and form a complex. During spindle orientation, this complex is recruited to the cell cortex to define axial polarity (Goldstein & Macara, 2007; Suzuki & Ohno, 2006). Par/Insc/Pins/Gαi complex provides the ability to orient spindle location during asymmetric cell division (Fig. 1.11).

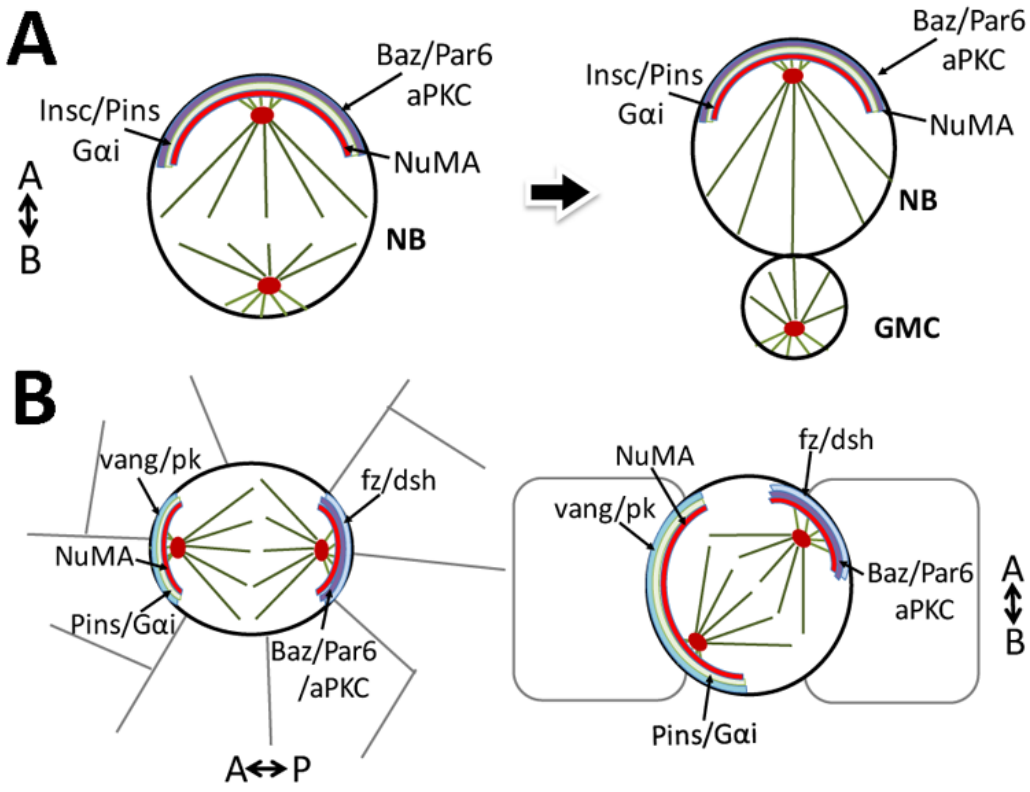

Figure 1.11. Distribution of cPCP proteins and Insc/Pins/Gαi during cell division of neuroblasts and sensory organ precursor cells. (A) During neuroblast division, the Par complex recruits the Insc/LGN/Gαi complex at the apical cortex of the dividing cell. After the asymmetric division, one neuroblast and a smaller ganglion mother cell (GMC) are generated. (B) During cell division of the sensory organ precursor (pI cell), cPCP proteins are asymmetrically distributed along the anterior-posterior axis (left). Vang/pk recruits the Gαi/Pins and NuMA to the anterior end, whereas fz/dsh are distributed at the posterior end with Par complex, which also binds NuMA, to establish planar orientation of the spindles. At the same time, the distribution spindle orientation along the apical-basal plane (right) is tilted slightly clockwise towards the posterior. Both cPCP proteins and Pins/Gαi are required to establish this spindle orientation. Figures are adapted from published work (di Pietro, Echard, & Morin, 2016; Morin & Bellaiche, 2011; Siller & Doe, 2009).

During *Drosophila* central nervous system development, embryonic neuroblasts divide asymmetrically along the apical-basal axis to generate a new neuroblast (NB, a stem cell) and a small ganglion mother cell (GMC), which will further differentiate into a neuron. During this process, Par complex recruits Insc/Pins/Gαi complex via interaction with Insc. Par/Insc/Pins/Gαi complex interacts with the coiled-coil domain protein, NuMA (nuclear and mitotic apparatus) that binds to Dynein/Dynactin motor complex to pull the spindle. All together they establish the apical-basal axis to divide cells asymmetrically and maintain the neuroblast fate (Fig. 1.11A, (Siller & Doe, 2009)).

In addition to establishing the apical-basal polarity, these proteins also function to mediate cell division along the anterior-posterior axis of sensory organ precursors in *Drosophila*, also referred as the pI cell (Fig. 1.11B). The Par and Gαi/Pins complexes are distributed along the anterior-posterior axis. However, different from the neuroblasts, the complexes are distributed at opposite ends of pI cells, which are under the influence of cPCP pathway (Lancaster & Knoblich, 2012; Morin & Bellaiche, 2011; Siller & Doe, 2009). Fz/dsh recruits the Par complex to the posterior side, which drives the cell fate

determination to the anterior side. On the other hand, Pins/Gαi, being excluded by fz/dsh to the anterior side, interact with NuMA. These two complexes, Pins/Gαi and Par, at opposite poles of the cells, determine the anterior-posterior orientation of mitosis spindle for mediating asymmetric cell division (Bellaiche et al., 2001; Segalen & Bellaiche, 2009; Segalen et al., 2010). Therefore, Pins/Gαi and the cPCP pathway maintain the spindle location along the apical-basal and anterior-posterior axis (Fig. 1.11B). However, how these protein complexes interact with each other to orient the spindles are not clear.

In mammals, spindle orientation proteins are also important for cell fate determination. For instance, in the absence of *Insc*, cells in the retina and neurons tend to undergo more symmetric divisions than normal, which leads to more cell proliferation and less differentiation. Gain of mInsc has the opposite effect (Postiglione et al., 2011; Zigman et al., 2005). The role of these proteins in spindle orientation requires further exploration.

b. Scrb/Dlg/Lgl complex

The Scrb/Dlg/Lgl signal pathway is another example that plays a role in orienting subcellular organelles. Scribble (Scrb) is a leucine-rich protein with PSD95/Dlg/ZO-1 (PDZ) domains. Discs-large (Dlg) belongs to the membrane-associated guanylate kinase (MAGUK) family. As a scaffold protein, Dlg assemble the Scrb/Dlg/Lgl (Lethal giant larvae) complex in response to other polarity signaling. In *Drosophila*, Scrb interacts with Vang and Insc to mediate polarities along apical-basal and planar planes (H. May-Simera & Kelley, 2012; Rivera et al., 2013). This complex could interact with Par/Insc/LGN/Gαi complex to orient spindle orientation (Lancaster & Knoblich, 2012;

Morin & Bellaiche, 2011; Siller & Doe, 2009). However, in *Drosophila* epithelial cells and neuroblasts, Scrb/Dlg/Lgl complex is basally located and antagonist to Par complex (Humbert, Dow, & Russell, 2006). Based on these results from different systems, it is clear that Scrb/Dlg/Lgl complex can interact with both cPCP pathway and Par/Insc/LGN/Gαi complexes to establish the intracellular polarity.

c. Ciliogenesis proteins

In *Drosophila*, the location of trichomes in the distal end of wing cells is a readout of the tissue's planar polarity (Gray et al., 2011). Likewise, primary cilium or cilia are also readout of planar polarity of cells in vertebrates. The primary cilium develops from the basal body, in a pattern of nine outer pairs with or without a central pair of microtubules. The 9+2 pattern is found in motile cilia, similar to the kinocilium of HCs of the inner ear. However, 9+0 is found in immotile cilia of the embryonic node, which provide the directionality of fluid flow to determine left-right asymmetry (Cardenas-Rodriguez & Badano, 2009; Dawe, Farr, & Gull, 2007).

Since protein synthesis does not occur in the cilium, proteins that are needed for cilia formation and maintenance are being transported to the cilium from cytoplasm via intraflagellar transport (IFT) (Cardenas-Rodriguez & Badano, 2009; Silverman & Leroux, 2009). Proteins participated in this process are critical for ciliogenesis (Cardenas-Rodriguez & Badano, 2009). For example, Ift88, one of the proteins required to form IFT particles, and Kif3a, which provides the motor for this transportation as a kinesin, are both important for ciliogenesis. Mutations on these two genes in mice lead to a series of ciliogenesis problems (Jones et al., 2008; Sipe & Lu, 2011). Additionally, genes that are

associated with Bardet-Biedl Syndrome (BBS) have also been identified as ciliogenesis proteins. For example, *BBS6*$^{-/-}$ mice show flattened and splayed stereocilia in inner ear HCs (H. L. May-Simera et al., 2010; H. L. May-Simera et al., 2009). However, ciliogenesis and cilium function are complicated systems: same gene can lead to different phenotypes and one disease can be caused by different genes (Dawe et al., 2007; Norris & Grimes, 2012). Thus, how the ciliogenesis proteins connect to other polarity signals are still under investigation.

B. Polarity signals regulating cell arrangements: vulva and ommatidia

There are several examples of polarity signals regulating cellular arrangements such as formations of the vulva in *c. elegans* and ommatidia in the *Drosophila* eye. Both of these tissues exhibit a polarity reversal in cell arrangement, which requires planar polarity signals.

1. Vulva

During vulva development in *c. elegans*, three vulva progenitor cells (VPC), P5-7.p within the epithelium undergo three rounds of asymmetric cell division to generate 22 cells with 7 different cell types (Fig. 1.12). The progeny align in a linear array and display palindrome symmetry, like "ABCDEFFEDCBA". The cell fate reversal is induced by the anchor cell (AC), the "invaded" cell from the uterus. The proximity of AC to P6.p progenitor is required to establish this patterning. The P6.p progenitor cell will receive high level of Wnt ligands, LIN-44 and MOM-2, which is expressed in AC. The high level of LIN-44 and MOM-2 induce the P6.p to adopt 1^{o} VPC fated to generate

the mirror-imaged progenies "EFFE" next to the AC. P5.p and P7.p, instead, will receive low levels of LIN-44 and MOM-2 to adopt the 2° VPC fate. In addition to the Wnt signaling from AC, another Wnt ligand, EGL-20 is also involved, which is expressed in the tail. EGL-20 establishes a posterior-to-anterior concentration gradient to provide directional instructive information and induce the posterior P7.p to orient cell division towards the AC, which are reversed from the ones from P5.p. EGL-2 mediates this effect via the Wnt/PCP pathway, regulating Vang expression and Ror2 tyrosine kinase receptor, CAM-1. Thus, the vulva formation requires multiple Wnt morphogens utilizing both canonical, β-catenin and non-canonical, PCP pathways (Fig. 1.12; (Green, Inoue, & Sternberg, 2008; Schindler & Sherwood, 2013)).

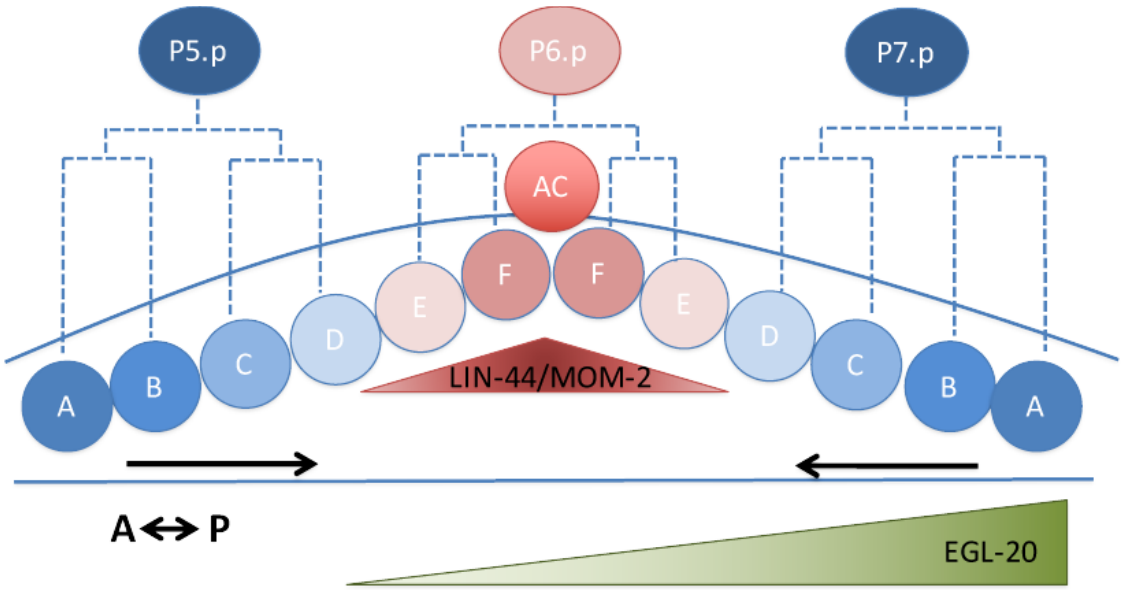

Figure 1.12. Various Wnt signals contribute to palindromic cell divisions in vulva formation. During vulva development, the P6.p adapts 1° VPC fate (pink) to generate four "EFFE" progenies under the influence of Wnt/Lin-44 and Wnt/MOM-2 that are expressed by the AC. P5.p and P7.p, in contrast, adapt the 2° VPC fate (blue) and generate "ABCD" vulva cells in a row. The arrows indicate the orientation of the asymmetric cell division and order of the "ABCD" progenies from P5.p and P7.p. The orientation of cells divided from P7.p is inverted by the posterior Wnt/EGL-20 signals. Figure is adapted from published work (Green et al., 2008; Schindler & Sherwood, 2013).

2. Ommatidia

During *Drosophila* eye development, collaborations of Wg and cPCP proteins are required to establish a mirror-imaged reversal of ommatidia across the equator (Fig. 1.13). Each ommatidium is comprised of eight photoreceptor cells, arranged in a trapezoid form. R1/R2 and R5/R6 are aligned in a plane beside R7 and R8. R7 and R8 are located in the center of the trapezoid and the two are aligned in the apical-basal plane. R3 and R4 are located on the tip of the trapezoid as the polarity determinator. During development of a given ommatidium, the specified R8 recruits pairwise R2/R5 and R3/R4 to form the five-cell precluster. Then, the precluster starts to rotate and brings R3 closer to the pole. At the same time, R1, R6 and R7 are differentiating and recruited to form the final trapezoid form. During this process, cell fate specification and relative position determination of the R3 versus R4 is the critical step that R3 is more polar localized, whereas the R4 is more equatorial positioned. Across the equator, the polarity of the trapezoid of ommatidia is reversed (Fig. 1.13). How is this mirror-image established? First, expression of *Wg* at both poles of the eye imaginal disc, which create a concentration gradient with the lowest at the equator is important (Fig. 1.13). Then, the asymmetric distribution of cPCP components plays a key role. At the precluster stage, the cPCP proteins are first enriched in a double horseshoe-like pattern in R3/R4, which guide the rotation of the R3/R4 towards polar side. Then, the fz and dsh are concentrated in the R3 side at the R3 and R4 boundary, which is required for the R3 specification. In contrast, the vang and pk are concentrated in R4, especially at the boundary with R3. At this stage, cPCP proteins are also concentrated in horseshoe-like of R4 at the polar end. These polarized distributions of cPCP proteins contribute to the polarity of the trapezoid

formation during division and differentiation. The polarity of ommatidia is random or no R4 forms in the *fz* null and overexpression mutants (Andreas Jenny, 2010; Maung & Jenny, 2011).

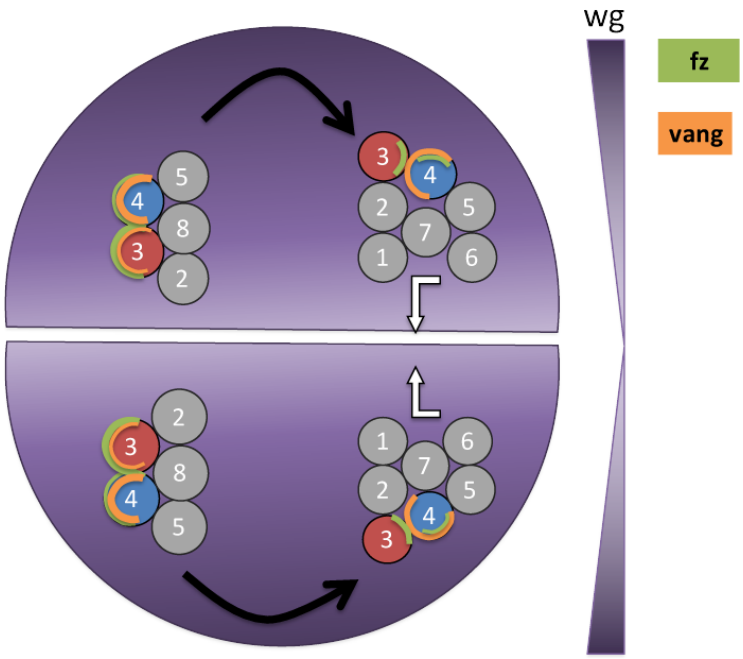

Figure 1.13. Polarity reversal of the ommatidia in the *Drosophila*. Expression of *Wg* at the two poles of the *Drosophila* eye defines the equator (white line). The gradient of *Wg* concentration guides the asymmetric distribution of cPCP proteins (green and orange) in the R3 (red) and R4 (blue). As a result, ommatidia differentiate and rotate along the polar-equator axis (black arrows), forming a mirror-image pattern of cell arrangements across the equator (white arrows). Figure is adapted from published work (Andreas Jenny, 2010).

Considering that the mechanism involved in LPR formation of the maculae is not known, the examples of vulva and ommatidia formation provide insight into how the LPR could be established. Could the morphogens and cPCP pathway also mediate some sort of cell rearrangement or just stereocilia reversal to establish the LPR? I will discuss this question in later sections.

C. Polarized ciliated cells

In addition to cellular arrangement, polarity signals also play a role in the asymmetric distribution of subcellular organelles. Polarized cilia in epithelial cells are important for their functions. The cilium could be single or multiple located on the surface of the cell (Wallingford, 2010). Multi-ciliated cells include ependymal cells in ventricular system, and epithelial cells in the oviduct and airway tract. The cilia are aligned parallel and polarized on the apical surface of a given cell. These polarized cilia are essential for directional flow, such as the cerebrospinal fluid (Guirao et al., 2010; Mirzadeh, Han, Soriano-Navarro, Garcia-Verdugo, & Alvarez-Buylla, 2010). Additionally, the mono-cilia within the nodal cells of the mouse and other equivalent structures in vertebrates are also polarized and control the directional fluid flow in the node to establish left-right asymmetry of embryos (Fig. 1.6F; (Essner, Amack, Nyholm, Harris, & Yost, 2005; Hirokawa et al., 2006; Kramer-Zucker et al., 2005)). The similarly polarized mono-cilium in the HCs is responsible for hearing and maintaining balance (Fig. 1.1; (Tilney et al., 1992)). Cilia dysfunction can alter structure and location of cilia that lead to ciliopathies. For example, dysfunction of cilia in HCs results in hearing loss and vestibular phenotypes (Dawe et al., 2007; Norris & Grimes, 2012).

The planar polarity signals are known to be involved in various types of polarized ciliated cells. The cPCP pathway is asymmetrically distributed in all of the cell types listed above: multiciliated ependymal (Boutin et al., 2014), airway tract cells (Vladar, Bayly, Sangoram, Scott, & Axelrod, 2012), monociliated nodal (Borovina et al., 2010) and sensory HCs (Deans et al., 2007; Montcouquiol et al., 2006; Y. Wang, Guo, & Nathans, 2006). Mutations of cPCP proteins lead to randomly oriented cilia in these cells.

For example, cilia are not polarized along the functional axis of ependymal cells with *Celsr1* null mutation (Boutin et al., 2014). The null mutation of *vangl2* leads to random polarization of epithelial cells in Kupffer's vesicle (Borovina et al., 2010). The mouse mutant, *Vangl2*$^{lp/lp}$, causes randomly oriented HCs (Montcouquiol et al., 2003; Montcouquiol et al., 2006). Thus, these polarized cell types are good models for studying planar polarity signaling in animals.

III. Polarity establishment of sensory hair cell organs

A. Mechanism of stereocilia orientation: analysis from expression and mutants

The establishment of stereocilia polarity is a complicated process. Most signaling pathways that are known to be involved in PCP formation appear to play a role in establishing the orderly array of HC polarity in the inner ear. The intracellular polarity signals establish the asymmetrical localization of stereociliary bundle on the apical surface. Intercellular polarity signals coordinate neighboring cells to align HCs pointing to the same direction. Even though there is currently insufficient supporting evidence, the global polarity signals are believed to establish the polarity pattern of HCs within the entire sensory organ [14]. Known polarity signaling pathways that regulate HC polarity in the inner ear are summarized in the following sections (Fig.1.14, Table 1).

Name	Phenotype	Functional level
Wnt5a/7a	Defects in convergent and extension of the cochlea and refinement of stereocilia orientation	Global?
Fat4	Defects in convergent and extension of the cochlea and stereocilia misoriented	Intercellular (Ds/Ft/Fj)
Vangl2	Random polarized stereocilia	Intercellular (Core PCP)
Fz3/6	Random polarized stereocilia	Intercellular (Core PCP)
Dsh	Random polarized stereocilia	Intercellular (Core PCP)
Rac1	stereocilia malformation in addition to misorientation	Effectors of core PCP (Rho GTPase gamily)
Cdc42	abnormal orientation of cochlear HCs	Effectors of core PCP (Rho GTPase gamily)
Gαi	polarity reversal and random orientation in outer HCs	Intracellular (Par/Insc/LGN/Gαi)
LGN	randomness of stereocilia polarity and malformations in the shape of stereocilia	Intracellular (Par/Insc/LGN/Gαi)
Dlg1	mis-orientation of cochlear HCs	Intracellular (Scrb/Dlg/Lgl)
Lis1	stereocilia misorientation and cellular disorganization	Intracellular (Lis1/Dynein)
Ift88	Defects in convergent and extension of the cochlea and stereocilia are circular with a centralized kinocilium on the apical plane of HCs	Intracellular (Ciliogenesis)
Kif3a	The basal body in the mutants is no longer associated with stereocilia nor located at the apical surface of HCs	Intracellular (Ciliogenesis)

Table 1. Summary of polarity proteins required for stereocilia polarity establishment. Phenotypes resulting from loss of these proteins and whether these proteins are functioning at the inter- or intracellular level are shown.

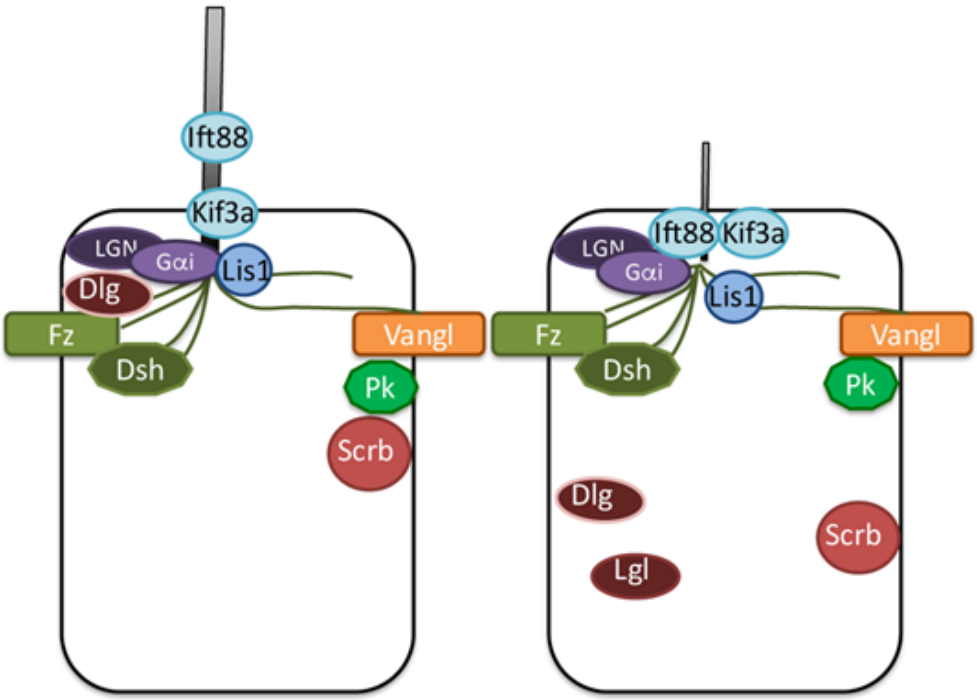

Figure 1.14. Projected summary of various polarity protein locations within the sensory epithelium of the inner ear. Cross-cell-boundary complex is formed between the hair cell on the left and supporting cell on the right. Locations for some of the proteins such as Scrb and Lgl are not known.

1. Global polarity signaling: Morphogens - Wnt5a and Wnt7a

Morphogens Wnt5a and Wnt7a have been reported to participate in hair bundle polarity regulation. Despite the role of Wnts in establishing global patterning in other systems, analyses of Wnt mutants suggest that Wnts only has a minor role in mediating stereocilia orientation (Dabdoub et al., 2003; Qian et al., 2007). Overexpression of Wnt7a in a cochlear explant resulted in a mild stereocilia orientation defect (Dabdoub et al., 2003). Further supportive evidence that Wnts are important for stereocilia patterning was observed when Frzb (secreted Frizzled-related protein 3) an antagonist of Wnt pathway, was added to cochlear explants and resulted in misorientation of hair bundles and a shortened cochlea (Qian et al., 2007). In contrast, even though the cochlear duct is

shorter and wider in *Wnt5a*$^{-/-}$ mutants, there is not much stereocilia orientation defects. The third row of outer HCs, occasionally have rotated alignment with relative normal hair bundle, suggesting that there could be functional the redundancy of Wnts in stereocilia polarity formation (Qian et al., 2007). Furthermore, defects in stereocilia orientation and neural tube closure are enhanced by *Wnt5a*$^{-/-}$;*Vangl2*$^{lp/lp}$, which indicates the genetic interaction between Wnt and cPCP pathway (Qian et al., 2007). Thus, these results suggest that Wnts have global effects on convergent and extension of the developing cochlea and an effect on the refinement of stereocilia orientation (Fig. 1.14 , Table 1).

2. Intercellular signaling:

a. Ds/Ft/Fj pathway—Fat4

Ds/Ft/Fj pathway is conserved in mammals. Published results show that loss of *Fat4* in the mouse inner ear leads to a shorter cochlear duct (Saburi et al., 2008). All four rows of HCs stereocilia in the cochlea exhibit some deviations from the normal position. In short, *Fat4* mutants show a mild global polarity phenotype but clear hair bundle polarity defects. Given multiple Fats in vertebrate, it is possible that there is redundancy of the Ds/Ft/Fj pathway in stereocilia orientation. In addition, compound mutants of *Fat4*$^{-/-}$;*Vangl2*$^{lp/+}$ show an enhanced polarity defects, suggesting a genetic interaction of the two pathways (Saburi et al., 2012). These results indicate that the Ds/Ft/Fj pathway may have redundant role in the stereocilia orientation (Fig. 1.14, Table 1).

b. Core PCP pathway

Core PCP proteins are distributed at cell junctions. In cochlear HCs, Fz3 and Vangl2 form a complex at the HC-supporting cell junctions, in which Fz3 is distributed at HCs side and Vangl2 is distributed in the opposing membrane in the supporting cell (Giese et al., 2012; Montcouquiol et al., 2006). More importantly, Dsh1/2 rather than Fz is co-localized with the stereocilia (J. Wang et al., 2006). This pattern of Fz, which is not co-localized with the stereocilia, is different from the pattern in the *Drosophila* wing disc.

The *looptail* mouse mutant, $Vangl2^{lp/lp}$, is the first mutant reported to have a HC phenotype (Montcouquiol et al., 2003). In the mutants, the cPCP complex is lost, which resulted in HC mis-orientation in all sensory organs of the inner ear (Deans et al., 2007; Montcouquiol et al., 2006). In the maculae, HCs are randomly oriented and the LPR is obscured. However, the hair bundles on the apical HC surface remain normal shape and distributed at the lateral edge of HCs (Montcouquiol et al., 2003; Montcouquiol et al., 2006). Similar but milder phenotypes are observed in $Fz3^{-/-};Fz6^{-/-}$ double mutants. In these double knockout mutants, inner HCs are inverted in the cochlea. In the vestibular organs, strong polarity defects are observed in the cristae but milder hair bundle mis-orientation is observed in the utricle (Y. Wang et al., 2006). Dsh is known to interact with Fz in other systems, and essential for polarity formation (A. Jenny, Reynolds-Kenneally, Das, Burnett, & Mlodzik, 2005). Although Dsh is not associated with Fz in cochlear HCs, null mutants of *Dsh1/2* show randomly polarized third row of outer HCs and the cochlear duct is shorter and wider, suggesting that Dsh is still required for stereocilia orientation (J. Wang et al., 2006). In summary, the intercellular polarity pathway, cPCP, functions in mediating convergent and extension of the cochlear duct as

well as regulating stereocilia alignment among HCs (Fig. 1.14).

A small Rho family GTPase, which could act downstream of cPCP signaling pathway, is also involved in polarity formation (Park, Mitchell, Abitua, Kintner, & Wallingford, 2008; D. I. Strutt, Weber, & Mlodzik, 1997). Rho GTPases have been reported to participate in various PCP processes such as cell migration, microtubule dynamics and cilia orientation. In the inner ear, Rho-ROCK2 (Rho-associate kinase) is required for Ptk7 (Protein tyrosine kinase) at cell junctions to polarize HC stereocilia (Andreeva et al., 2014; J. Lee et al., 2012; Xiaowei Lu et al., 2004). Ptk7 is a known effector of cPCP pathway: required for membrane localization of Dsh via interaction with cPCP components in neural crest migration (Shnitsar & Borchers, 2008). Thus, Rho family members could also function as effectors of cPCP pathway in stereocilia orientation. Notably, tissue-specific knockout of *Rac* that encodes a member of Rho family of GTPases, resulted in stereocilia polarity defects. Rac1, which interacts with p21-activated kinase (PAK), is found to be involved in HC polarity formation (Grimsley-Myers, Sipe, Geleoc, & Lu, 2009). However, different from the mutants of cPCP complex, which only affected the alignment of the stereociliary bundles, loss of Rac1 resulted in stereocilia malformation in addition to misorientation (Grimsley-Myers et al., 2009). This phenotype suggests that Rho GTPase have additional functions than cPCP pathway. In addition, conditional knockout Cdc42, another Rho GTPase family member, also results in abnormal orientation of cochlear HCs (Kirjavainen, Laos, Anttonen, & Pirvola, 2015). This function of Cdc42 requires aPKC to establish the stereocilia polarity (see below). Based on these results, Rho GTPase family members could be effectors of cPCP pathway but they could also respond to other signaling besides cPCP, which makes

this group of proteins excellent candidates as linkers between inter- and intracellular polarity pathways (Fig. 1.14, Table 1).

3. Intracellular polarity proteins:

a. Par/Insc/LGN/Gαi complexes

What are the intracellular mechanisms that regulate stereocilia orientation? Existing results suggest that the Par/Insc/LGN/Gαi complexes are important for this process (Ezan et al., 2013; Tarchini, Jolicoeur, & Cayouette, 2013). In the HCs, Gαi3, LGN, Insc, and Par3 are associated with the kinocilium and form a crescent. In contrast, the Par6 and aPKC have a distribution pattern that are complementary to the LGN/Gαi complex, located on the opposite side of the kinocilium (Ezan et al., 2013; Tarchini et al., 2013). In the cPCP mutants such as *Vangl2*$^{lp/lp}$, the Gαi3 expression is still consistently associated with the kinocilium regardless of the stereocilia mis-orientation. Furthermore, ectopically generated HCs in the greater epithelial ridge of the cochlea, Gαi3 expression is intact and associated with the kinocilium, even though their polarities are random relative to the body axis (Ezan et al., 2013). Gαi3 in a complex with Par/Insc/LGN is thought to regulate the dynamics of microtubules via the dynein and pull the plus-end of microtubules in the HCs, and thus mediate the migration of kinocilium(Ezan et al., 2013; Tarchini et al., 2013). Based on these results, the Par/Insc/LGN/Gαi complex is responsible for intracellular kinocilium polarization (Fig. 1.14, Table 1).

Pertussis toxin (Ptx) is Gαi/o protein inhibitor. Overexpression of the catalytic subunit of the Ptx (Ptxa) in cochlear HCs causes polarity reversal in some of the HCs in the first and second rows of outer HCs and random orientation in the third row of outer

HCs (Ezan et al., 2013; Tarchini et al., 2013). Inhibiting Gαi signaling with Ptxa also causes a reduced accumulation of microtubules plus-ends at the apical surface. In addition to Gαi, *LGN* mutants exhibit some randomness of stereocilia polarity and malformations in the shape of stereocilia. In the *LGN* conditional knockout cochlea, stereocilia in outer HCs no longer maintain the V shape. The shape of stereocilia bundles can be split, shortened, or malformed, whereas the kinocilium can be randomly localized and centralized. In addition, overexpression of Gαi2 or LGN affects hair bundle migration and its mature pattern in the cochlear HCs (Ezan et al., 2013; Tarchini et al., 2013). In summary, the Par/Insc/LGN/Gαi complexes are required for proper subcellular polarization of stereociliary bundle, supporting their role as intracellular polarity signaling (Fig. 1.14).

b. Scrb/Dlg/Lgl complex

The function of Scrb/Dlg/Lgl complex in HC polarity formation is not clear. Knockout of *Dlg1* leads to mis-orientation of cochlear HCs (Rivera et al., 2013). In addition, *Dlg3* shares a similar distribution pattern as Gαi in cochlear HCs, and could interact with Dsh in apical docking of kinocilium (Gegg et al., 2014). Furthermore, Scrb and Vangl2 are known to interact in stereocilia orientation (Montcouquiol et al., 2003). Based on these results, the Scrb/Lgl/Dlg complex could receive the intercellular polarity information from cPCP proteins in individual HCs and regulate the intracellular polarity via their interaction with the Par/Insc/LGN/Gαi complex (Fig. 1.14, Table 1, (Bergstralh, Lovegrove, & St Johnston, 2013)).

c. Lis1/Dynein complex

Gαi complex is known to mediate the spindle position through Lis1/Dynein complex, which provides the pulling force of microtubules (di Pietro et al., 2016), which may occur in HCs as well (Siller & Doe, 2009). The Lis1/Dynein complex could also participate in stereocilia orientation intracellularly. In cochlear HCs, Lis1 is located at the pericentriolar region and it regulates microtubule organization and localization of dynein. Then, dynein forms the motor complex that pulls the microtubule plus-ends towards the lateral edge of the cell (Guo et al., 2006). In the cochlea, conditional knockout of *Lis1* resulted in stereocilia misorientation and cellular disorganization. These results suggest that Lis1/Dynein could be another intracellular mechanism for mediating stereocilia position in the HCs (Fig. 1.14, Table 1, (Sipe, Liu, Lee, Grimsley-Myers, & Lu, 2013)).

d. Ciliogenesis proteins—Ift88 and Kif3a

Kinocilium is the primary cilium derived from the basal body. Thus, the ciliogenesis proteins are important for cilia formation, could also participate in stereocilia polarity formation. For example, in the *Ift88* mutants, cochlear duct is shorter and stereocilia are circular with a centralized kinocilium on the apical plane of HCs (Jones et al., 2008). In *Kif3a* knockout mutants, hair bundles are flattened in cochlear HCs. In addition, Kif3a also participates in the apical docking of basal body through a non-ciliary function. Kif3a regulates the basal body position and its correlation with stereocilia through cortical PAK activity. The basal body in the mutants is no longer associated with stereocilia nor located at the apical surface of HCs (Sipe & Lu, 2011). These results

indicate multiple roles of ciliogenesis proteins functioning in hair bundle polarity, in addition to their role in ciliogenesis (Fig. 1.14, Table 1).

B. The polarity signals in the LPR establishment

How is the LPR established in the maculae? The kinocilium remains closely associated with the distribution of intracellular polarity proteins, Par/Insc/LGN/Gαi complex across the LPR (Fig. 1.15; (Ezan et al., 2013; X. Lu & Sipe, 2016; Tarchini et al., 2013)). In the *Vangl2*$^{lp/lp}$ mutants, the LPR is missing and stereocilia are randomly oriented (Ezan et al., 2013; Montcouquiol et al., 2006). However, distribution of the intercellular polarity proteins such as Pk2 and Vangl2 in a normal utricle are maintained at the medial side of HC-supporting cell boundary across the LPR and Fz3 expression at the lateral side is also maintained (Fig. 1.15; (Deans et al., 2007; Jones et al., 2014)). These results suggest that cPCP proteins are unlikely to mediate the LPR, and the loss of LPR in the *Vangl2*$^{lp/lp}$ mutants is likely to be a result of intercellular misalignment. Thus, the establishment of the LPR is different from vulva and ommatidia formation described earlier, which are both dependent, in part, on the cPCP pathway. Interestingly, it has been reported that in the null mutants of *Emx2* maculae, the LPR is absent and all HCs in the maculae are unidirectional (Holley et al., 2010). In addition, cochlear outer HCs are missing and the inner HCs are malformed, arranged in two rows instead of one.

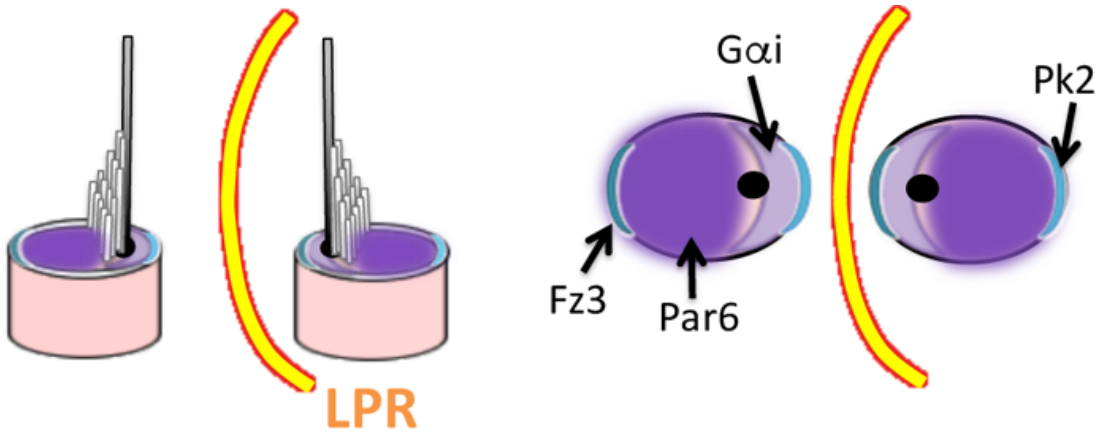

Figure 1.15. Schematics for the distribution of polarity proteins across the LPR in utricles. HCs are facing each other across the LPR (yellow line). However, distribution of the cPCP components, Fz3 (dark blue) and Pk2 (light blue) are not reversed across the LPR, which are asymmetrically distributed at the lateral and medial border of the HCs, respectively. The intracellular polarity proteins, instead, maintain their relationship with the kinocilium. Gαi (light purple) forms a crescent beside the kinocilium, whereas the Par6 (magenta) has a complementary pattern to Gαi.

IV. Emx2

A. The *ems* in the *Drosophila*

The *empty spiracles (ems)* gene was first isolated and identified in *Drosophila* (Dalton, Chadwick, & McGinnis, 1989; Jurgens, Wieschaus, Nussleinvolhard, & Kluding, 1984). This gene is named based on the mutant phenotype, in which the spiracles (tracheal system in flies) are empty, missing the filter lining. The *ems* encodes a homodomain transcription factor, isolated from a low stringency screen using the homeobox of *eve* (even-skipped). Homeobox is a conserved 180 base pairs DNA sequences, encoding a ~60 residues homeodomains that have a sequence-specific DNA binding activity (Dalton et al., 1989). The preferred DNA sequence of *ems* target in *Drosophila* is TAATTA that was identified by bacterial one-hybrid system (Meng &

Wolfe, 2006), which is a common recognition sequence identified among homeobox-containing proteins so far (Berger et al., 2008). In addition to homeodomain sequences, there are a proline-rich N-terminal sequence and an acidic profile in C-terminus, which are consistent with its role as a transcription factor. Given *ems* expression in the anterior part of the embryo and the severe patterning defects in the anterior head, *ems* is believed to be a gap gene that regulates transcription cascades in this region (Walldorf & Gehring, 1992).

There are two different spatial and temporal patterns of *ems* expression during embryogenesis: an early, head-specific pattern, and a later, metameric pattern. *Ems* protein is first detected around stage five of development in anterior region of the blastoderm as a stripe (Campos-Ortega & Hartenstein, 1985; Dalton et al., 1989). This stripe is in a gradient with increasing width from dorsal to ventral, with an average width of approximately eight cells. Most of the *ems* expressing cells in the procephalon are found in the antennal lobe, which gives rise to the antennal sense organ (Dalton et al., 1989; Walldorf & Gehring, 1992). The metameric expression of *ems* begins to emerge from stage 8 in lateral ectoderm of each germband segment primordium. During the germband elongation, *ems* expressing cells proliferate to elongate every *ems* patch dorsally. Then, in each patch, ventromedial and ventrolateral regions of *ems* expressing cells give rise to neuroblast and ventral epidermis, whereas tracheal pits and dorsal epidermis are derived from the lateral region (Dalton et al., 1989; Walldorf & Gehring, 1992).

The mutant phenotypes of *ems* are accountable by this broad expression pattern of *ems*. The missing head structures in the null mutants are due to *ems* expression in the

head primordia. The process of head involution fails, which leads to malformation of the cuticular and sensory structures of the head. The optic lobe is absent and antennal sense organs are missing. Several of the head skeletal elements are also missing. In addition, the loss of *ems* expression in the ventral nerve cord leads to an axonal patterning defects in the *ems* mutant, and the nerves do not migrate through the midline (Hartmann, Hirth, Walldorf, & Reichert, 2000). *Ems* was also suggested to participate in neuronal development and central nervous system formation, since this gene is expressed in neuroblast precursors (Dalton et al., 1989; Walldorf & Gehring, 1992).

B. The *Emx2* in the mouse: expression, function and conservation

1. Homologues of *ems* in the mouse

a. *Emx1*

In mouse, there are two homologues of *Drosophila ems* gene, *Emx1* and *Emx2*. Between these two homologues, there is about 80% identity at the amino-acid level. Only 4 residue differences are present in homeodomain of these two genes (Simeone et al., 1992). *Emx1* has more restricted expression in the brain, expressed in the dorsal telencephalon compared to *Emx2* (Briata et al., 1996; Cecchi & Boncinelli, 2000). *Emx1* is present in proliferating, differentiating and mature neurons in the central nervous system. For the trunk region, during development, *Emx1* is also expressed in branchial pouches, apical ectodermal ridge of limbs, kidney and the reproductive system (Briata et al., 1996). Different from *Emx2* mutants, *Emx1* knockout mice have minor phenotypes (Bishop, Garel, Nakagawa, Rubenstein, & O'Leary, 2003; Yoshida et al., 1997). The mutant mice are viable with no obvious behavioral impairment, which could be due to its

functional redundancy with *Emx2* since these two genes are co-expressed in multiple regions, such as the brain (Cecchi & Boncinelli, 2000). The more severe brain phenotypes in the *Emx1*$^{-/-}$;*Emx2*$^{-/-}$ double mutant further supports that the two *Emx* genes cooperate in cortical development (Bishop et al., 2003; Yoshida et al., 1997).

b. *Emx2*

The mouse *Emx2* has about 11 amino acids differences from the *Drosophila ems* in the homeodomain region indicating that this gene is highly conserved (Simeone et al., 1992). The mouse *Emx2* is located at 10q25.3-26.1 region that has a 2907 base pair long cDNA and encodes a protein of 252 amino acids (Fig. 1.16;(Noonan, Mutch, Ann Mallon, & Goodfellow, 2001)). Similar to the results in *Drosophila*, the target sequences of *Emx2* homeodomain is TAATTA based on high resolution DNA binding analysis (Berger et al., 2008).

The expression pattern of *Emx2* is similar between mouse and flies. In mice, *Emx2* expression is first detected at three-somite stage in the lateral-caudal forebrain primordia (Suda et al., 2001). Starting from E8.5, expression is detected at anterior-dorsal neuroectodermal regions of the embryos. Around E9.5, the cortical expression of *Emx2* is extended to the olfactory placodes. At E12.5, *Emx2* is expressing in the forebrain, olfactory epithelium, digit primordia, and the developing gonads and kidneys (Cecchi, 2002; Cecchi & Boncinelli, 2000; Mallamaci et al., 1998; Simeone et al., 1992). The expression patterns and phenotype in the null mutants of *Emx2* will be discussed in more details in the following sections.

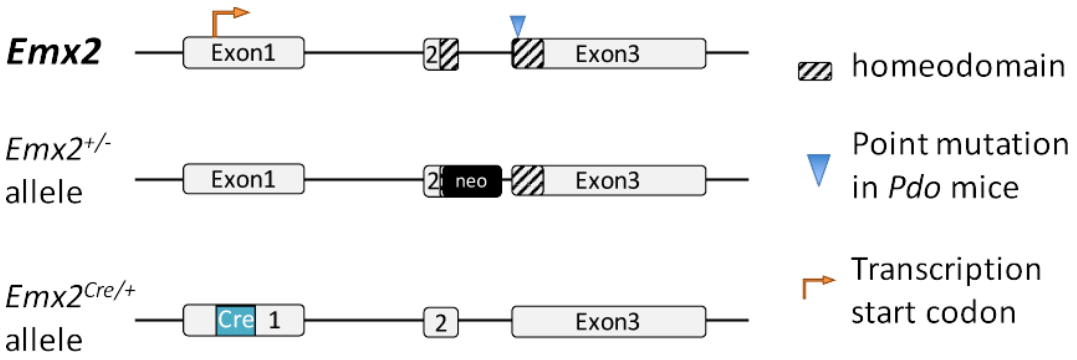

Figure 1.16. Schematic of the mouse *Emx2* locus in wildtype and mutants. *Emx2* has three exons. The homeodomain (striped) is located in Exon 2 and 3. The null allele is generated by replacing a portion of the homeodomain in Exon 2 with neomycin (black bar, (Pellegrini, Mansouri, Simeone, Boncinelli, & Gruss, 1996)). *Pardon* mutants harbor a point mutation in the homeodomain of *Emx2* (blue arrow; (Rhodes et al., 2003)). The $Emx2^{Cre}$ allele is generated by inserting the Cre sequences (cyan bar) right after the start codon, ATG (arrow, (Kimura et al., 2005)).

2. Roles of *Emx2* in nervous system development: regional patterning and cell proliferation

a. Regional patterning

The central nervous system of the mouse is derived from the neural plate, which becomes distinguishable around E7.5. Cerebral cortex development is initiated by cell divisions at the ventricular zone (VZ), where *Emx2* is expressed and this expression persists in the adult mouse cortex. During cortical development, *Emx2* is expressed in a gradient, higher in the medial-posterior region within the telencephalon. *Emx2* is required for in early cortical regionalization and specification (Cecchi, 2002).

Beyond the cortex, *Emx2* is also expressed in specific cell layers in the hippocampus, amygdala and mammillary bodies. Strong *Emx2* expression is still detected at postnatal day 5 hippocampus, especially in the dentate gyrus (Cecchi & Boncinelli, 2000;

Mallamaci et al., 1998). These expression patterns suggest a regional function for *Emx2*, which is further supported by the phenotypes observed in *Emx2* null mutants. The hippocampus is severely reduced in *Emx2*$^{-/-}$ brain (Fig. 1.16; (Pellegrini et al., 1996)). Since *Emx2* is expressed in the dentate gyrus at a high level, this region is complete missing in the *Emx2* knockout mice. Thus, *Emx2* is required for patterning the forebrain, and participate in proliferation and/or specification of the dentate gyrus development (Cecchi, 2002; Cecchi & Boncinelli, 2000; Pellegrini et al., 1996). In addition, the olfactory bulbs are significant reduced (Pellegrini et al., 1996). With the loss of this gene, the size of cerebral hemispheres is decreased in the cortical area that normally expresses *Emx2* and there is a relative expansion of the non-*Emx2* region (Cecchi, 2002; Cecchi & Boncinelli, 2000; Mallamaci, Muzio, Chan, Parnavelas, & Boncinelli, 2000; Pellegrini et al., 1996).

b. Cell proliferation and differentiation

In addition to regional patterning, *Emx2* also regulates cell proliferation and differentiation. Expression of *Emx2* in the VZ, the stem cell region, suggests a role for *Emx2* in maintaining the neuroblasts and inhibiting differentiation.

The loss of *Emx2* leads to more asymmetric division in vitro and decreases clonal size compared to controls (Heins et al., 2001). Infecting isolated cortical cells from E14 with *Emx2*-sense virus is able to promote symmetric division, increase the clone size, and boost proliferation (Heins et al., 2001). However, the function of *Emx2* may be different between embryonic and adult nervous system. *Emx2* is expressed in adult neural stem cells at a high level in vitro and this expression decreases upon differentiation.

Overexpression of *Emx2* in adult neural stem cells reduces cell proliferation. In contrast, adult neural stem cell culture generated from *Emx2* null mutants promotes more proliferation (Rossella Galli et al., 2002; Gangemi et al., 2001; Gangemi et al., 2006). Whereas the effects of Emx2 in neuroblasts and adult neural stems cells appear to be different, Emx2 is implicated in regulating the type of cell division in the brain.

c. Neuronal migration and projection

In the mouse, *Emx2* may also affects neuronal migration. Loss of *Emx2* affects the projection of the olfactory nerve projection to the olfactory bulbs (Mallamaci, Mercurio, et al., 2000; Miyamoto, Yoshida, Kuratani, Matsuo, & Aizawa, 1997). During the cortical neurogenesis, the newly differentiated neurons will bypass the early-formed neurons and migrate to the surface of the cortex. This is known as the "Inside-out" rule (Cecchi & Boncinelli, 2000). This pattern of migration is affected in the *Emx2* knockout mice. *Emx2* expression is detected in the Cajal-Retzius cells within the marginal zone, which are essential for the newborn neurons to radially migrate to the external layer. The migration defects could be attributed to the lack of Cajal-Retzius cells in the absence of *Emx2*. Further analyses indicate that the radial migration defects observed in *Emx2* knockouts is attributable to the loss of reelin protein in Cajal-Retzius cells (Cecchi, 2002; Cecchi & Boncinelli, 2000; Mallamaci, Mercurio, et al., 2000).

Besides the radial migration defects in the cortex, the distribution of thalamocortical projections are also affected in *Emx2*$^{-/-}$ mice. The thalamocortical projections are misrouted in the *Emx2*$^{-/-}$ cortex. There is an altered and delayed arrival of thalamic projections to the cortex, which could contribute to the absence of regional identity and

an axonal guidance defect at the diencephalic-telencephalic boundary (Lopez-Bendito, Chan, Mallamaci, Parnavelas, & Molnar, 2002). In addition, the olfactory sensory neurons fail to project and innervate the disorganized olfactory bulbs in the absence of *Emx2* (Pellegrini et al., 1996).

d. Functional conservation

The functions of *Emx2* are likely to be conserved among species. As mentioned above, loss of *ems* leads to missing of various regions of the nervous system in *Drosophila*. The expression of *ems* in the ventral nerve cord is believed to help the neurons cross the midline and migrate correctly (Hartmann et al., 2000). Thus, regional patterning of the brain and neuronal migration requirements of *ems* in the fly brain are similar to Emx2's function in the mouse. In addition, *Emx2* has been reported to express in telencephalon and diencephalon of zebrafish (Kawahara & Dawid, 2002; Morita, Nitta, Kiyama, Mori, & Mishina, 1995), frog (Pannese et al., 1998), newt (Beauchemin, Del Rio-Tsonis, Tsonis, Tremblay, & Savard, 1998), and chicken (Bell, Ensini, Gulisano, & Lumsden, 2001), among which *Emx2* has been suggested to function as a regional patterning factor. In comparisons between zebrafish and human, more than 90% of the amino acid residues of *Emx2* are identical (Noonan et al., 2001). Outside of the homeobox region, the conservation of *Emx2* sequences is strong. The alignment of nucleotides in the 3' UTR region of *Emx2* also suggests significant evolutionary conservation across vertebrates (Bell et al., 2001; Noonan et al., 2001). Therefore, based on sequence homologies, expression patterns, and defects in mutants across species suggest that Emx2 has a conserved role in brain development.

3. *Emx2* in urogenital system development

The *Emx2* knockout mutants die soon after birth, due to complete loss of the urogenital system. *Emx2* can be detected in the presumptive nephrogenic cord as early as E8.5. From E10.5 to E16.5, *Emx2* is expressed in the ureteric bud, epithelialized mesenchyme cells, and cortical region of the kidney (Miyamoto et al., 1997). How does the loss of *Emx2* affect kidney and ureters formation? During development, the kidney is formed by the reciprocal induction of mesenchyme and epithelium. In metanephrogenesis, the ureteric buds from the caudal region of nephric duct (Wolffian duct) invade into mesenchyme and induce mesenchyme to epithelial transition for nephron differentiation. In the absence of *Emx2,* the ureteric bud is not able to invade the mesenchyme for nephrogenesis. The failure of reciprocal induction of mesenchyme to epithelium leads to the absence of kidneys during embryonic development (Miyamoto et al., 1997).

As a part of the urogenital system, the gonad is formed through the mediodorsal migration of thickened embryonic coelomic epithelium to the mesenchyme compartment. The epithelium-to-mesenchyme transition is important for gonad formation. Failure of this transition causes the loss of gonads in the *Emx2* knockout mice (Kusaka et al., 2010). The expression of *Emx2* in the primodium promotes the proliferation and migration via the suppression of Egfr (Epidermal growth factor receptor), which normally enhances the tight junction assembly and inhibits the epithelium transition and migration (Kusaka et al., 2010; Miyamoto et al., 1997). These results suggest a potential role of *Emx2* in the epithelium-to-mesenchyme transition, which may involve polarity proteins such as the aPKC.

In addition to the mouse, mutations of *EMX2* in humans have recently been reported to be related to disorders of sex development. Direct sequencing of an infertile boy and a woman in case studies have revealed the correlation of *EMX2* mutation with the disorder of uterine development (Liu et al., 2015; Piard et al., 2014; Taylor, 2015).

4. *Emx2* in the inner ear

The expression of *Emx2* in the inner ear has been identified in both Xenopus (Pannese et al., 1998) and mouse (Cecchi, 2002), the conservation of which indicates the significance of *Emx2* in the inner ear development. In the mouse inner ear, *Emx2* expression was reported to be evident around E12.5 in the lateral region of the cochlear epithelium and the roof of the cochlear duct, maculae, endolymphatic duct, but not the cristae and endolymphatic sac (Holley et al., 2010). These expression patterns are consistent throughout embryonic development.

The investigation into the role of *Emx2* in the ear development began with hearing defects reported in the heterozygous *pardon (Pdo)* mice, which harbor a point mutation in the *Emx2* homeodomain locus, obtained from a large-scale N-ethyl-N-nitrosourea (ENU) mutagenesis screen (Fig. 1.16; (Rhodes et al., 2003)). The *Pdo* mice have a significant increase in compound action potential CAP thresholds in between 60-80dB. Gross dissection of middle ears from the heterozygous *Pdo* revealed defects in the ossicular chain such that the joints between incus and malleus are malformed. The phenotypes in the middle ear account for the conducting hearing defects but the threshold shift in compound action potential suggest that there is additional sensorineural hearing loss. Increased number of outer HCs and inner HCs are observed in the heterozygous *Pdo*

cochlea, which supports the hypothesis of sensorineural hearing impairment. Similar phenotypes are also observed in the *Emx2*$^{+/-}$ inner ear (Fig. 1.16; (Pellegrini et al., 1996; Rhodes et al., 2003)).

In the *Emx2*$^{-/-}$ cochlea, the outer HC compartment is missing, with doubling of inner HCs in the organ of Corti (Holley et al., 2010). Increased number of inner HCs could be single, doublet, triplet, or even form a groups of four or five in the sensory epithelium. Supporting cells between the inner HCs were either reduced or missing. The doublet inner HCs retain their intracellular polarity but lose polarity in relationship to the body axis. In the maculae, HCs maintained their global and intrinsic polarities. However, the LPR is reportedly missing in the mutant maculae and all the HCs are pointing towards the lateral edge in the saccule and utricle. In addition, similar to the cochlear epithelium, maculae were reported to be about one third smaller in size compared to the wildtype. No phenotype was observed in any of the cristae in the null mutants (Holley et al., 2010). Based on these phenotypes and expressions pattern in the inner ear, and with its known functions in other systems, the role of *Emx2* in the inner ear was proposed to be an early regulator in cell proliferation and differentiation but not as a mediator of HC polarity (Holley et al., 2010).

Chapter 2: Transcription factor Emx2 controls stereocilia polarity of sensory hair cells

Manuscript in preparation.

All the experiments in this chapter are conducted by me under the guidance of Drs. Doris Wu and Katie Kindt

In the vertebrate inner ear, the asymmetric location of the stereociliary bundle on the apical surface of sensory hair cells (HCs) dictates the direction in which a given HC can be activated. Hence, each sensory organ of the inner ear displays a well-defined stereocilia pattern. Notably, vestibular maculae of vertebrates and neuromasts of zebrafish exhibit a line of polarity reversal (LPR), across which stereocilia are arranged in mirror images. Here, we show that this LPR is established by restricted expression of *Emx2* to only HCs exhibiting similar stereocilia polarity within these sensory organs. The lack of *Emx2* reverts stereocilia polarity in its region to the default state and thus abolishes the LPR. In contrast, ectopic expression of *Emx2* in HCs that do not normally express this gene causes stereocilia polarity reversal by approximately 180^{o}. Effector(s) of *Emx2* mediates this effect, in part, via heterotrimeric G-protein activities.

I. Introduction

The asymmetric location of cilia on the apical surface of epithelial cells is related to the function of the tissue. For example, abnormal positioning of the monocilium in the node and multicilia of ependymal cells lining the brain ventricles can lead to left-right asymmetry defects and hydrocephalus, respectively (H. Song et al., 2010; Tissir et al., 2010). Similarly, the asymmetrical location of stereociliary bundle on top of the inner ear HCs is also linked to the function of this organ (Shotwell et al., 1981). Each stereociliary bundle is comprised of specialized microvilli arranged in a staircase pattern that are tethered to a kinocilium (true cilium). Formation of the asymmetric stereociliary bundle begins with docking of the basal body to the center of the apical HC surface to form the kinocilium. The nascent kinocilium then moves from the center to the periphery where specialized microvilli are gradually built adjacent to the kinocilium in a staircase pattern (X. Lu & Sipe, 2016; Tilney et al., 1992). Deflection of the stereociliary bundle in response to sound or head movements towards its kinocilium leads to opening of the mechanotransduction channels located on the tip of stereocilia and HC depolarization, whereas bundle displacement in the opposite direction results in hyperpolarization (Fig. 1A; (Shotwell et al., 1981)).

Planar polarity of any tissue can be regulated by global, intercellular and intracellular signaling mechanisms. Global signaling dictates the overall pattern of the tissue according to the body axis or its surrounding tissues. Morphogens such as Wnt have been demonstrated to function in this context for establishing long-range directional planar polarity in the developing mouse limb bud and *Drosophila* wing (Gao et al., 2011; J. Wu et al., 2013). A well-established intercellular polarity signaling is the core planar

cell polarity (cPCP) pathway, named for its conserved function among species. This pathway is comprised of transmembrane proteins such as Van Gogh (Vangl), Frizzled (Fz), and Cadherin EGF LAG seven-pass G-type receptors (Celsr) as well as cytoplasmic proteins such as Dishevelled (Dvl) and Prickle (Pk) (Goodrich & Strutt, 2011; Wallingford, 2012). All but Celsr are asymmetrically distributed at cell junctions to coordinate polarity among adjacent cells. How do individual cells interpret these global and intercellular polarity signals and undergo a specific plane of cell division or erect an organelle/appendage asymmetrically on the apical surface are not always clear (Devenport, 2016). Genetic studies in *Drosophila* have identified a group of cPCP effector genes such as *inturned*, *fritz* and *fuzzy*, which encode proteins that function downstream of the cPCP pathway in a cell autonomous fashion (Wong & Adler, 1993).

The orderly array of the four rows of stereocilia in the organ of Corti (oC), the sensory organ for sound detection, is regulated by both intercellular (cPCP) and intracellular polarity signaling (Goodrich & Strutt, 2011; X. Lu & Sipe, 2016). Mutations of the cPCP components such as Vangl2 and Dvl, affect the coordinated alignment of stereocilia among HCs but not the peripheral positioning of stereociliary bundle within a given HC (Montcouquiol et al., 2003; J. Wang et al., 2006; J. Wang et al., 2005). By contrast, many known intracellular components such as Par/Insc/LGN/Gαi complex required for mediating spindle orientation during mitosis (Morin & Bellaiche, 2011), intraflagella transport proteins required for ciliogenesis, and Rho GTPase for regulating cytoskeletal structures, are all important for establishing the polarized stereociliary bundle on the apical HC surface (X. Lu & Sipe, 2016). Presumably, the Par/Insc/LGN/Gαi complex, tethered to the cell cortex by Par and Gαi, binds

microtubule-associated proteins such as NuMA. Then, these proteins pull the basal body/nascent kinocilium to the cell periphery via the attached-microtubule, in a manner similar to pulling the centrioles during mitosis (Ezan et al., 2013; X. Lu & Sipe, 2016; Tarchini et al., 2013). In humans, mutations of LGN (also known as GPSM2) cause syndromic and non-syndromic hearing loss (Doherty et al., 2012; Yariz et al., 2012). How global and intercellular polarity cues coordinate with intracellular machinery to form the orderly stereocilia alignment is not well understood.

Other sensory organs of the inner ear also exhibit a well-defined polarity pattern. Notably, the maculae of the utricle and saccule are divided by the LPR into two regions of opposite stereocilia polarity. In the utricle, stereocilia face each other across the LPR whereas they point away from each other in the saccule (Fig. 2.1A). Similar mirror images of stereocilia polarity and functionality as the utricle are observed in neuromasts of the lateral line in zebrafish (Lopez-Schier et al., 2004). Previous studies suggest that cPCP complex is not involved in establishing the LPR. First, distribution of cPCP components such as Prickle-like 2 (PK2) and Vangl2 are not reversed across the LPR in maculae as predicted by the HC polarity (Deans et al., 2007; Jones et al., 2014). Furthermore, although stereocilia are misoriented in *Vangl* mutant maculae, the LPR does not appear to be obliterated (Montcouquiol et al., 2006; Yin, Copley, Goodrich, & Deans, 2012). However, it was reported that LPR failed to form in knockout maculae of *Emx2,* which encodes a homeobox-containing transcription factor (Holley et al., 2010). The unidirectional polarity defect was attributed to an imbalance between proliferation and differentiation of sensory precursors rather than defects in stereocilia polarity. Here, we show that expression of *Emx2* in sensory HCs is sufficient to reverse the "default"

stereocilia polarity by approximately 180°. The restricted expression of *Emx2* in maculae and neuromast defines the LPR.

II. Material and methods

A. Mouse strains

The $Rosa^{Emx2\text{-}GFP}$ (designated $Rosa^{Emx2}$) mouse strain was generated by knocking in the cassette, *attb-pCA* promoter-*lox-stop-lox-Emx2-T2A-Gfp-WPRE-polyA-attb,* to the Rosa locus using integrase technology (conducted by Applied Stem Cell) (Tasic et al., 2011). One founder with the correct insertion, identified based on PCR analyses, was propagated and maintained in the FVB background. Primers used for genotyping offspring are as follow: PR425 (GGTGATAGGTGGCAAGTGGTATTC) and pCA-R2 (GGCTAT GAACTAATGACCCCGT) for the $Rosa^{Emx2\text{-}GFP}$ allele, and R10 (CTCTGCTGCCTCCTGGCTTCT) and R11 (CGAGGCGGATACAAGCAATA) for the wildtype allele with expected fragment sizes of 369 and 311 base pairs, respectively.

$Emx2^{+/-}$ mice were provided by Peter Gruss at the Max-Planck Institute (Pellegrini et al., 1996) and maintained in a mixed C57BL/6J and CD1 background. $Emx2^{Cre}$ mice were obtained from Shinichi Aizawa at RIKEN Center for Developmental Biology and maintained in C57BL/6J background (Kimura et al., 2005). $Gfi1^{Cre}$ knock-in mice were obtained from Lin Gan at University of Rochester (H. Yang et al., 2010), $Sox2^{CreER}$ mice from Konrad Hochedlinger at Harvard University (Arnold et al., 2011), and the $Foxg1^{Cre}$ mice from Susan McConnell at Stanford University (Hebert & McConnell, 2000). $Gfi1^{Cre}$ and $Sox2^{CreER}$ strains were maintained in a CD-1 background, while $Foxg1^{Cre}$ strain was maintained in a mixed background of C57BL/6J and Swiss Webster.

Rosa26R^{tdTomato} (designated *Rosa*^{tdT}, JAX #007914, (Madisen et al., 2010)) and *Rosa26R*$^{mtdTomato/mGfp}$ (designated *Rosa*$^{mT/mG}$, JAX #007506, (Muzumdar, Tasic, Miyamichi, Li, & Luo, 2007)) were purchased from Jackson laboratory and maintained in a C57BL/6J background. All animal experiments were conducted under approved NIH animal protocols and according to NIH animal user guidelines (protocol # 1212-14).

B. Zebrafish strains

Zebrafish were maintained under standard conditions. All transgenic fish were maintained in a TAB5 wildtype background (S. Burgess, NIH). The transgenic line, *Tgmyo6b:emx2-p2A-nls-mCherry*, designated as *m6b:emx2-mCherry*, was generated using Gateway cloning Technology. First, a middle entry clone, pME-*emx2*, was constructed using a zebrafish *emx2* cDNA clone (IMAGE: 7403786) using PCR primers encoding attB sites: attB1 *emx2* forward primer (GGGGACAAGTTTGTACAAAAAAGCAGGCTGCCACCATG TTTCAACCCACACCGAAGAGGTG) and attB2 *emx2* reverse primer (GGGGCACTTTGTACAAGAAAGCTGGGTGATCGTCTGAGGTGACGTCAATTTC CTC). Then, the *myosin6b:emx2-p2A-nls-mCherry* plasmid was constructed using a 5' entry clone containing the HC-specific promoter of *myosin6b* (Obholzer et al., 2008), the middle entry clone *pME-emx2*, a 3' entry clone encoding *p2A*-nuclear localized *mCherry* (*p3E-p2A-nls-mCherry,* gift from Kristen Kwan at the University of Utah), and a destination vector containing the transgensis marker *pcmcl2-gfp* (tol2kit #395, (Kwan et al., 2007)). Larvae injected with this plasmid at one-cell stage were selected based on GFP signal within the heart and raised to adulthood. These founders were bred to

wildtype or to the previously described transgenic line, *Tgmyo6b: βactin(actb1)-EGFP*^{vo8}, designated as *m6b:βactin-EGFP* fish (Kindt, Finch, & Nicolson, 2012) for stereocilia polarity analyses.

Knockout *emx2* zebrafish were generated using CRISPR/Cas9 technology as described (Varshney et al., 2015). Two target sites on Exon1 of *emx2* were chosen for generating guide RNA: GGTAAAACACCTCTTCGGTGTGG and GGCTTTCACTCCAGCGGCAGGGG (Fig. S6A). Genotyping of injected larvae and F1 larvae was conducted by PCR using the primers emx2-fPCR-Fwd (TCACTTAAACTGGGGAATCTTGA) and emx2-fPCR-Rev (GGAGGAGGTACTGAATGGACTG), followed by subcloning and sequencing of the PCR fragments. F1 generated fish were analyzed for stereocilia polarity between 3 to 5 days post fertilization (dpf).

C. In situ hybridization

Section and whole mount in situ hybridization of utricle and saccule were performed as described previously (Morsli et al., 1998). In situ probes for *Emx2* (Simeone et al., 1992), *β-tectorin* (Rau, Legan, & Richardson, 1999), and *Lfng* (Morsli et al., 1998) were prepared as described.

D. Whole mount immunostaining

In general, E18.5 mouse embryos were harvested and fixed with 4% paraformaldehyde in PBS at 4°C overnight. For anti-Pk2 and anti-Vangl2 staining, hemi-sectioned embryo heads were fixed for 30 min at 4°C. After fixation, samples were washed with PBS and

various inner ear sensory organs were dissected, blocked with PBS containing 0.2% Triton-X and 4% donkey serum for 30 minutes before incubating with primary antibodies diluted in blocking solution overnight at 4°C. Then, samples were washed extensively with PBS before incubating with secondary antibodies at 1:250 dilutions in blocking solution for 2 hours at room temperature. Samples were mounted with ProLong Gold Antifade (Invitrogen) after extensive washing with PBS and imaged with a Zeiss LSM780 confocal microscope.

For staining zebrafish larvae, 3-5 dpf embryos were fixed with 4% paraformaldehyde in PBS for 3.5h at 4°C. Post-fixed larvae were rinsed with PBS and treated with pre-chilled acetone for 3-5 minutes at -20°C. Then, larvae were incubated with a blocking solution (2% goat serum, 1% BSA in PBS solution for 2 hours at room temperature), followed by incubation with primary antibodies diluted in PBS with 1% bovine serum albumin (BSA) at 4°C overnight. The next day, larvae were washed 4 times with PBS for 5 minutes each before incubating with secondary antibodies at 1:250 dilutions in blocking solution for 2 hours at room temperature. Then, larvae were washed and mounted with Antifade and imaged with a Zeiss LSM780 confocal microscope.

Primary antibodies used in this study are listed as follow: mouse anti-βII-spectrin (1:500; BD Bioscience, 612562), rabbit anti-Emx2 (1:250; Trans Genic, KO609), rabbit anti-Gαi (1: 1,000; provided by B. Nurnberg (Gohla et al., 2007) (Ezan et al., 2013), goat anti-oncomodulin (1:250; Santa Cruz, sc-7446), rabbit anti-Pard6 (1:250; Santa Cruz, sc-67393), mouse anti-parvalbumin (1:5,000; Millipore, MAB1572), rabbit anti-Pk2 (1:250; (Deans et al., 2007)) and goat anti-Vangl2 (1:250; Santa Cruz, sc-46561). In addition, two rabbit polyclonal antibodies, anti-Pk2 and anti-Emx2 were generated for this study

(Thermo Fisher) using the synthetic peptide of Pk2 as described (Deans et al., 2007)) and the full-length mouse Emx2 protein, respectively. Both antibodies were affinity-purified and used at a 1:1000 dilution and show immunostaining patterns indistinguishable from those of the anti-Pk2 and anti-Emx2 described above. Fluorescence-labeled phalloidin (1:50; Life Technologies, #F432) was used to visualize actin in the stereocilia bundle on top of sensory HCs.

Secondary antibodies that were used in these studies are listed as follow: Alexa Fluor® 405 Donkey anti rabbit IgG (Abcam, ab175651), Alexa Fluor® 405 Donkey anti mouse IgG (Abcam, ab175658), Alexa Fluor® 405 Donkey anti goat IgG (Abcam, ab175664), Alexa Fluor® 488/568/647 Donkey Anti-Rabbit IgG (Life Technologies; A-21207/A-10042/A-31573), Alexa Fluor® 488/568/647 Donkey Anti-Rabbit IgG (Life Technologies; A-21202/A-10037/A-31571), Alexa Fluor® 488/568/647 Donkey Anti-Rabbit IgG (Life Technologies; A-11055/A-11057/A-21447), Alexa Fluor® 647 Goat Anti-Mouse IgG (Life Technologies; A-21235), and Alexa Fluo® 568 Goat Anti-Rabbit IgG (Life Technologies; A-11079).

E. Tamoxifen administration

A stock solution of 30 mg tamoxifen (Sigma Aldrich, T5648) in 1 ml of corn oil was prepared. To avoid premature abortion of fetuses due to tamoxifen, 0.2 mg β-estradiol (20 mg/ml of ethanol; Sigma Aldrich, E8875) was added per ml of tamoxifen stock solution. On designated gestation days at noon, pregnant females were gavaged with the tamoxifen containing β-estradiol stock solution at 1 mg/10 g body weight. The morning of a found plug was considered as embryonic day 0.5.

F. EdU administration and cell cycle exit analysis

Pregnant mice were injected intraperitonealy with 5-ethynyl-2'-deoxyuridine (EdU; 1mg/ml solution; Life Technologies) three times (10 am, 12 pm and 2 pm) on a given day between embryonic day (E) 11.5 and E16.5 at an amount of 10 mg EdU/g of body weight, and all embryos were harvested and fixed with 4% paraformaldehyde at E18.5 (Fig. 1A). EdU-labeled cells were detected with a Click-iT reaction ((Bok, Zenczak, Hwang, & Wu, 2013); Life Technologies). Processed utricles were then flat-mounted and imaged using LSM780 confocal microscopy.

Under this injection regiment, HC precursors that underwent terminal mitosis soon after EdU incorporation should be strongly labeled, whereas precursors that have already exited from the cell cycle at the time of EdU delivery should not be labeled. HC precursors that underwent several rounds of cell division after EdU incorporation should have weak or no EdU labeling in the nucleus. Since weak EdU labeling can also be a result of HC precursors that incorporated EdU at the end of S phase of the last cell cycle, we scored all Myosin VIIa-positive HCs that have robust or distinct EdU labeling in the nuclei (Fig. S3I). For quantification of EdU-labeled HCs, the utricle was divided into three regions: striola, lateral and medial extrastriolar regions (LES and MES). Oncomodulin-positive region was marked as striola. The separation between LES and MES was defined by drawing a straight line linking the two ends of oncomodulin-positive striolar region to the edge of the utricle as shown in Figure S3H. Approximately 300, 450, and 500 HCs were counted in the striola, LES and MES of each utricle, respectively.

G. Quantification and statistical analyses

For quantification of HC density and surface area in the utricle, a straight A-P line between the two widest points of a given utricle along the anterior-posterior axis was drawn on a stitched confocal image taken at 40x magnification. Two lines perpendicular to the A-P line, marking the middle-third region were drawn and this region was sub-divided into 4 equal parts marked as 1, 2, 3, and 4 (Fig. 3O). Within regions 1 and 3, total number of HCs per 0.01 mm^2 and apical surface area of HCs were scored as representatives for the lateral and medial region of the utricle, respectively.

For stereocilia orientation analyses, regions 1 and 3 were further divided into three equal sections. Stereocilia angles were measured in the middle one-third, defined as regions L (lateral) and M (medial, Fig. 3P). Each region contains at least 50 HCs. The stereocilia angle of each HC was measured based on the position of the kinocilium on the apical surface by defining 0^o as the anterior apex of the utricle and the medial side as 90^o. Since LPR falls within region L of controls, we identified two different groups of HCs in controls (Fig. 3P).

In *Ptx* alone or *Emx2* and *Ptx* epistatic experiments of utricles, we defined HC polarity between 30-150^o as pointing medial (Fig. 6G, 7M-N, green) and between 210-330^o as pointing lateral (Fig. 6G, 7M-N, pink). Polarities of HCs that are outside of these ranges are considered misorientated (Fig. 6G, 7M, grey, and 7N, white). In order to avoid confusion in accessing polarity phenotypes of mutants, oncomodulin-positive HCs in control and Ptx specimens of region L were not included in the quantification of stereocilia angles shown in Figures 3P, 7M and N).

To quantify stereocilia orientation in the saccule, a line drawn along the notch of the saccule was defined as the anterior-posterior axis. Then a perpendicular dorsal-ventral line was drawn, which bisected the A-P line into two halves. We defined the dorsal end as 0^o and the posterior end as 90^o. Three 50 μm^2 squares in the anterior region of the IR and OR were selected and HC polarity within were scored (Fig. 6O). These regions were selected to avoid variation in polarity among HCs of controls and to specifically exclude the striola, which is bisected by the LPR in the saccule (Fig. 1B,H, 2K). At least 50 HCs were counted from each region. HC polarity in the IR and OR of a normal saccule is between 30-150 degrees (Fig. 6O,P, green) and 210-330 degrees (Fig. 6O,P, pink), respectively. The stereocilia polarity of HCs outside of these two ranges is considered misorientated (Fig. 6O, grey and 6P, white).

Statistical analyses of our quantification were performed using Prism 5 (GraphPad Software). HC density, apical surface area of HC, and stereocilia orientation were analyzed using an unpaired Student's t test or one-way ANOVA with the appropriate post hoc test.

III. Results

A. The border of *Emx2* expression domain coincides with the LPR in maculae

We investigated the reported stereocilia polarity defect in *Emx2*$^{-/-}$ maculae (Holley et al., 2010) by examining where Emx2 is normally expressed. Both in situ hybridization and immunostaining results indicate that Emx2 expression is restricted to the lateral region (lateral extrastriolar region, LES) of the utricle and inner region (IR) of the saccule (Fig. 2.1B,B', E,E', 2.2 A-F). The border of the Emx2 expression domain (Fig. 2.1B,B', E,E', green region bordered by the cyan line) appears to coincide with the reported LPR

at the lateral edge of the oncomodulin-positive striola in the utricle and at the center of saccule bisecting the striola (blue outline; (Desai et al., 2005; Li et al., 2008)). The coincidence of the Emx2 border (cyan line) with the LPR (yellow line) was confirmed by comparing Emx2 immunoreactivity to stereocilia polarity using anti-spectrin staining, which labels the cuticular plate except at the kinocilium location (Fig. 2.1C-G'; (Deans et al., 2007)).

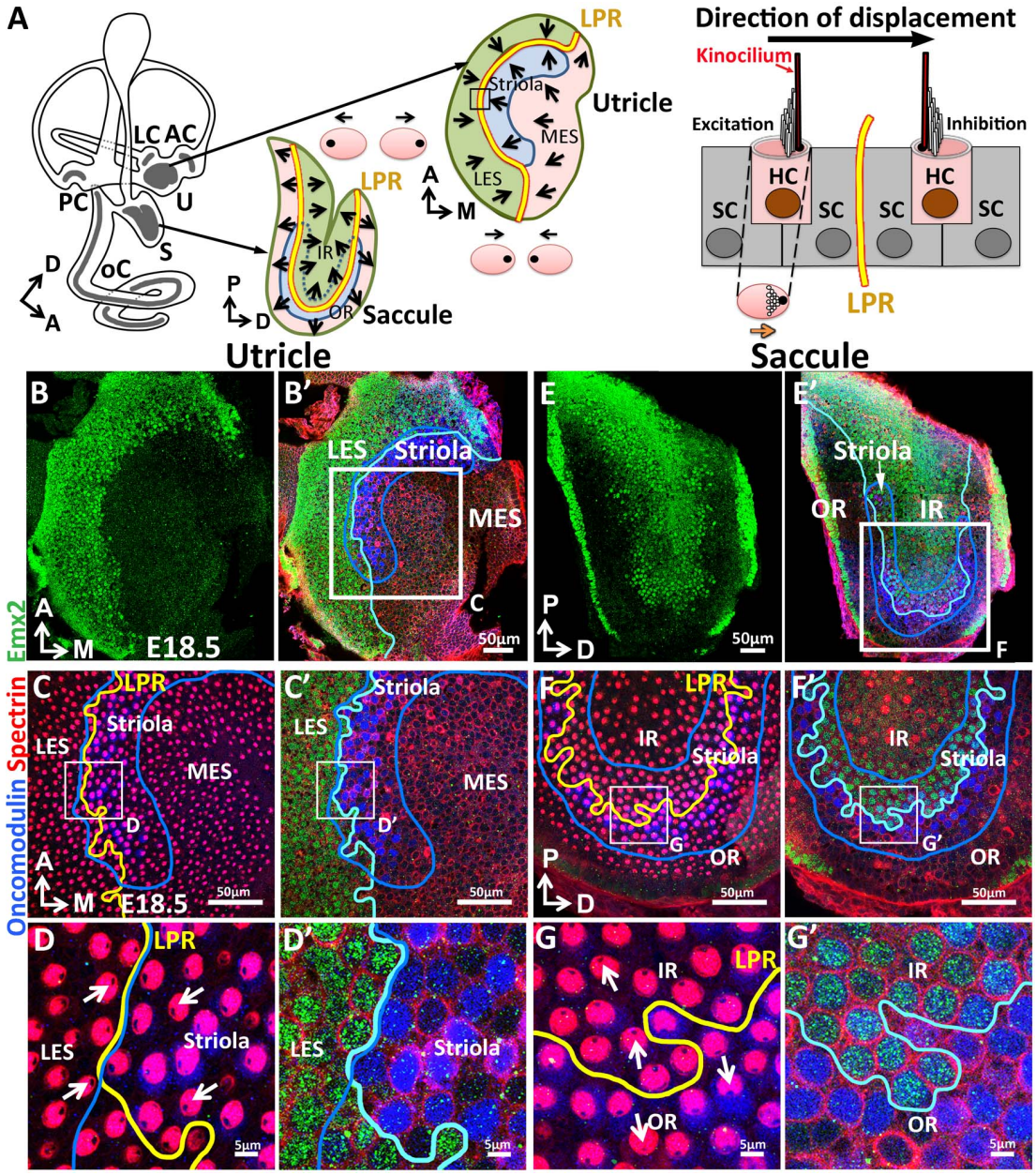

Figure 2.1. Regional expression of *Emx2* in the maculae. (A) Medial view of a left mouse inner ear with its six sensory organs (grey). Enlarged are the two maculae, utricle and saccule, showing their HC polarity, LPR (yellow line), striola (blue), and Emx2 positive regions. Displacement of the stereociliary bundle towards or away from the kinocilium results in depolarization and hyperpolarization of HC, respectively. (B-G') Utricle (B-D') and saccule (E-G') stained for anti-Emx2 (green), anti-spectrin (red) and anti-oncomodulin (blue) antibodies (n=6). Stereocilia polarity is determined by the location of the kinocilium, which is devoid of anti-spectrin staining (red). (C,D,F,G) and (C',D',F',G') are confocal images of the same HCs taken at the apical surface and nuclei level, respectively. (B,B',C',D') Anti-Emx2 (green) staining is located in the LES (lateral extrastriola) lateral to the oncomodulin-positive striola (blue) of the utricle. Stereocilia in LES face those in the striola and medial extra striola region (MES) of utricle (D). (E,E',F',G') Anti-Emx2 staining is restricted to the (IR) of saccule and the LPR bisects the striola. Stereocilia in the IR point away from those in the outer region (OR) of saccule (G). The border of the Emx2-positive domain (cyan line, C', D', F', G') coincides with LPR (yellow line, C,D,F,G) in both maculae. A, anterior; AC, LC, and PC, anterior, lateral and posterior crista; D, dorsal; IR, inner region; M, medial; oC, organ of Corti; OR, outer region; P, posterior; S, saccule; U, utricle.

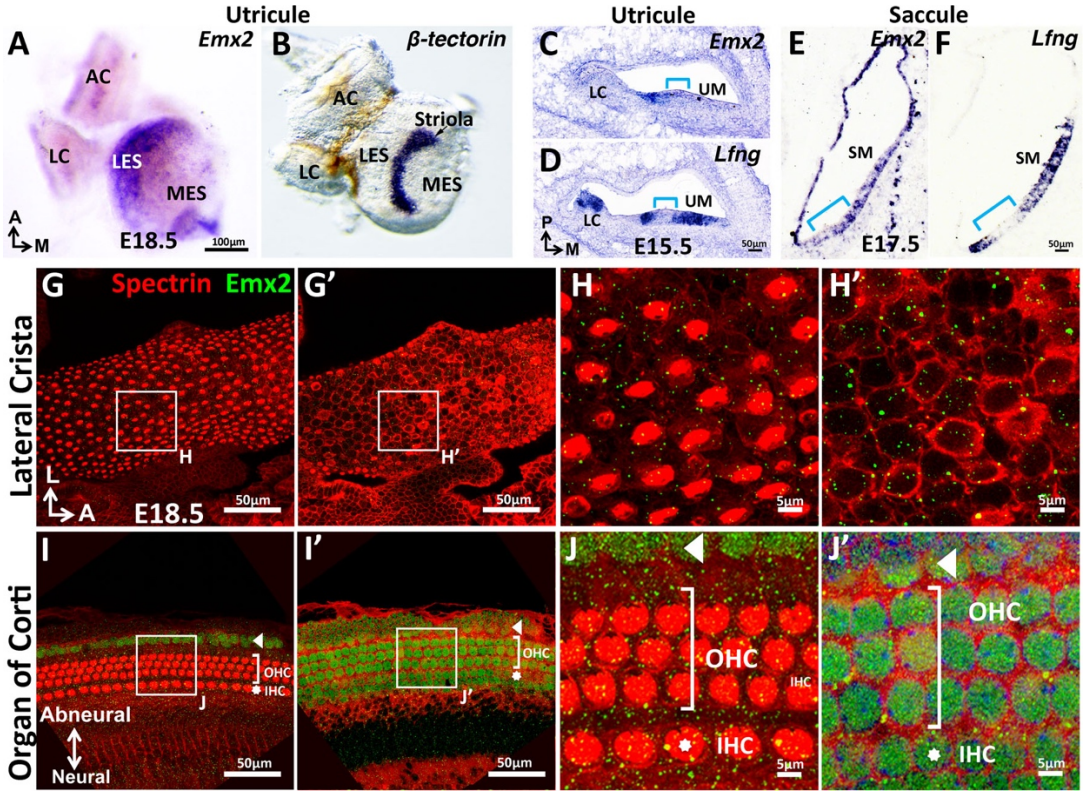

Figure 2.2. Expression of Emx2 in sensory organs of the mouse inner ear. (A-B) Whole mount in situ hybridization of the utricle showing *Emx2* hybridization domain (A) lateral to that of the *β*-tectorin-positive striola (B). Neither genes are expressed in the anterior and lateral cristae (AC & LC). (C-F) Section in situ hybridization of the utricle (C, D) and saccule (E, F) showing *Emx2* expression (C, E) within the *Lfng*-positive sensory epithelium (D, F). Bracket indicates the *Lfng*-negative striola. (G-J') No Emx2 immunoreactivity is detected in the lateral or in other cristae (G-H'). In contrast, anti-Emx2 immunoreactivities are broadly detected in the cochlea (I-J') including inner and outer HCs (IHC, asterisk; OHC, bracket), as well as the Hensen's and Claudius cell region (arrowhead, I-J').

B. No loss of region in *Emx2*$^{-/-}$ maculae

The restricted expression of *Emx2* to sensory regions that share the same HC polarity, and the unidirectional polarity reported in *Emx2* knockouts, suggest that this gene has a role in regional stereocilia patterning. However, since *Emx2* encodes a transcription factor, HC polarity phenotypes reported in *Emx2*$^{-/-}$ maculae could be caused by loss of

Emx2-positive domains. Indeed, the size of *Emx2*$^{-/-}$ utricles was reported to be smaller than wildtype (Holley et al., 2010). To address this question, we first investigated the lineage of *Emx2* in *Emx2*$^{Cre/+}$ strain (Kimura et al., 2005) by crossing it to *Cre* reporter mice, *Rosa*$^{tdT/+}$ or *Rosa*$^{mT/mG}$. The lineage domain of *Emx2* corresponded to its expression pattern, regionally restricted to the LES of utricle and IR of saccule (Fig. 2.3A-D,I-L). Within the *Emx2* domain of the utricle and saccule, stereocilia were oriented in the opposite direction from the rest of the sensory organ (Fig. 2.3B-C,J-K, green). The border of *Emx2* lineage domain (cyan line) in the maculae (Fig. 2.3A-C,I-K) also coincides with the LPR (yellow line) except in the posterior-ventral region of the saccule where the two lines diverge (double-headed arrow). We further determined that *Emx2*^{Cre}, in which *Cre* is inserted into Exon1 of the *Emx2* locus, generates a functional null allele since both *Emx2*$^{Cre/Cre}$ and *Emx2*$^{Cre/-}$ embryos exhibit brain and kidney phenotypes similar to *Emx2*$^{-/-}$ mutants (Fig. 2.4). Thus, this *Emx2*^{Cre} strain allowed us to investigate the *Emx2* lineage domain in an *Emx2* functional null mutant. The *Emx2* lineage domain remained in both *Emx2*$^{Cre/-}$*;Rosa*$^{tdT/+}$ maculae and its spatial relationship with the striola was maintained, whereas stereocilia within the domain were reversed (Fig. 2.3E-H, M-P, green), compared to controls (Fig. 2.1C,K, green). These results indicate that the unidirectional phenotype in *Emx2*$^{-/-}$ maculae is not caused by the loss of a domain and suggest that Emx2 has a role in establishing regional stereociliary pattern.

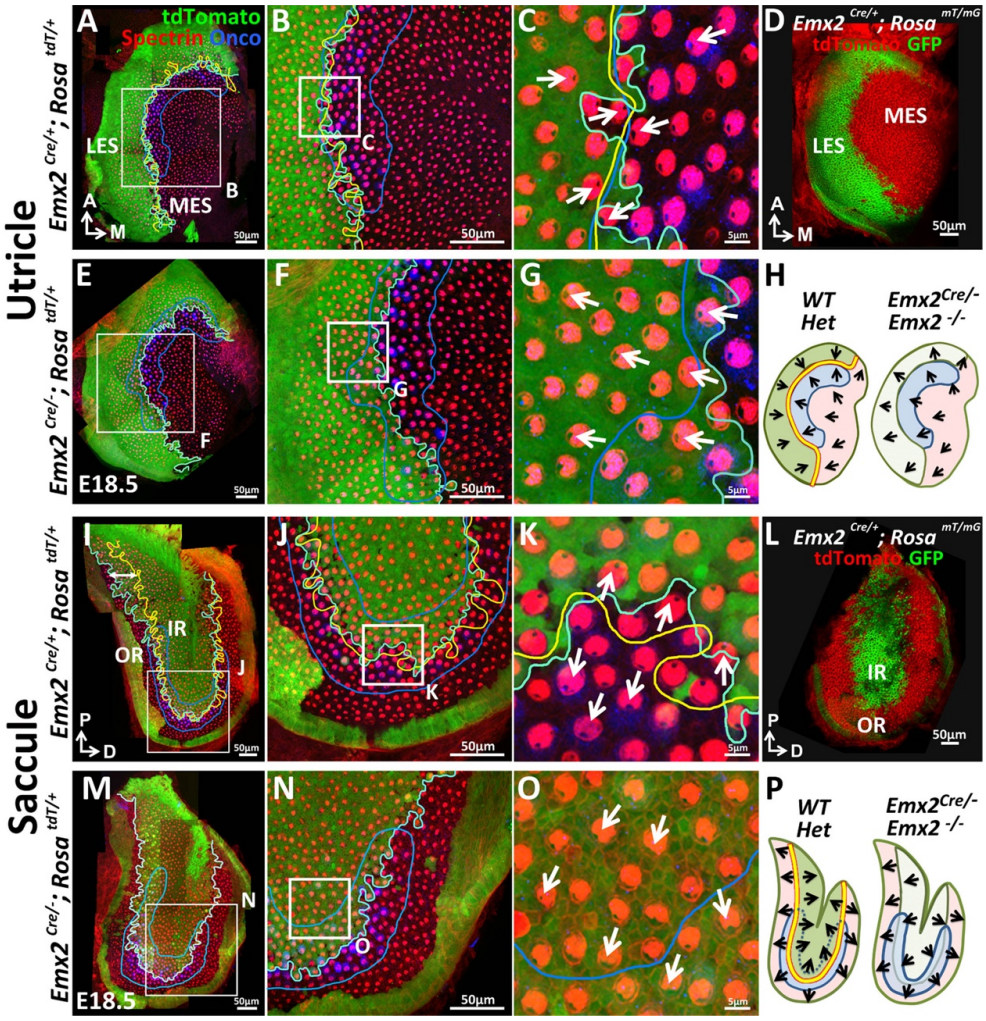

Figure 2.3 Emx2 lineage domain are present in *Emx2* functional null maculae. (A-C) In *Emx2*$^{cre/+}$;*Rosa*$^{tdT/+}$ utricles, the border of *Emx2* lineage domain (cyan line) coincides with LPR (yellow line), located at the lateral edge of oncomodulin-positive striola (blue outlined; n=5). HCs point toward each other (arrows) across the LPR. (D) Similar *Emx2* lineage domain (GFP) is observed using a different cre reporter, *Rosa*$^{mT/mG}$ strain. (E-G) *Emx2* lineage domain (green) remained in *Emx2*$^{cre/-}$;*Rosa*$^{tdT/+}$ utricles but stereocilia polarity in this region is reversed (G; n=5), compared to controls (C; n=5). (I-K) In *Emx2*$^{Cre/+}$;*Rosa*$^{tdT/+}$ control saccules, the border of *Emx2* lineage domain (cyan line) coincides well with the LPR except in the ventral-posterior region (I, double-headed arrow). Across the LPR, HCs are pointing away from each other (K, arrows). (L) Similar lineage domain (GFP) is observed using the cre reporter, *Rosa*$^{mT/mG}$ strain. (M-O) In *Emx2*$^{Cre/-}$;*Rosa*$^{tdT/+}$ mutant saccules, the border of the *Emx2* lineage domain (cyan line) remained located in the middle of the striolar region (blue outline) but the stereocilia within the lineage domain are reversed (O; n=5), relative to controls (green region in K). (H) and (P) Schematics of respective utricles and saccules showing relationships among the *Emx2* expression domain (green), stereocilia polarity pattern, LPR (yellow line) and striola (blue outline) in controls and *Emx2* mutants.

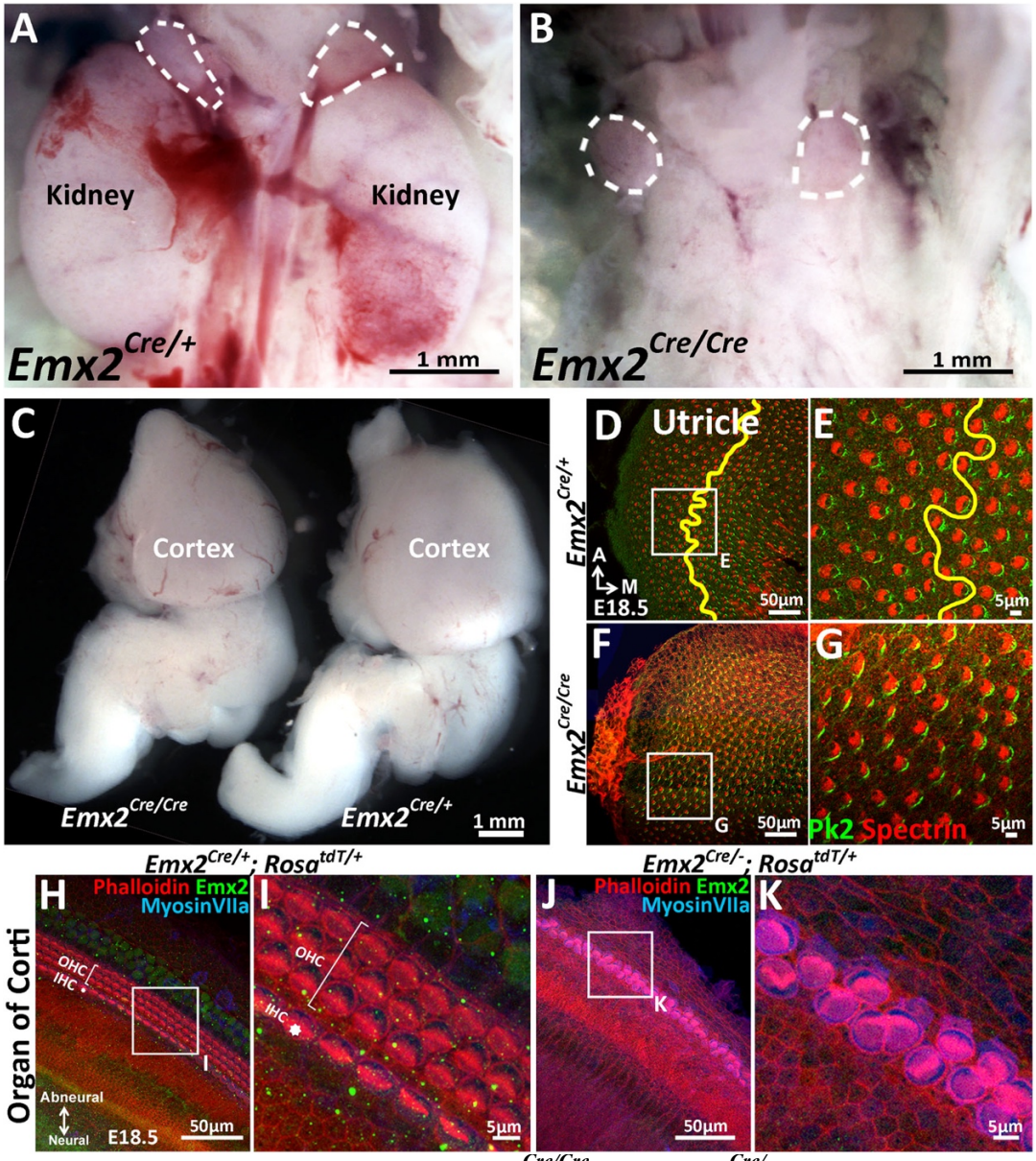

Figure 2.4. Mutant phenotypes of *Emx2*$^{Cre/Cre}$ and *Emx2*$^{Cre/-}$ embryos are similar to *Emx2* $^{-/-}$ mutants. (A-B) The kidneys below the adrenal glands (dotted lines) are absent in *Emx2*$^{Cre/Cre}$ (B) compared to *Emx2*$^{Cre/+}$ embryos (A). (C) The size of the cortex is smaller in *Emx2*$^{Cre/Cre}$, compared to *Emx2*$^{Cre/+}$ embryos. Both kidney and cortical phenotypes have been described in *Emx2* $^{-/-}$ mutants (Holley et al., 2010). (D-G) In contrast to controls (D, E), LPR (yellow line) is absent in *Emx2*$^{Cre/Cre}$ utricles (F, G) and stereocilia polarity defects are similar to those reported in *Emx2*$^{-/-}$ ears (Holley et al., 2010). The distribution of Prickle-like 2 (Pk2) immunostaining in *Emx2*$^{Cre/Cre}$ utricles is associated with the medial border of HCs (G), similar to control (E) and *Emx2*$^{-/-}$ utricles (Fig. 5D-E). (H-K) Compared to controls (H-I), outer HC are absent and two rows of inner HCs with aberrant stereocilia polarity are evident in *Emx2*$^{Cre/-}$*;Rosa*$^{tdT/+}$ cochlea (J-K), similar to the phenotypes reported in *Emx2* knockout mutants (Holley et al., 2010).

C. No obvious change in timing of terminal mitosis of HC precursors in *Emx2*$^{-/-}$ utricles

Since *Emx2* has been implicated in regulating symmetric and asymmetric cell divisions in the brain (R. Galli et al., 2002; Heins et al., 2001), stereocilia polarity defects in the *Emx2* mutants could be related to the timing of terminal mitosis. For example, sensory progenitors expressing Emx2 may remain in cell cycle longer and do not respond to polarity signal(s) that are instructing post-mitotic HCs in non-Emx2 regions. We addressed this possibility by comparing the timing of terminal mitosis of HCs between *Emx2* heterozyous and knockout utricles. A thymidine analog, EdU, was injected to pregnant dams between embryonic day (E) 11.5 to E16.5 and embryos were harvested at E18.5. Myosin VIIa-positive HCs with strong EdU labeling served as a proxy for the time of terminal mitosis. Although our results indicate HC precursors in the LES (where Emx2 is normally expressed) undergo terminal mitosis later than the rest of the maculae, we did not observe any obvious difference in this timing between controls and *Emx2*$^{-/-}$ utricles (Fig. 2.5). These results suggest that *Emx2* does not mediate stereocilia polarity by regulating the timing of terminal mitosis.

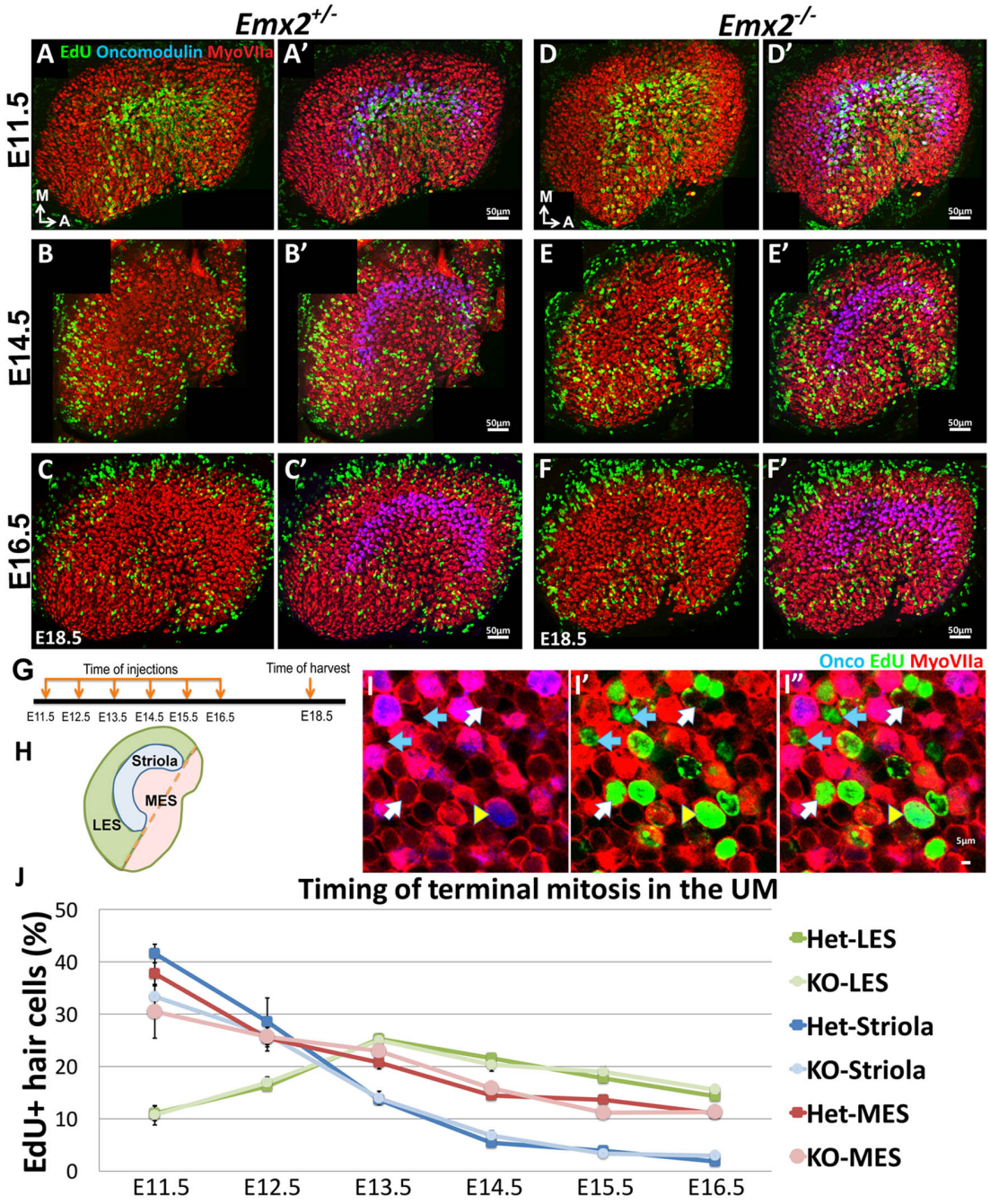

Figure 2.5. Regional differences in timing of cell cycle exit are maintained in the *Emx2* null utricle. (A-F) E18.5 *Emx2*$^{+/-}$ utricles injected with EdU at E11.5 (A-A'), E14.5 (B-B') or E16.5 (C-C') and harvested at E18.5 (G) were processed for anti-Myosin VIIa (HC marker), anti-oncomodulin (striolar marker), and incorporated EdU. Abundant labeling is observed in the striola when the utricle is exposed to EdU at E11.5 (A) and not at E14.5 (B) and E16.5 (C), whereas labeling in the MES is observed in all three ages but weakest at E16.5 (C). In contrast, EdU labeling is not apparent in the LES at E11.5 (A) but only at E14.5 and E16.5 (B, C). (D-F) In *Emx2*$^{-/-}$ utricles, the regional differences of

EdU labeling are maintained, compared to the controls. (H) The subdivision of an utricle into the oncomodulin-positive, striola (blue), LES (green) and MES (pink) is shown. The orange dotted line joining the two ends of the striola was used as an arbitrary division between the LES and MES. (I) Triple labeling of the utricle with anti-Myosin VIIa, anti-oncomodulin and EdU. HCs that are triple-labeled (yellow arrowhead), EdU-positive HCs (white arrow) and non HCs (blue arrow) are marked. (J) No significant difference between various regions of the *Emx2*$^{+/-}$ and *Emx2*$^{-/-}$ utricles in percentages of EdU-labeled HCs. Blue, green and pink lines represent the percentages of EdU-positive HCs in the striola, LES and MES, respectively. Highest percentages of EdU-positive HCs in the striola are detected at E11.5 for both heterozygous (dark lines) and mutant (light lines) utricles and this percentage decreases quickly after E13.5, whereas the peak of EdU labeling in the LES starts at E13.5. EdU-labeled HCs in the MES is relatively high between E11.5 and E13.5 and becomes lower after E14.5.

D. Ectopic *Emx2* inverts stereociliary bundle polarity

If Emx2 directly affects stereocilia polarity, one would predict ectopic expression of *Emx2* in naïve HCs should alter their polarity. Thus, we generated *Rosa*^{Emx2} mice, which allow spatial and temporal activation of *Emx2* depending on the presence of Cre. We first ectopically expressed *Emx2* in all prosensory domains of the inner ear by breeding *Sox2*^{CreER} to *Rosa*^{Emx2} mice and administered tamoxifen to pregnant dams at E12.5/E13.5 (Sox2-GOF early). Compared to stereocilia facing the LPR in control utricles (Fig. 2.6A-C), the LPR was absent in *Sox2*-GOF early mutants and all HCs in the entire utricle were uniformly facing the medial direction (Fig. 2.6D-F, O-Q). This ability of *Emx2* to invert stereocilia polarity is developmentally dependent. By delaying the tamoxifen administration to E15.5 and E16.5 (*Sox2*-GOF late), at which time many HC precursors have undergone terminal mitosis and started to differentiate (Fig. 2.5), only a partial polarity phenotype was observed in the medial utricle (Fig. 3G-I, P-Q, region M). These results suggest that once the kinocilium position is established, it no longer responds to

Emx2. Ectopic expression of *Emx2* during early prosensory development also resulted in increased apical HC surface area and reduced HC density, which may not be related to the stereocilia polarity phenotype (Fig. 2.6D-F,M-O). To better pinpoint the role of *Emx2* in stereocilia polarity, we overexpressed *Emx2* specifically in nascent HCs using the $Gfi1^{Cre}$ strain. In $Gfi1^{Cre/+}$;$Rosa^{Emx2/+}$ mutant utricles, all HCs in the utricle were uni-directionally pointing towards the medial edge (Fig. 2.6J-L,P-Q). The stereocilia reversal in the medial utricle is approximately 180° compared to controls (Fig. 2.11, compare region M between control and *Emx2*).

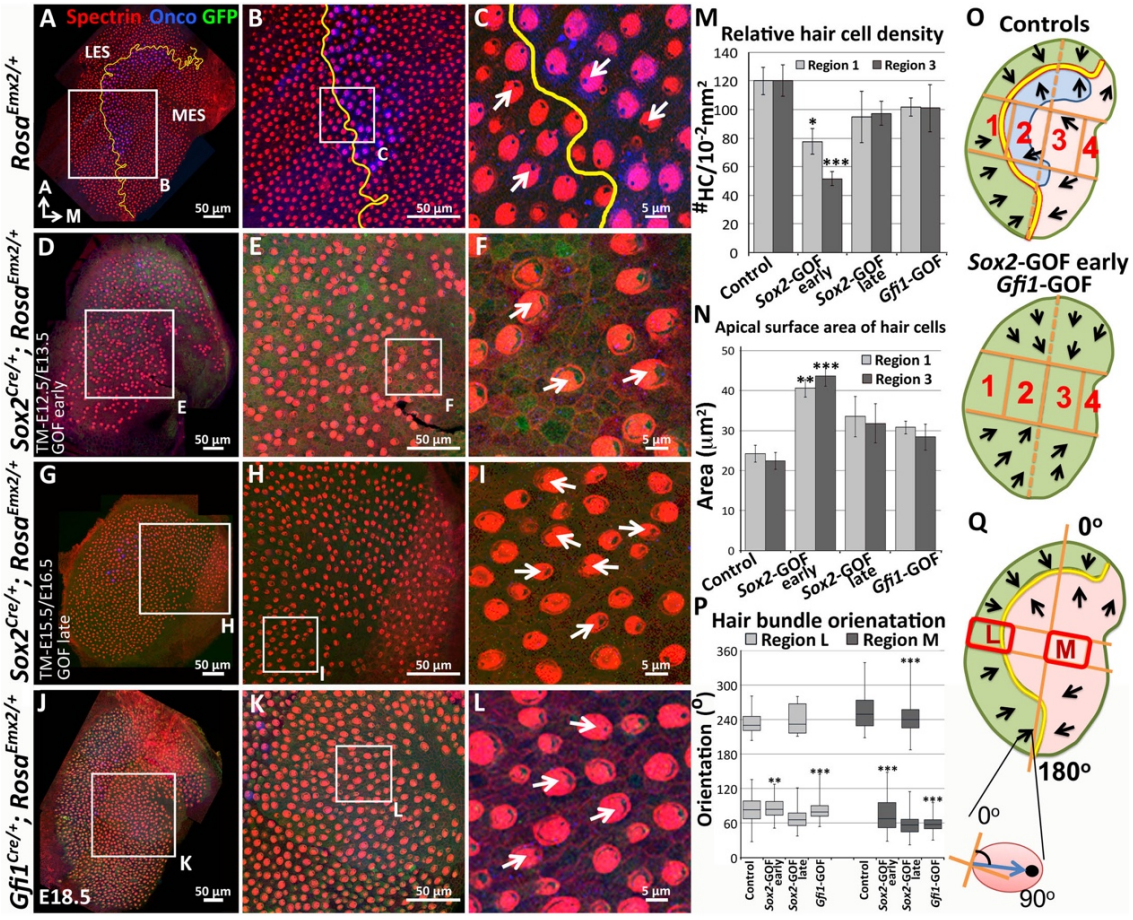

Figure 2.6. Ectopic *Emx2* inverts HC polarity in the utricle. Compared to controls (A-C, right of LPR), HC polarity (arrows) in the medial region of $Sox2^{CreER/+}$;$Rosa^{Emx2/+}$ (D-F, tamoxifen administered at E12.5 and E13.5, gain-of-function (GOF) early; n=3) and $Gfi1^{Cre/+}$;$Rosa^{Emx2/+}$ utricles (J-L) are reversed (n=7). (G-I) $Sox2^{CreER/+}$; $Rosa^{Emx2/+}$ utricles (tamoxifen administered at E15.5 and E16.5, GOF late) show a mixed phenotype of normal and reversed stereocilia polarities (white arrows, n=3). (M-N) Quantification of HC density (M) and surface area (N) in Regions 1 and 3 of utricles from various genotypes. Only utricles of *Sox2*-GOF early show a significant decrease in HC density and an increase in apical surface of HCs, compared to controls. Error bars represent SEM. *p<0.05; **p<0.01; ***p<0.001. (O) Schematic diagrams illustrating stereocilia polarity pattern in control and *Emx2* gain-of function (GOF) utricles. (P-Q) Box-plots of stereocilia polarity in regions L (LES) and M (MES) of utricles. Region L of controls includes the LPR and thus show HCs with both medial and lateral polarities but only medial-pointing stereocilia are present in all *Emx2* GOF utricles except *Sox2*-GOF late. Box represents 1 to 3 quartile. Line within box is the median and bar represents maximum and minimum number. ** p< 0.01, *** p< 0.001, compared to controls.

Similar findings were observed in the saccule: only the OR of the saccule where *Emx2* is not normally expressed showed a stereocilia reversal phenotype (Fig. 2.7C-D,O), compared to controls (Fig. 2.7A-B). Emx2 immunostaining was not detected in the cristae (Fig. 2.2G-H'; (Holley et al., 2010)), and likewise stereocilia polarity was reversed in $Gfi1^{Cre/+}$;$Rosa^{Emx2/+}$ cristae (Fig. 2.7H-J,O), compared to controls (Fig. 2.7E-G). In contrast, Emx2 is normally expressed in the cochlea including the oC (Fig. 2.2I-J'; (Holley et al., 2010)). As expected, no stereocilia polarity phenotype was observed in the mutant oC (Fig. 2.7K-O). Taken together, these results suggest that *Emx2* has a dominant, cell-autonomous effect in dictating stereocilia polarity pattern in the inner ear.

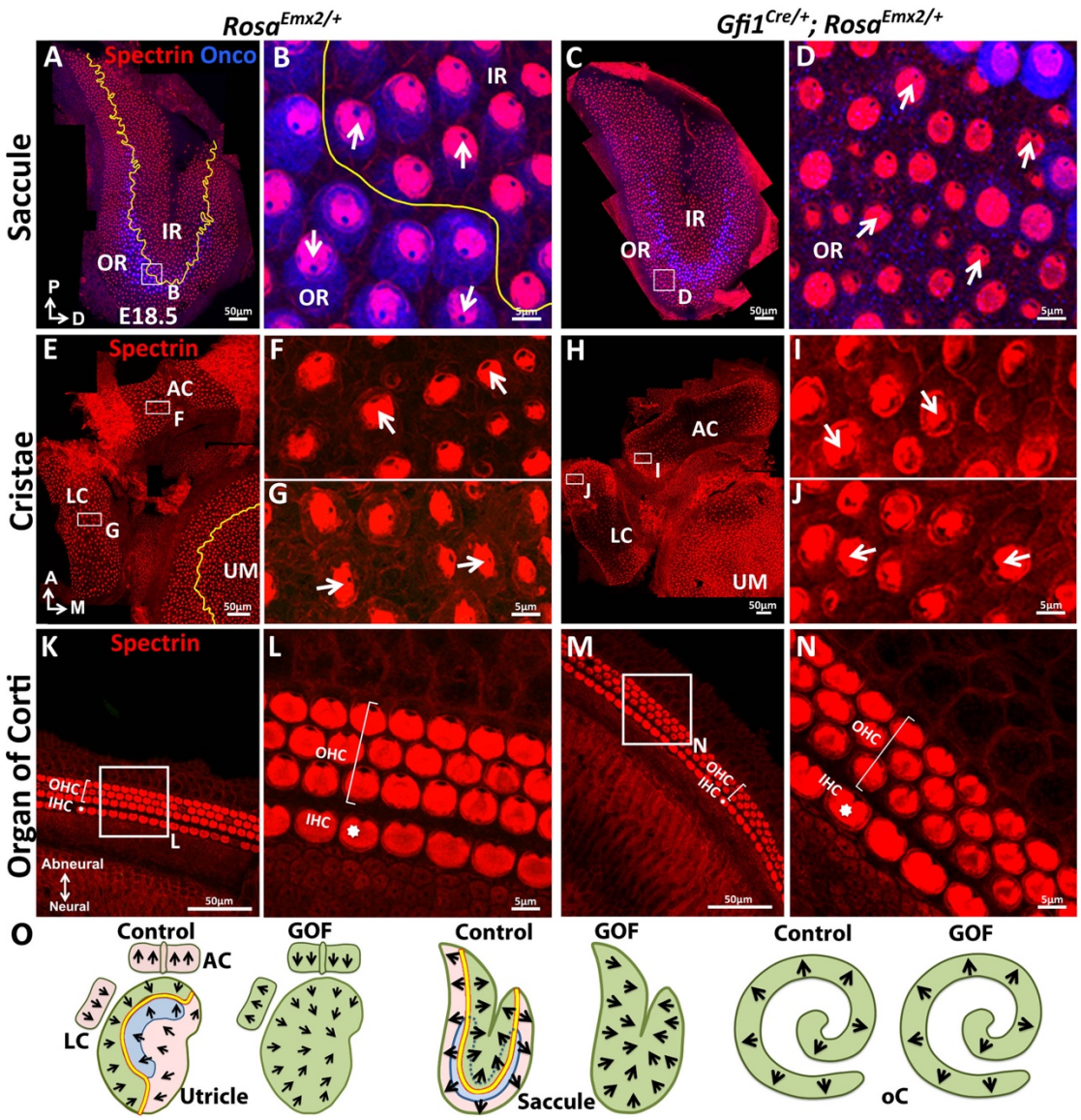

Figure 2.7. Ectopic *Emx2* inverts HC polarity in the saccule and cristae but not organ of Corti. (A-D) Saccule, (E-J) anterior and lateral cristae (AC and LC), and (K-N) oC of $Rosa^{Emx2/+}$ (A-B, E-G, K-L) and $Gfi1^{Cre/+};Rosa^{Emx2/+}$ (C-D, H-J, M-N) inner ears at E18.5 (n=7). In the $Gfi1^{Cre/+};Rosa^{Emx2/+}$ saccule, HC polarity in the OR (outer region) is reversed by approximately 180° (C-D), compared to controls (A-B). (E-J) In control cristae, stereocilia point toward the anterior direction in the AC (F) and medial direction in the LC (G), whereas these polarities are reversed in AC (I) and LC (J) of $Gfi1^{Cre/+};Rosa^{Emx2/+}$ ears, pointing toward posterior and lateral directions, respectively (H-J). (K-N) No difference in HC polarity is apparent between control (K-L) and $Gfi1^{Cre/+};Rosa^{Emx2/+}$ (M-N) cochlea. Inner HCs (IHC, asterisk); outer HCs (OHC, bracket). (O) Schematic diagrams illustrating stereocilia polarity pattern in control and *Emx2* GOF sensory organs of the inner ear.

E. Normal distribution of cPCP and intracellular polarity components in *Emx2* mutants

To investigate how downstream effector(s) of Emx2 mediates stereocilia orientation, we first compared distribution of some of the cPCP proteins such as Pk2 and Vangl2 between control and *Emx2* mutant utricles. We validated in control utricles that Pk2 immunoreactivities are concentrated on the medial side of HC and supporting cell border and this pattern is maintained across the LPR (Fig. 2.8A-C; (Deans et al., 2007)). This distribution pattern of Pk2 is similar in both loss and gain of *Emx2* function utricles (Fig. 2.8D-G), compared to controls (Fig. 2.8B-C). The distribution of Vangl2 in control utricles, though strongest between supporting cells, is not changed across the LPR similar to that of Pk2 (Fig. 2.9A-B; (Jones et al., 2014)). This expression pattern of Vangl2 is also maintained in the *Emx2* mutants (Fig. 2.7C-F). Together, these results suggest that distribution of cPCP components in the utricle are not altered by gain or loss of *Emx2* function.

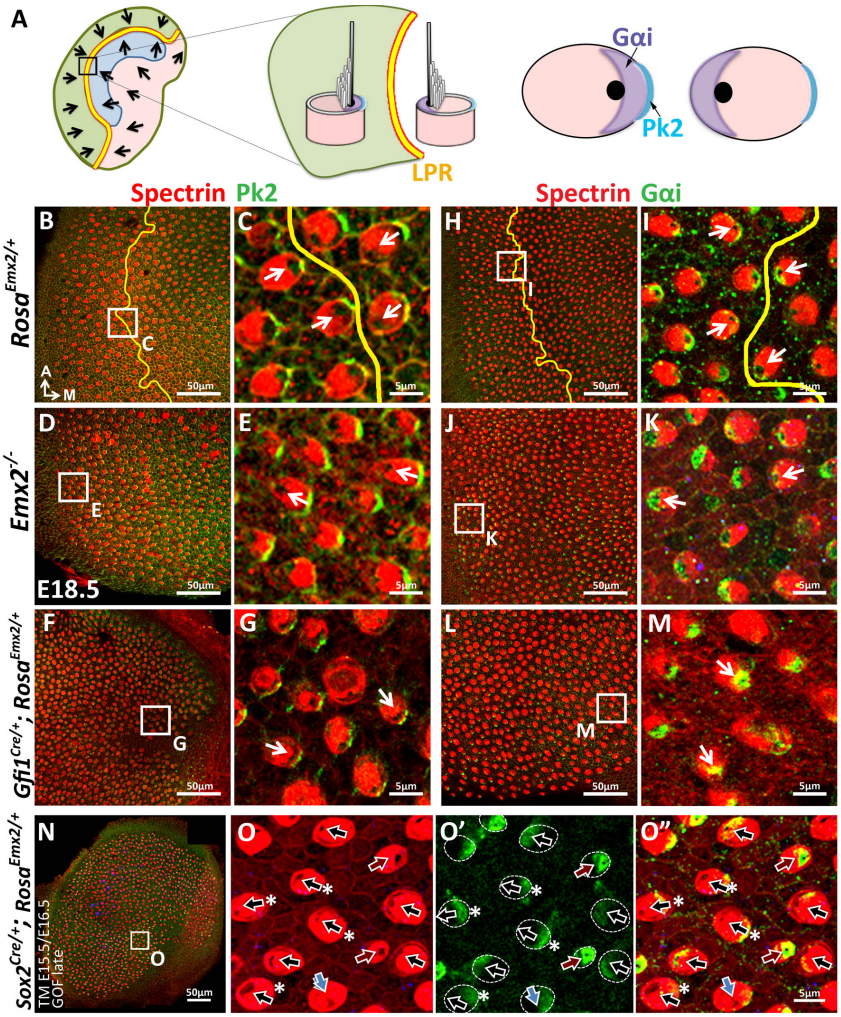

Figure 2.8. Distribution of PK2 and Gαi immunoreactivites are maintained in *Emx2* mutants. (A) Schematic diagram illustrating the distribution of an intercellular polarity protein, Pk2, and an intracellular polarity protein, Gαi, in HCs across the LPR of a control utricle. (B-C) In $Rosa^{Emx2+/-}$ control utricles, Pk2 staining (green) is concentrated on the medial side of HC and supporting cell border and such pattern is not changed across the LPR (n=15). (D-G) In the lateral region of $Emx2^{-/-}$ utricle (D-E, n=5) and medial region of $Gfi1^{Cre/+};Rosa^{Emx2/+}$ utricle (F-G, n=4), in which the stereocilia polarity is reversed compared to the respective left and right of LPR of controls (C), but Pk2 staining remained on the medial side (green). (H-I) In control utricles, Gαi immunostaining (green) is associated with the kinocilium. This relationship is consistent among all HCs of the utricle and the staining pattern of Gαi is reversed across the LPR (yellow line), following the kinocilium position (I, n=8). Similar relationship between Gαi and kinocilium position is observed in $Emx2^{-/-}$ (J-K, n=4) and $Gfi1^{Cre/+};Rosa^{Emx2/+}$ (L-M, n=5) utricles as controls. (N-O") $Sox2^{CreER/+};Rosa^{Emx2/+}$ utricles (tamoxifen administered at E15.5 and E16.5, GOF late) show mixed phenotypes of normal (black arrows), mis-oriented (blue arrows), and reversed (red arrows) kinocilia (n=3). Some HCs with normal polarity show abnormal Gαi distribution (asterisks).

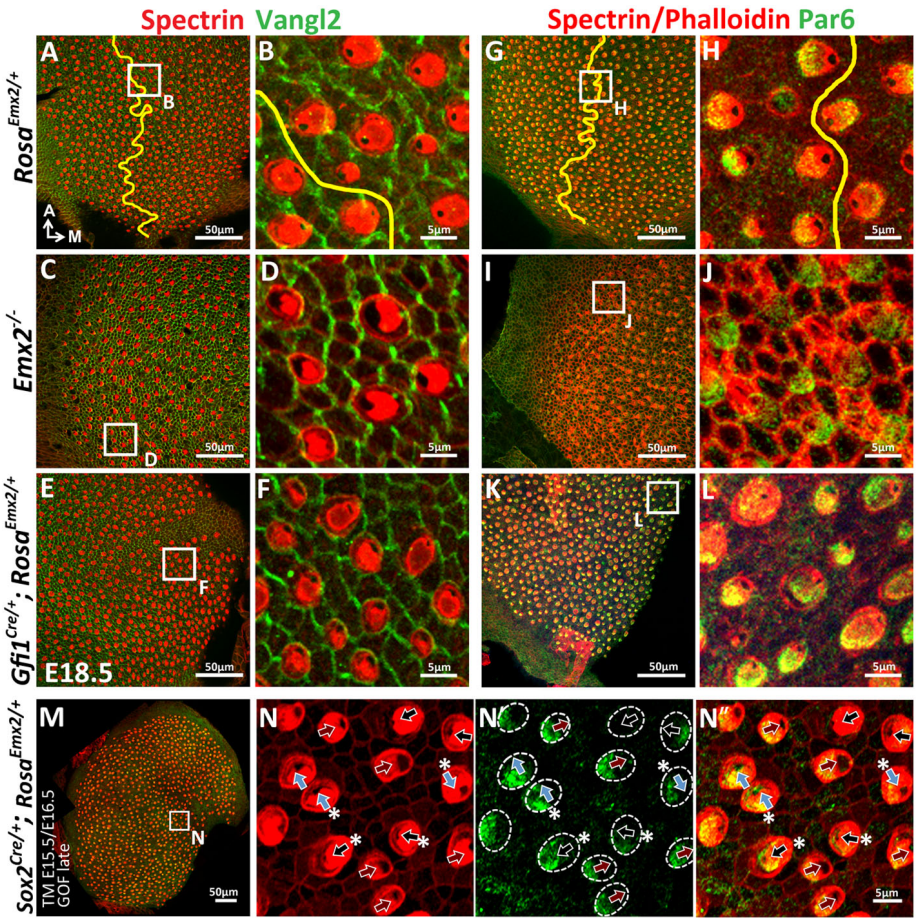

Figure 2.9. Distribution of Vangl2 and Par6 immunoreactivites in apical HCs are not changed in *Emx2* mutant utricles. (A-B) In *Emx2*$^{+/-}$ utricles, Vangl2 immunostaining (green) are restricted, stronger between adjacent supporting cells and weaker between HC and supporting cell junction. Staining pattern of Vangl2 is not changed across the LPR (Jones et al., 2014). (C-F) In the lateral region of *Emx2*$^{-/-}$ utricle (C-D) and medial region or *Gfi1*$^{Cre/+}$;*Rosa*$^{Emx2/+}$ utricle (E-F), in which the stereocilia polarity is reversed compared to controls (B), there is no obvious change in the distribution of Vangl2 immunostaining. (G-H) In control utricles, the distribution of Par6 (green) is in the apical HC region opposite to the kinocilium (H). This relationship among kinocilium and Par6 is consistent in all HCs and the staining pattern of Par6 is reversed across the LPR (yellow line), following the change in kinocilium position. Similar immunostaining pattern of Par6 in relationship to the kinocilium position is observed in *Emx2* $^{-/-}$ (I-J, n=3) and *Gfi1*$^{Cre/+}$;*Rosa*$^{Emx2/+}$ (K-L, n=3) utricles as controls. (M-N") Activating *Emx2* at a later age by administering tamoxifen at E15.5 and E16.5 causes mixed phenotypes in *Sox2*$^{CreER/+}$;*Rosa*$^{Emx2/+}$ utricles (GOF late): normal (black arrows), reversed (red arrows) or mis-oriented (blue arrows) kinocilia. In some HCs with normal stereocilia polarity, anti-Par6 distribution is no longer complementary to the kinocilium position (asterisks).

The intracellular complex, Par/Insc/LGN/Gαi, is required to guide the migration of kinocilium to its asymmetrical apical location of HCs (Ezan et al., 2013; Tarchini et al., 2013). This complex is distributed as a crescent-shape that is always associated with the kinocilium at the apical surface of HCs (Ezan et al., 2013; Tarchini et al., 2013). In contrast, distribution of one of the Par proteins, Par6, is complementary to that of Gαi and located opposite to the stereocilia. Thus, unlike the cPCP proteins, the distribution pattern of Gαi and Par6 are reversed across the LPR, in alignment with the kinocilium (Fig. 2.8H-I, 2.9G-H). These relationships among Gαi, Par6, and kinocilium are preserved in the loss and gain of *Emx2* function mutants (Fig. 2.8J-M, 2.9I-L). However, in the Sox2-GOF late utricles, in which the stereocilia reversal phenotype is only partially penetrant, some of the HCs with normally-positioned kinocilium loss their relationship with Gαi and Par6 (Fig. 2.8N-O", 2.9M-N", black arrows with asterisks). These results suggest that while delaying ectopic *Emx2* expression can no longer change the kinocilium position, it can still effectively alter the distribution of apical polarity proteins, Gαi and Par6, suggesting that effector of Emx2 may normally mediate its effects by altering the intracellular polarity complex.

F. Blocking Gαi partially rescues the stereocilia phenotype induced by ectopic *Emx2*

Blocking Gαi activities with Pertussis Toxin (Ptx) or knocking out one of the genes that encodes Gαi, *Gnai3,* can lead to misoriented or even reversed stereocilia polarity in cochlear HCs (Ezan et al., 2013; Tarchini et al., 2013). We tested whether ectopic expression of *Ptx* also affects stereocilia polarity in macular HCs by breeding $Rosa^{Ptx/+}$ to $Foxg1^{Cre/+}$, in which cre is activated at the otic placode stage. Compared to controls (Fig.

2.10A-C',I-K'), stereocilia mis-orientation (blue arrows) and reversal (red arrows) were observed in *Emx2*-positive, LES of utricles (15% in Fig. 2.10D-E',G-H) and IR of saccules (46% in Fig. 2.10L-M',O-P) of $Foxg1^{Cre/+}$;$Rosa^{Ptx/+}$ ears. No apparent phenotype was observed in the medial utricle or OR of saccule where *Emx2* is absent (Fig. 2.10F-F',G-H,N-N',O-P), comparable to controls (Fig. 2.10C-C,K-K). Despite the regional-specific stereocilia phenotype, diffused or reduced Gαi immunostaining was broadly evident, suggesting that Ptx is affecting the entire mutant maculae (Fig. 2.10E',F',M',N', arrowheads). These results indicate that whereas Ptx seems to affect Gαi accumulation in the entire maculae, it is preferentially affecting kinocilium position within the *Emx2*-positive regions. Additionally, some of the kinocilia within the *Emx2*-positive domain, regardless of whether their position is normal or reversed, are no longer associated with Gαi (Fig. 2.10E-E',M-M', asterisks).

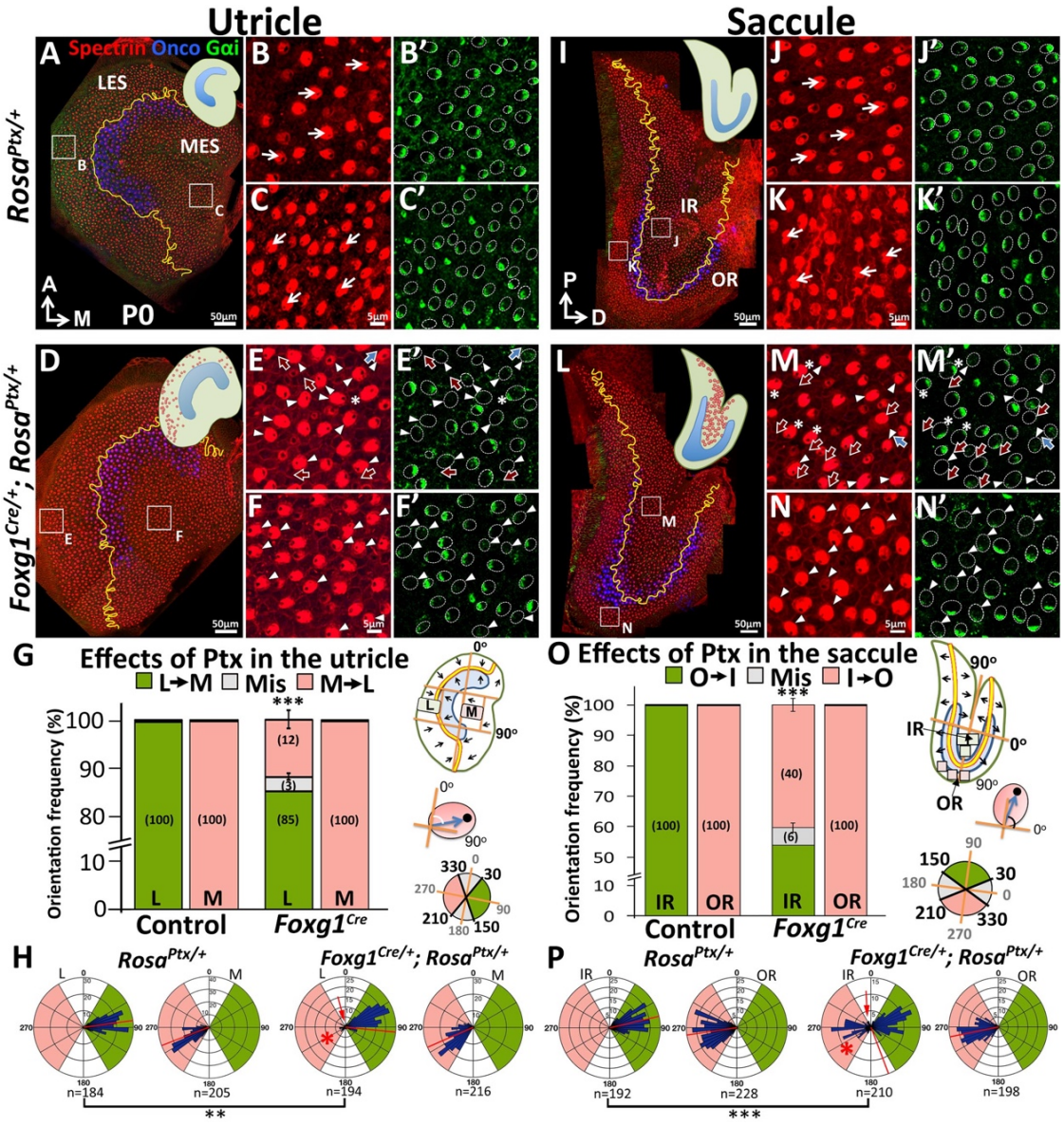

Figure 2.10. Inhibition of Gαi inverts stereocilia orientation in the *Emx2*-positive domain of maculae. (A-C) In control utricles, stereocilia are pointing toward the LPR (yellow line) and Gαi is associated with the kinocilium within each HC (B-C; n=3). (D-F') In *Foxg1*$^{Cre/+}$;*Rosa*$^{Emx2/+}$ utricles, stereocilia in LES are sometimes inverted (red arrows) or misoriented (blue arrows, E-E', G) but not in MES (F-F', n=3). The distribution of Gαi in HCs can be reduced or diffused across the utricle (E-F', arrowheads). Occasional HCs can be found in the LES, in which the kinocilium and Gαi concentration are no longer coupled to each other (asterisks, E-E'). (G) Quantification of stereocilia orientation scored in regions L and M of control and *Foxg1*$^{Cre/+}$; *Rosa*$^{Emx2/+}$ utricles. Anterior axis of the utricle is zero degree, kinocilium position within 30^0 to 150^0 are green (pointing medial), 210^0 and 330^0 are pink (pointing lateral) and ranges in between are grey (misoriented). Fifteen percent of HCs in region L of

Foxg1$^{Cre/+}$;*Rosa*$^{Emx2/+}$ utricles show abnormal orientations. (H) Circular histograms summarizing stereocilia orientation in region L and M for specimens shown in (G). (I-N') In control saccules (I-K'), stereocilia point away from the LPR (yellow line) but Gαi immunoreactivity is always associated with the kinocilium. In *Foxg1*$^{Cre/+}$;*Rosa*$^{Ptx/+}$ saccules (L-N'), misoriented (blue arrows) and reversed (red arrows) kinocilia are found in IR (M-M') but not OR (N-N'). Distribution of Gαi is often reduced or diffused (arrowheads), including some that are no longer coupled to the kinocilium (asterisks). (O) Quantification of stereocilia orientation scored within the six selected squares of the inner (IR) and outer regions (OR) of control and *Foxg1*$^{Cre/+}$;*Rosa*$^{Ptx/+}$ saccules. Stereocilia in the inner region (IR) point toward the inner margin within the range of 30^{o} to 150^{o} (green), whereas stereocilia in the outer region (OR) point toward the outer margin of the sensory organ within the range of 210^{o} to 330^{o} in control saccules (pink). In *Foxg1*$^{Cre/+}$;*Rosa*$^{Ptx/+}$ saccules, 46% of stereocilia polarity were affected in IR, compared to controls (n=3). (P) Circular histograms of specimens shown in (O). Stereocilia in IR of *Foxg1*$^{Cre/+}$;*Rosa*$^{Ptx/+}$ saccules are misoriented but no obvious misorientation is evident in OR (N-N'). Red asterisk, arrow and line represent stereocilia reversal, stereocilia misorientation, and average degree of HC orientation, respectively. Inset in (D) and (L) indicate distribution of all abnormal stereocilia in the specimen shown. ** $p< 0.01$, *** $p< 0.001$.

Next, we investigated the epistatic relationship between *Emx2* and *Ptx* in the utricle. Since *Foxg1*$^{Cre/+}$;*Rosa*$^{Emx2/Ptx}$ compound mutants are early lethal, we generated compound mutants of *Emx2* and *Ptx* using *Gfi1*$^{Cre/+}$. First, HC-specific induction of Ptx in *Gfi1*$^{Cre/+}$;*Rosa*$^{Ptx/+}$ utricles showed similar but milder stereocilia phenotypes than those of the *Foxg1*$^{Cre/+}$;*Rosa*$^{Ptx/+}$ (Fig. 2.10). Only 7% of stereocilia in the LES were affected, while polarity was normal in the MES of *Gfi1*$^{Cre/+}$;*Rosa*$^{Ptx/+}$ utricles (Fig. 2.11D-F',M-N). Additionally, similar abnormality in Gαi distribution as *Foxg1*$^{Cre/+}$;*Rosa*$^{Ptx/+}$ maculae was observed as well (Fig. 2.11E-F', arrowheads and asterisks). Comparing the LES of *Ptx* single to *Ptx* and *Emx2* compound mutant utricles (*Gfi1*$^{Cre/+}$;*Rosa*$^{Ptx/+}$ and *Gfi1*$^{Cre/+}$;*Rosa*$^{Emx2/Ptx}$), no significant change in HC polarity was observed (Fig. 2.11E-E',J-K',M-N, 7% versus 9%). However, despite the lack of polarity defect in

Gfi$^{Cre/+}$;*Rosa*$^{Ptx/+}$ medial utricles (Fig. 2.11F-F',M-N), a moderate but significant rescue of HC polarity reversal induced by ectopic *Emx2* (Fig. 2.11G-I) was observed in *Gfi1*$^{Cre/+}$;*Rosa*$^{Ptx/Emx2}$ mutants (Fig. 2.11L-L', yellow arrows, M-N, 22%). Together, these results suggest that Ptx affects stereocilia polarity in HCs that express Emx2 either endogenously or ectopically, and Emx2 requires Gαi to mediate stereocilia polarity (Fig. 2.11O). The absence of Ptx effects in macular regions that do not normally express Emx2 suggests that other mechanisms for establishing stereocilia polarity are involved.

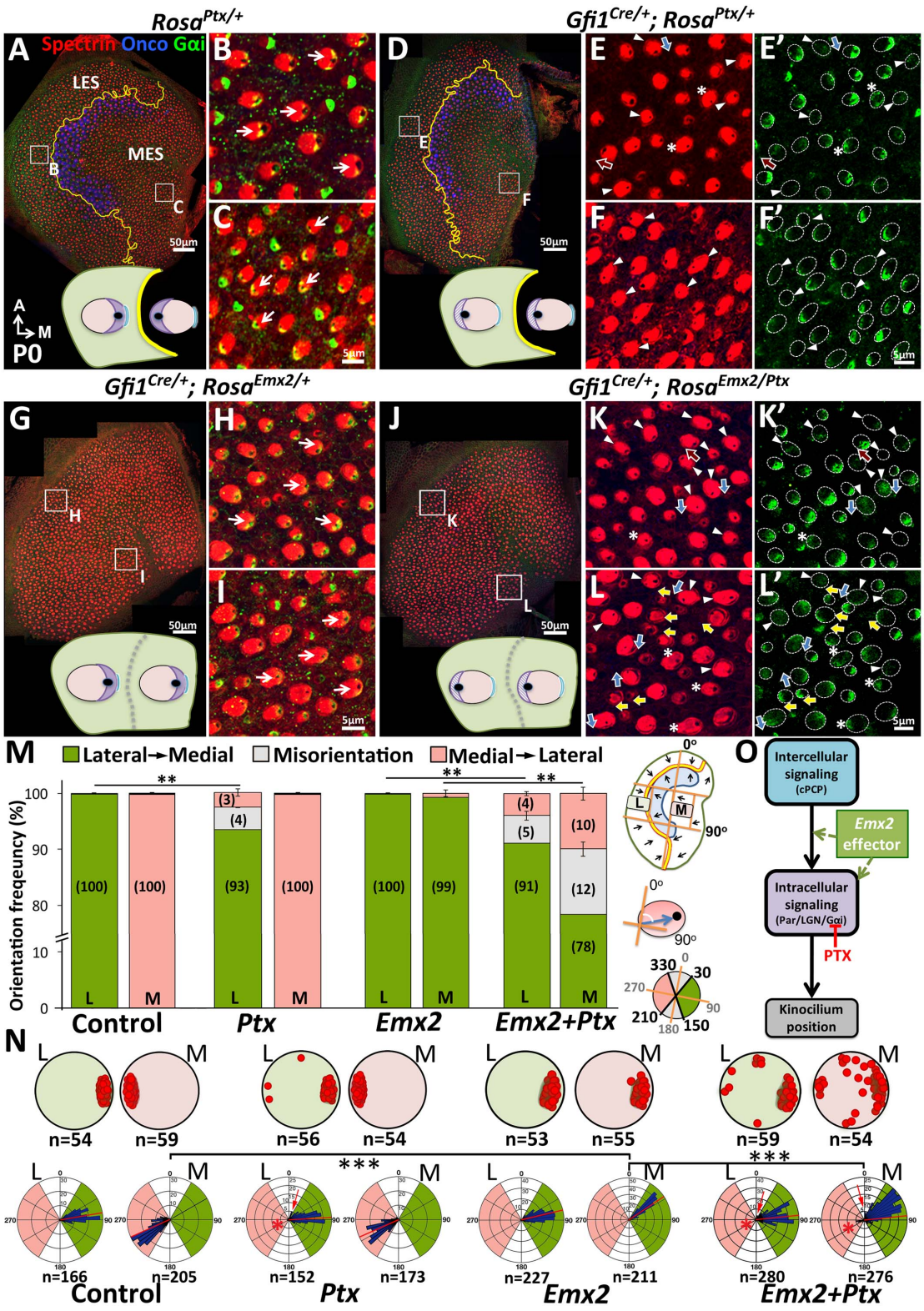
Rosa^Ptx/+
Gfi1^Cre/+; Rosa^Ptx/+
Gfi1^Cre/+; Rosa^Emx2/+
Gfi1^Cre/+; Rosa^Emx2/Ptx
Spectrin Onco Gαi
LES
MES
P0
50μm
5μm
M Lateral→Medial
Misorientation
Medial→Lateral
Orientation freqeuncy (%)
Control
Ptx
Emx2
Emx2+Ptx
Intercellular signaling (cPCP)
Emx2 effector
Intracellular signaling (Par/LGN/Gαi)
PTX
Kinocilium position
n=54
n=59
n=56
n=54
n=53
n=55
n=59
n=54
n=166
n=205
n=152
n=173
n=227
n=211
n=280
n=276

Figure 2.11. *Emx2*-mediated stereocilia polarity change requires heterotrimeric G-proteins. Compared to $Rosa^{Ptx/+}$ controls (A-C), some stereocilia polarity are reversed in LES (D-E') but not MES (F-F') of $Gfi1^{Cre/+}$;$Rosa^{Ptx/+}$ utricles. Ectopic *Ptx* and *Emx2* in $Gfi1^{Cre/+}$;$Rosa^{Emx2/Ptx}$ utricles rescued HC polarity reversal in MES (L-L') but not in LES (J-K') of $Gfi1^{Cre/+}$;$Rosa^{Emx2/+}$ utricles (G-I). Red, blue and yellow arrows represent reversed, misoriented and rescued HC polarity, respectively. Arrowheads and asterisks represent anti-Gαi staining that is reduced/diffused or no longer associated with the kinocilium, respectively. (M) Percentages of stereocilia orientation. Ptx causes abnormal HC polarity in region L of controls (7%) and ectopic *Emx2* (9%). Reversed HC polarity induced by *Emx2* in region M is partially rescued by ectopic *Ptx* (22%, **$p<0.01$). (N) Upper - plots of kinocilium location (red dots) in HCs within regions L and M of one specimen. Lower - Circular histograms summarizing HC orientation distribution in regions L and M for each genotype indicated. (O) Model of Emx2 effector mediating stereocilia position by regulating Par/Insc/LGN/Gαi complex (purple) but not cPCP proteins (light blue).

G. Conserved role of *Emx2* in establishing stereocilia polarity pattern

Since the LPR is conserved among vertebrates (Desai et al., 2005; Hammond & Whitfield, 2006; Huss, Navaluri, Faulkner, & Dickman, 2010), we investigated whether *Emx2* has a role in establishing LPR in other species. Both the lagena (an additional macula not present in mice) of the chicken inner ear and neuromasts of the lateral line system in zebrafish exhibit a similar LPR as the mouse maculae. Our immunostaining results indicate that the border of Emx2 expression domain in the three maculae of the chicken inner ear, utricle, saccule, and lagena also coincides with the LPR, similar to those of the mouse (Fig. 2.12).

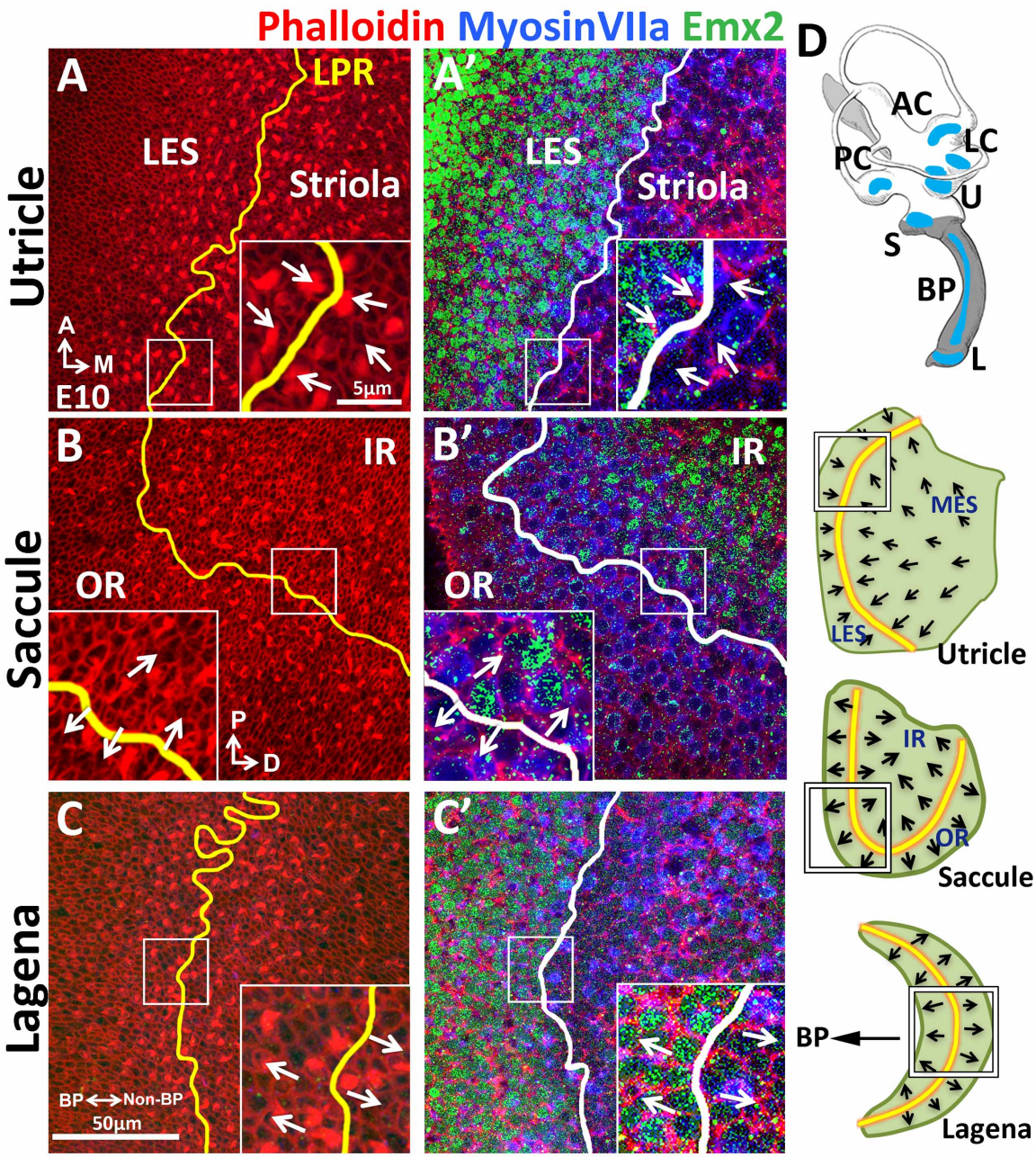

Figure 2.12. Conserved expression of Emx2 in the three chicken maculae. Anti-Emx2 immunostaining of the chicken utricle (A, A'), saccule (B, B') and lagena (C, C') at E10. (A-C) Phalloidin staining (red) showing opposite stereocilia orientation across the LPR (yellow line). In the same regions shown in (A), (B), and (C) but at the level of the cell body, the border (white line) of the Emx2-positive region (green) is restricted to only one side of the LPR: lateral region of the utricle (A'), inner region of the saccule (B'), and proximal region of the lagena, closer to the cochlea/basilar papilla (BP) (C'), respectively (n=3). HCs are stained with anti-Myosin VIIa (blue). (D) Schematic diagram of the chicken inner ear and its three macular organs.

The lateral line system is responsible for detection of water pressure changes including schooling behavior in aquatic vertebrates (Chitnis et al., 2012). Depending on the neuromast, the HCs within are arranged in pairs facing each other and aligned in either anterior-posterior (A-P) or dorsal-ventral (D-V) direction along the body axis (Fig. 2.13A-C, (Lopez-Schier et al., 2004)). Similar to the ear, whereas cPCP regulates stereocilia polarity in neuromasts, its distribution is not altered across LPR (Mirkovic, Pylawka, & Hudspeth, 2012). We found that emx2 is expressed in half of the HCs, oriented towards the posterior or ventral direction within the respective A-P and D-V neuromast (Fig. 2.13B-C’’’).

To test the role of emx2 in establishing stereocilia polarity in zebrafish, we generated gain and loss of *emx2* zebrafish mutants. Using the CRISPR/Cas9 technology, we generated *emx2* knockouts (Fig. 2.14A). In F1 generation of *emx2* knockouts, all stereocilia were uniformly polarized toward the anterior and dorsal direction in the respective A-P and D-V neuromasts (Fig. 2.13D-D’’’). In contrast, neuromasts of *m6b:emx2-mCherry* transgenic fish, which overexpress *emx2* under a hair cell-specific promoter *myosin6b*, showed stereocilia pointing toward only the posterior or ventral direction in A-P and D-V neuromasts, respectively (Fig. 2.13E-E’’’). Additionally, the utricle and cristae, which have similar polarity patterns as mice, demonstrated loss of LPR and the predicted HC polarity reversal phenotype in *emx2* gain- and loss-of-function larvae (Fig. 2.14B-J). Taken together, these results indicate that Emx2 has a conserved role in determining stereocilia polarity of sensory HCs and establishing the LPR.

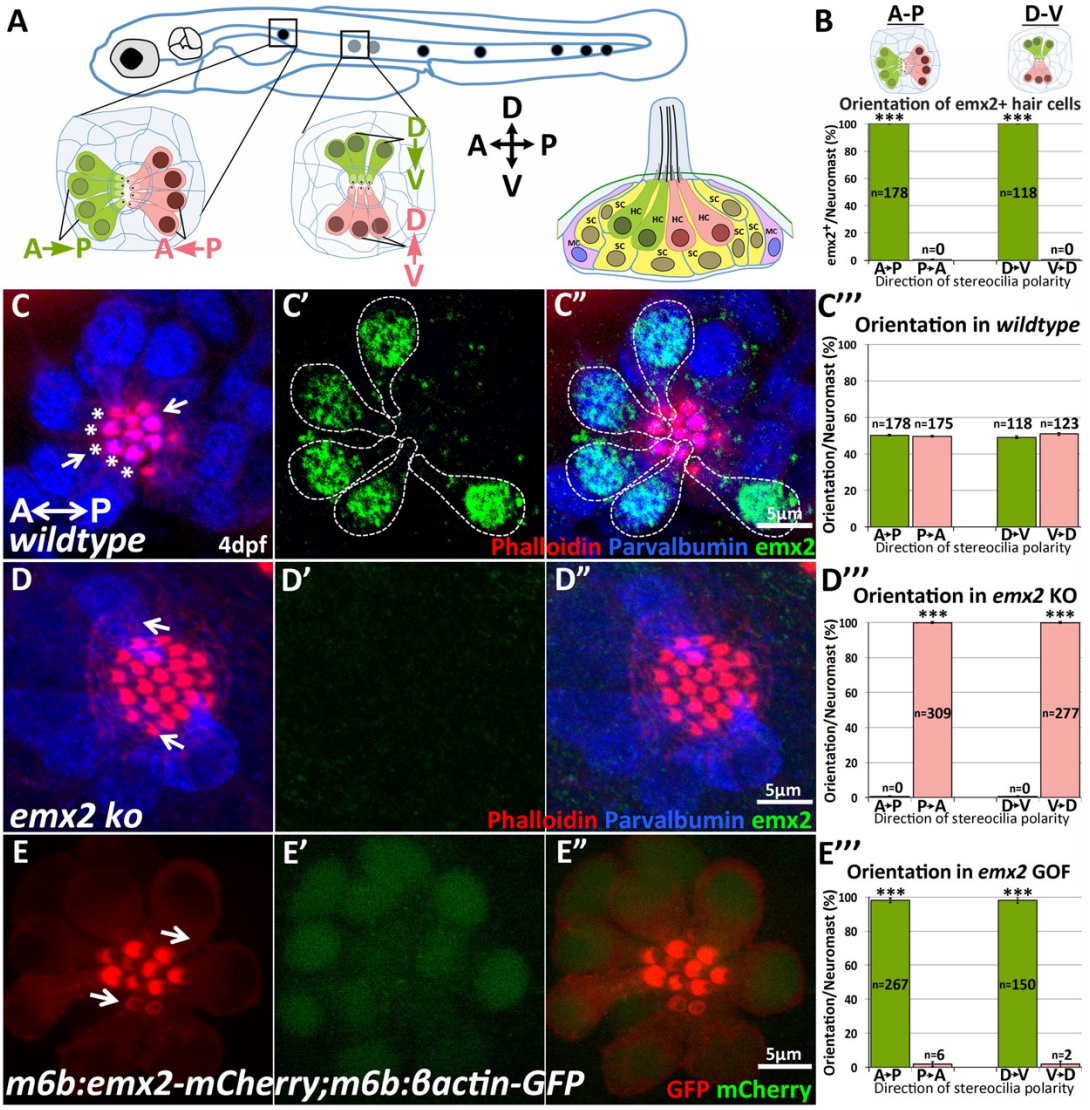

Figure 2.13. *emx2* regulates stereociliary bundle polarity in neuromasts. (A) Surface view of an A-P and D-V oriented neuromast and a sagittal view of the cellular architecture of a neuromast in the lateral line of zebrafish. (B-C''') Only HCs (parvalbumin-positive, blue, asterisks) with stereociliary bundles (phalloidin, red) pointing toward the posterior or ventral direction are positive for anti-Emx2 staining (green) in A-P and D-V neuromasts, respectively (54 neuromasts from 26 larvae, ***p<0.001). (D-D") Illustrations and (D''') quantification of HCs in F1 generation of *emx2* knockouts showing all HCs are *emx2*-negative and pointing unidirectionally (43 neuromasts, 18 larvae, p<0.001). (E-E''') *m6b:emx2-mCherry* neuromasts. (E-E") All stereociliary bundles (visualized using *m6b:βactin-GFP,* red) are emx2-positive (green) and pointing towards the posterior. (E''') Quantification of HC polarity in 36 A-P and D-V neuromasts from 23 larvae. ***p<0.001.

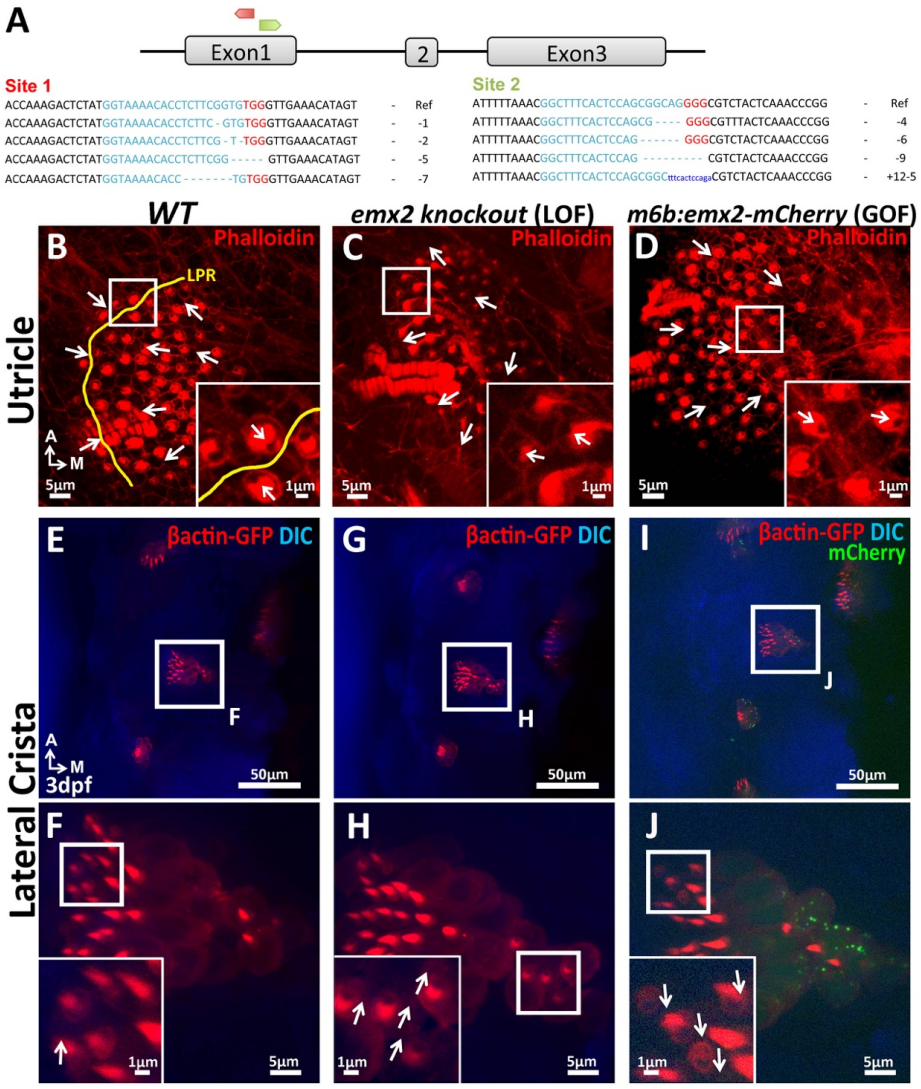

Figure 2.14. Polarity phenotypes in the utricle and lateral crista of *emx2* gain- and loss-of function zebrafish mutants. (A) Example of deletions created in two targeted sites (site 1 red and site 2 green) in exon1 of *emx2* using CRISPR/Cas9 technology. Guide targets (blue), PAM sequences (red), and examples of deletions found are shown. (B-D) Utricle and (E-J) lateral crista of controls (B, E, F), *emx2* knock out (C, G, H), and *emx2* gain of function, *m6b:emx2-mCherry*, zebrafish (D, I, J). (B-D) LPR is by the lateral edge of the utricle in zebrafish (B, n=10), which is absent in *emx2* knockout utricles (C, n=13) as well as *m6b:emx2-mCherry* utricles (D, n=9). Based on phalloidin staining (red), HCs at the edge of *emx2* knockout utricles point toward the lateral (inset in C), whereas HCs in the medial region of *m6b:emx2-mCherry* utricles now point toward the medial (inset in D), opposite from controls (B). (E-J) Arrows indicate the direction of stereocilia polarity based on βactin-GFP label (red). Stereocilia in the lateral crista of control are pointing toward the anterior direction (E, F, n=6) and this polarity is not affected in the *emx2* knockout fish (G, H, n=3) but stereocilia polarity are all reversed in the *m6b:emx2-mCherry* GOF cristae (I, J, n=3).

IV. Discussion

A. Conserved role of Emx2 in dictating sensory HC polarity

Our results provide direct evidence that Emx2 is capable of reversing endogenous stereocilia orientation in HCs that do not normally express Emx2 in the inner ear and neuromasts. Consistently, the loss of *Emx2* in maculae and neuromasts abolishes their LPR. Polarity defects in the cochlea, however, are not readily evident in the *Emx2*$^{-/-}$ mutants due to the absence of outer HCs and the poor organization of the double rows of inner HCs (Fig. 2.4, (Holley et al., 2010)). We attributed these phenotypes to an earlier requirement of *Emx2* function prior to kinocilium positioning. Nevertheless, taken into consideration the expression patterns of this transcription factor in mouse, chicken and fish, as well as our gain- and loss of function results in both mouse and fish, we propose that Emx2 has a conserved role in mediating stereocilia polarity in all sensory HCs.

B. Polarity reversal phenotypes

Whereas mutations in components of the cPCP pathway affect stereocilia orientation (Montcouquiol et al., 2003; J. Wang et al., 2006; J. Wang et al., 2005), few cause a fully penetrant polarity reversal of 180^{o}. Similar types of polarity reversal phenotypes, however, have been reported when a cPCP component, pk, was disrupted in *Drosophila*. Abnormal ratio of isoforms between *pk* and *spiny-legs (pk:sple*) leads to polarity reversal in trichomes of fly wings and abdomen (Ayukawa et al., 2014; Gubb et al., 1999), similar to stereocilia phenotypes reported here. In *pk* and *sple* mutants, distributions of cPCP components such as fz and strabismus (analogous to Vangl in mammals) are concomitantly reversed, corresponding to the changes in tissue polarity (Ayukawa et al.,

2014; Olofsson et al., 2014). In contrast, distribution of Pk2 and Vangl2 remained unchanged in utricles of gain- or loss-of *Emx2* function mouse models suggesting that Emx2 effector functions either independent or downstream of cPCP proteins.

C. Emx2 mediates stereocilia polarity via the Par/Insc/LGN/Gαi complex

The Par/Insc/LGN/Gαi complex is thought to pull the basal body/kinocilium from the center of the HC to the periphery during stereocilia formation (Ezan et al., 2013; Tarchini et al., 2013). The ability of ectopic *Emx2* to relocate this complex despite the establishment of the kinocilium suggests that Emx2 regulates the Par/Insc/LGN/Gαi complex. Furthermore, our results suggest that the function of this complex in kinocilium positioning is more important for *Emx2*-positive than negative HCs. First, HCs in both the cochlea and lateral utricle, which express *Emx2*, were affected by Ptx (Fig. 2.10, 2.11; (Ezan et al., 2013; Tarchini et al., 2013)). However, under similar conditions, HC polarity was not affected in the *Emx2*-negative, medial utricle. Second, despite the fact that Ptx did not affect stereocilia polarity in the medial utricle, it was able to rescue some of the polarity defects elicited by ectopic *Emx2* in this region. Together, these results suggest that the Par/Insc/LGN/Gαi complex is important for kinocilium positioning in HCs that express *Emx2* and other mechanisms may be more important for proper targeting of the kinocilium in *Emx2*-negative HCs.

D. Emx2 effector and signaling

The regional expression pattern of Emx2 in the maculae and its requirement to reverse stereocilia polarity within this domain qualifies Emx2 as a global polarity cue. The gain-of-function results, however, suggest that this transcription factor bypasses the

cPCP proteins and functions at the intracellular level. As a result, the normal relationship between cPCP distribution and intracellular polarity appears to be reversed. For example, localizations of Fz3 and Fz6 are opposite to the stereociliary bundle in the cochlea (Montcouquiol et al., 2006; Y. Wang & Nathans, 2007). This relationship differs from the pattern found in the fly wing and ciliated cells in mouse trachea for example, in which Fz is localized with the hair and cilia, respectively (D. I. Strutt, 2001; Vladar et al., 2012). Likewise, the association of Pk2 with stereocilia in the lateral utricle where Emx2 is expressed, also differs from the PK2/Vangl distribution in the fly wing and ependymal cells in the mouse ventricle, where these two proteins are located opposite to the trichome and cilia, respectively (Boutin et al., 2014; Guirao et al., 2010; Tree et al., 2002). In contrast, in the Emx2-negative medial utricle, the relationship between stereociliary bundle and Pk2 is similar to those described in other systems, located on opposite side of the cell (Fig. 2.8C, (Deans et al., 2007)). HCs in the lateral utricle that lack Emx2 also exhibit similar complementary relationship between stereociliary bundle and Pk2 (Fig. 2.8E). Taken together, these expression patterns support the hypothesis that Emx2 either functions independently or changes the interpretation of the cPCP polarity signals, and it causes a switch in the location of kinocilium and this positioning requires G-protein activities via the Par/Insc/LGN/Gαi complex (Fig. 2.11O).

Where could the Emx2 effector be functioning? One possibility is that the Emx2 effector is a Fz-like seven-transmembrane receptor, which competes with the known Fz proteins in coupling to Dvl and Gαi complex. These results in the segregation of Dvl and Par/Insc/LGN/Gαi complex, followed by the kinocilium to the opposite pole of the cell, away from Fz3 and Fz6 (Montcouquiol et al., 2006; Y. Wang & Nathans, 2007). Another

possibility is that Emx2 effector could change one of the cPCP effectors such as *inturned* and *fuzzy*, which have been shown to regulate ciliogenesis and cilia polarity in vertebrates (Park, Haigo, & Wallingford, 2006; Wong & Adler, 1993). This scenario is analogous to the *sple* mutants, in which the interpretation of the Dachsous and Four-jointed gradients, components of another intercellular polarity signaling pathway (Matis & Axelrod, 2013), is changed resulting in a reversed microtubule orientation and distribution of fz to the opposite end of the cell in the *Drosophila* wing disc (Ayukawa et al., 2014; Merkel et al., 2014; Olofsson et al., 2014). Finally, given the numerous examples of cytoskeletal changes in response to cPCP proteins in multiple systems (Devenport, 2016), Emx2 effector could also function directly at this level by regulating one or more of the Rho family of GTPase [4] and thereby changing the cytoskeleton and location of the Par/Insc/LGN/Gαi complex of HCs. Nevertheless, whatever the mechanism(s) might be, the presence of Emx2 causes 180^{o} switch in stereocilia polarity in otherwise normal macular and neuromast HCs.

E. Other roles of Emx2

Our results link Emx2 to basal body positioning in sensory HCs. Notably, Emx2 has been implicated in regulating symmetric versus asymmetric cell division in the brain (R. Galli et al., 2002; Heins et al., 2001), which could also be a result of changing spindle orientation. Though speculative, it is possible that Emx2 effector could function at multiple steps of a cell cycle: spindle orientation during mitosis and/or basal body positioning during differentiation. Identifying these effectors will be important. Furthermore, in both maculae and neuromasts, HCs with opposite polarities are

innervated by different populations of neurons and they project, at least in the maculae, to different regions of the brain (Maklad et al., 2010; Nagiel et al., 2008; Pujol-Marti et al., 2014). These innervation patterns could be guided by downstream targets of Emx2 as well. In summary, our results reveal a largely unexplored cellular process of planar targeting of the cilium at the apical cell surface, which has profound effects on HC function and may have a broader implication in other ciliated cells and neural development.

Chapter 3: Discussion

I. Transcription factors that regulate planar polarity

The absence of hippocampus and urogenital system in *Emx2* knockout mutants suggest that *Emx2* functions like a selector gene, the loss of which results in the absence of a specific compartment or conversion to another structure during embryogenesis (Miyamoto et al., 1997; Pellegrini et al., 1996). In the inner ear, the lack of outer HCs in the cochlea of *Emx2* mutant is consistent with this hypothesis (Holley et al., 2010). However, my results show that Emx2 also functions as a global polarity signal in the maculae, mediating stereocilia polarity in a restricted region. Although effectors of *Emx2* that mediate this global polarity signaling have not been identified yet, a transcription factor such as Emx2 could mediate its global effect through several mechanisms: 1) cPCP pathway, 2) effectors of cPCP pathway, and/or 3) pathways that are independent of cPCP. Below are known examples of transcription factors functioning via one of these mechanisms.

A. Transcription factors that mediate polarity via cPCP proteins

An example of a transcription factor that mediates its effects through cPCP is Tbx20 in its requirement during neuronal migration. Neuronal migration during development is important for generating complexity of neuronal circuitry (Marin & Rubenstein, 2003). Branchiomotor neurons in the trigeminal nerve (V), facial nerve (VI), and vestibuloacoustic nerve (VIII) all undergo specific migration patterns during hindbrain

development. However, mechanisms regulating their migration are complex. Among these neurons, only facial branchiomotor neurons express cPCP and mutations of cPCP components such as Vangl2, Pk2, and Celcr1/2 lead to failure of neuronal migration in both zebrafish and mice (M. R. Song et al., 2006; Tissir & Goffinet, 2013). Although Tbx20 is expressed in all three types of neuronal precursors and display neuronal migration phenotypes in knockout mice, the migration defect in the facial branchiomotor nerve is attributed to the down regulation of cPCP proteins (M. R. Song et al., 2006).

In addition to Tbx20's role in mammalian neuron migration, the transcription factor *grainy head* also regulates the orientation of trichomes in *Drosophila* wing via transcription of cPCP proteins. In *grh* mutants, the expression of a cPCP component, fmi (homolog of Celsr in mice), is reduced and other cPCP components fail to localize asymmetrically. As a result, multiple trichomes are formed with abnormal polarity (H. Lee & Adler, 2004). Compound double heterozygous mutants of *grh* and cPCP components such as fz, vang, and fmi display enhanced polarity defects in the wing. Although *grh* mediates its effect by regulating cPCP proteins in the *Drosophila* wing disc, additional global patterning defects are observed in *grh* mutants that are independent of cPCP. Taken together, results of *grh* and *Tbx20* suggest that transcription factors can regulate polarity at multiple levels: via the cPCP pathway or other mechanisms (see below).

B. Transcription factors that regulate polarity via cPCP effectors

Transcription factors could also regulate planar polarity without affecting the expression of cPCP proteins. Unlike the role of *grh* in the *Drosophila* wing, a homolog

of *grh* in the mouse*, Grhl3,* regulates planar polarity without affecting cPCP protein expression. Introducing the null allele of *Grhl3* to cPCP mutants, *Vangl2*$^{lp/+}$, increases the severity of defects in wound repair, stereocilia orientation and neural tube closure (Caddy et al., 2010). These results indicate that *Grhl3* genetically interacts with cPCP pathway. However, gene expressions of cPCP components are not altered in *Grhl3* knockout mice suggesting that the interaction does not occur at the cPCP protein level. Instead, transcription of *RhoGEF19,* which encodes an activator of Rho GTPase, is significant reduced with loss of *Grhl3*. Thus, the more severe phenotypes observed in the double heterozygous mutants of *Grhl3* and *Vangl2* could be explained by cPCP proteins and *Grhl3* both regulating *RhoGEF19*.

Other examples of transcription factors that mediate planar polarity without affecting the cPCP proteins are *Cdx* family of genes, which are homologs of the *caudal* in *Drosophila*. During mouse development, *Cdx* family is involved in anterior-posterior patterning during mouse development (Savory, Mansfield, Rijli, & Lohnes, 2011). Mutations of *Cdx1, 2,* and *4* lead to neural tube closure failure, axial patterning defects, and craniorachischisis, which are phenotypes associated with defects of cPCP components (Savory et al., 2011; Tissir & Goffinet, 2010; Y. Wang & Nathans, 2007). However, expression of cPCP proteins is not affected in the *Cdx1/2* compound knockout mice (Savory et al., 2011). Instead, the severe neural tube closure phenotype in *Cdx1/2* mutants is similar to the knockout mutants of protein tyrosine kinase 7 (*Ptk7*), which suggests that Cdx gene family could regulate planar polarity via *Ptk7* (Xiaowei Lu et al., 2004; Savory et al., 2011). *Ptk7* is a transmembrane protein that has been demonstrated to be a mediator of cPCP pathway. It interacts with cPCP effector, Rack1, to mediate

Dsh membrane localization during *Xenopus* development (Shnitsar & Borchers, 2008; Wehner, Shnitsar, Urlaub, & Borchers, 2011). Mouse mutant analyses indicate that *Ptk7* genetically interacts with cPCP components such as Vangl2 and Fz3/6. Introduction of a *Ptk7* null allele into the $Vangl2^{lp/+}$ mutant background shows a more severe phenotype than $Vangl2^{lp/+}$ alone (J. Lee et al., 2012; Xiaowei Lu et al., 2004). In addition, several Cdx binding sites are identified in the promoter region of *Ptk7*. Consistently, transcription of *Ptk7* are downregulated in *Cdx1/2* knockout mutants (Savory et al., 2011). Thus, whereas Cdx does not mediate polarity via regulating cPCP proteins, it genetically interact with the cPCP pathway and may regulate cPCP effector, *Ptk7* (Savory et al., 2011). Taken together, both Grhl3 and Cdx1/2 are good examples of transcription factors that interact with the cPCP pathway but do not directly affect the transcription or translation of the cPCP proteins themselves.

C. Transcription factors that mediate polarity independent of cPCP pathway

Last but not least, transcription factors have been demonstrated to regulate planar polarity independent of the cPCP pathway. During *Drosophila* germ band elongation, cells within the germ band epithelium undergo organized cell rearrangements, asymmetric cell division, and morphological changes to elongate along the anterior-posterior axis and simultaneously narrow the width across the dorsal-ventral axis (Vichas & Zallen, 2011). As demonstrated in Chapter 1, two pair rule genes, *eve* and *runt,* provide the global polarity cues for this process, resulting in the asymmetrical but complementary distribution of Myosin II and Bazooka (homolog of Par3) within individual cells to mediate coordinated cell movements. Interestingly, the cPCP proteins

are not required for this process (Zallen & Wieschaus, 2004). Thus, transcription factors could bypass the cPCP pathway that directly affect the distribution of intracellular polarity proteins.

D. *Emx2* regulate polarity as a transcription factors

The transcription factor, Emx2, functions as a global polarity cue in stereociliary polarity patterning, and could also mediate its effects via some of the aforementioned mechanisms. However, unlike Tbx20's role in branchiomotor neuronal migration of mice and grh's function in *Drosophila* wing development, the expression and distribution patterns of cPCP proteins are not changed by the loss of Emx2. In addition, my preliminary results also suggest that expression of *emx2* in the neuromasts is not disrupted in *trilobite* (mutations in *vangl* homolog) zebrafish larvae (see Appendix I). Together, these results indicate that *Emx2* does not mediate its effects via regulating cPCP proteins. Instead, effectors of *Emx2* are likely to mediate stereocilia orientation either independent or downstream of cPCP proteins.

II. Other regulators of the LPR formation

Since my results demonstrated that regional-expressed *Emx2* acts as a global signal to regulate stereocilia polarity on one side of the LPR, there could easily be other global signals that activate and/or collaborate with *Emx2* to establish the LPR in the maculae. As described in Chapter 1, the establishments of polarity reversal of cell arrangement in the vulva of *c. elegans* and ommatidia in *Drosophila* eye are mediated by gradients of morphogens. It is possible that a morphogen "X" expressed as a gradient in the maculae

establishes the initial lateral-medial and inner-outer regions within the utricle and saccule, respectively.

Even though there is no evidence for a morphogen that has been identified during macular development thus far, the Wnt family of proteins could be potential candidates. Wnt family of proteins have been demonstrated to function as morphogens to establish polarity axes in tissues from *c. elegans* to mammals (Y. Yang & Mlodzik, 2015). In addition, Wnt signaling regulates the regional specification of the mouse brain, which collaborates with other factors such as Emx2 (Backman et al., 2005; Muzio, Soria, Pannese, Piccolo, & Mallamaci, 2005). In the regional patterning of the occipito-hippocampal anlage, there could be a feedback loop between *Emx2* and Wnt signaling (Muzio et al., 2005). In addition, during dorsal telencephalon development, Wnt regulates *Emx2* and binding sites for Tcf and Smad (transducer of Wnt signaling) are located in the *Emx2* enhancer region. Ectopic expression of β-catenin to activate Wnt signaling stimulates the *Emx2* enhancer activity (Theil, Aydin, Koch, Grotewold, & Ruther, 2002). However, binding sites for *Emx2* are also found in the *Wnt-1* enhancer, which negatively regulates Wnt-1 expression in the forebrain (Iler, Rowitch, Echelard, McMahon, & Abate-Shen, 1995). Even though how *Emx2* regulates Wnt is unknown, the regulatory loop between *Emx2* and Wnt family participates in the regional patterning of the central nervous system.

Based on the above results, there could be a mutual-regulatory pathway to form the LPR during macular development. A concentration gradient of morphogen "X" in the utricle, for example, could originate from the medial side opposite to where *Emx2* will express. A low concentration of "X" activates the expression of *Emx2* in the lateral

utricle. The expression of *Emx2* in turn, down regulates the "X" expression in the lateral utricle. As a result, "X" and Emx2 collaborate to establish the medial-lateral axis within the utricle and define the LPR. However, there is no existing Wnt mutant that exhibits a phenotype to support the idea of a potential morphogen. Since there are multiple Wnt proteins, more work needs to be done to explore this idea further.

III. Polarity reversal phenotype

The presence of *Emx2* inverts the polarization of kinocilium in HCs by approximately 180 degrees. To understand how *Emx2* regulates the polarity, comparisons to other existing polarity reversal phenotypes are helpful. Since Emx2 mediates stereocilia reversal via the Par/mInsc/LGN/Gαi complex, phenotypes of 180-degree polarity reversal as well as phenotypes resulted from reversal of Par proteins in *Drosophila* will be described in the following sections.

A. *Spiny-legs* mutants in *Drosophila*

Whereas mutations in many components of cPCP affect polarity, reversal phenotype is only observed in the *Drosophila sple* mutant, in which orientation of the trichomes in wings and abdomen, as well as the cell arrangement in eye are reversed (Ayukawa et al., 2014; Y. Y. Lin & Gubb, 2009; Olofsson et al., 2014). Mutant phenotype of s*ple* is similar to the stereocilia phenotype in $Emx2^{-/-}$ that polarity of a cellular organelle is reversed. The reversed trichomes phenotype in *sple* mutant is caused by disrupted expression ratio of Pk^{pk} (*prickles*) and Pk^{Sple} (*spiny-legs*) isoforms, which resulted in inverted orientation of microtubules. This reversal of microtubule direction leads to inverted intracellular accumulation of cPCP components such as fz, which promotes

trichome formation. As a result, trichome orientation and cell arrangement in the ommatidia are inverted (Olofsson et al., 2014). The inversion of microtubule orientation by sple requires the ds/ft systems and the phenotype caused by overexpression of *sple* is absent in *ds* or *ft* mutants (Ayukawa et al., 2014). A possible mechanism is that increased sple bind to ds and polarized at the higher ds level side of a cell, which changes the microtubule orientation and thus switch the cPCP proteins trafficking within a given cell, without disturbing the ds/ft pathway.

Unlike the *sple* mutant, the distribution pattern of cPCP proteins is normal in the *Emx2* mutants (Fig. 5, S4). These results suggest that *Emx2* does not regulate the LPR formation at the cPCP level. However, it is possible that expression of *Emx2* switches the intracellular polarity by inverting the orientation of microtubules plus-ends within a given HC. Existing data suggested that the organization and relative relationship of microtubule and kinocilia is the same in *Emx2* and non-Emx2 expressing cells (Ezan et al., 2013). Thus, *Emx2* may change the orientation of microtubules independently from cPCP pathway. To test this hypothesis, further experiments on the microtubule orientation and its relationship to the distribution of intercellular and intracellular polarity proteins are needed. For example, live imaging of polarity proteins trafficking within the HC, and their relationships with the microtubule orientation may answer these questions. This will help us to decipher any changes in the relationship between microtubules and polarity proteins in the presence or absence of Emx2.

B. Cell fate switch in sensory organ precursor cells of *Drosophila*

A reported phenotype that is associated with reversed distribution of Par3 protein, a component of Par/Insc/LGN/Gαi complex, is observed in the sensory organ precursor cells (pI cells) of *Drosophila.* During the mechanosensory organ development, the pI cells divide along the anterior-posterior axis to form a pIIa and pIIb, which further divide to generate the mechanosensory organ (Morin & Bellaiche, 2011). Within each pI cell, Pins (homolog of LGN) is asymmetrically distributed, located at the anterior cortex together with Gαi, whereas Bazooka is located at the posterior cortex together with Par6 and aPKC (Fig. 1.11B). The Insc is not normally expressed in the pI cells. In the absence of Insc, Pins/Gαi and Par protein complex are normally distributed at opposite ends of the pI cell along the anterior-posterior axis, established by cPCP proteins. Ectopic expression of Insc in the pI cells resulted in reversed localization of Bazooka, from posterior to anterior cortex but the normal anterior localization of Pins and Gαi are not changed. As a result, Bazooka, Insc, Pins and Gαi form a complex at the anterior cortex of pI cells. Since Bazooka normally excludes the cell fate determination factor, Numb, from the posterior end during normal asymmetric division of pI cells, the reversed Bazooka location results in Numb location to the posterior and causes a switch in the cell fates of the descendants (Bellaiche et al., 2001). Thus, this is an example of reversal phenotype, which involves a cell fate change.

Unlike the scenario in the pI cells, Insc is likely to be present in both Emx2-positive and Emx2-negative HCs (Tarchini et al., 2013) and the Par/Insc/LGN/Gαi complex is likely to be similar between these two types of HCs (Ezan et al., 2013). Nevertheless, it is possible that the presence of an Emx2 effector could switch the location of the entire

Par/Insc/LGN/Gαi complex to the opposite side of the HC, analogous to the effects of Insc in the pI cells, and leads to 180^{o} change in stereocilia position. Based on these discussions, we proposed that the polarity regulation role of *Emx2* in sensory hair cell organs provides a new model to study polarity reversed.

IV. Intracellular signaling in establishment of stereocilia polarity

A. Effects of Ptx

Our results demonstrate that *Emx2*'s effects on stereocilia polarity require Gαi. Ptx blocks ADP-ribosylation of α subunit in the $G_{i/o}$ family (Carbonetti, 2010), which could inhibit the G-protein dependent polarity establishment in some systems. For example, inhibition of G-proteins with Ptx rescues the shape and polarity defects observed with overexpression of fz in the ommatidia (Katanaev, Ponzielli, Semeriva, & Tomlinson, 2005; Katanaev & Tomlinson, 2006). HeLa and MDCK cells treated with Ptx show abnormal oriented cell division due to reduced accumulation of LGN in the cell cortex and affected spindle orientation in metaphase (Woodard et al., 2010). Similarly, in the HCs, establishing the intracellular polarity and orienting cellular organelles require Gαi to interact with Par/Insc/LGN to form a complex, which is concentrated asymmetrically at the apical surface. The blockage of Gαi by Ptx leads to a severe reduction of endogenous Insc/LGN expression in cochlear HCs (Tarchini et al., 2013). This phenotype suggests that inhibiting Gαi production inhibits the recruitment of LGN, mInsc and Par to a destined location at the apical surface where they bind to microtubules and guide the kinocilium to the periphery. The requirement of Gαi in establishing

stereociliary bundle polarity in *Emx2*-positive HCs of the maculae is consistent with previous reports (Ezan et al., 2013; Tarchini et al., 2013).

Although Ptx was proposed to inhibit Par/mInsc/LGN/Gαi complex formation and thus affect the ability to bind to microtubules and polarize the kinocilium (Ezan et al., 2013), other mechanisms are possible. For example, Gαi inhibits cAMP signaling in other systems (Katada, 2012). It is possible that reduced Gαi by Ptx treatments in HCs resulted in increased cAMP, which could affect the transcription of *Emx2* or its downstream targets causing a reduction of the polarity phenotype. This idea can be tested by investigating the levels of *Emx2* transcripts in Ptx expressing maculae using qPCR and in situ hybridization. Thus, the mechanisms of Ptx in inhibiting the polarization of kinocilium in *Emx2*-expressing cells will need further investigation.

B. Other intracellular polarity proteins

The introduction of Ptx only partially rescued the phenotypes induced by *Emx2* (Fig. 6, 7). Although it is possible that Ptx may not be expressed at sufficient levels to block Gαi activity at the critical developmental time when kinocilium is migrating, other explanations are possible. For example, the Lis1/Dynein complex, as mentioned in Chapter 1, has been demonstrated to be important for kinocilium positioning in cochlear HCs as well (Sipe et al., 2013). Lis1 regulates organization of microtubule and localization of dynein, which is a motor complex that pull the microtubule plus-ends towards the lateral edge of the cell (Guo et al., 2006). Conditional knockout of *Lis1* leads to stereocilia misorientation and cellular disorganization in cochlear HCs (Sipe et al.,

2013). Thus Lis1/Dynein could be another intracellular mechanism that normally functions to mediate stereocilia position in sensory HCs.

Furthermore, our results indicate that Ptx has no effect on stereocilia orientation in HCs within the *Emx2*-negative region such as cristae, medial utricle, and OR of saccule (Fig. 6, 7). Although the Lis1/Dynein complex was demonstrated in cochlear HCs where Emx2 is expressed, it is possible that this Lis1/Dynein complex or other mechanisms that have yet to be identified are more important in mediating kinocilium position in Emx2 negative HCs.

V. Emx2 **changes the interpretation between inter- and intracellular polarity signals**

How does *Emx2* regulate HC polarity? I hypothesize that intercellular polarity signals such as cPCP proteins, establish a "default" polarity orienting all HCs pointing toward the lateral edge in the utricle and inner side of the saccule. The presence of *Emx2* changes the interpretation between intercellular and intracellular polarity signals, without interrupting the expression of these proteins. The intracellular Par/Insc/LGN/Gαi complex is utilized by Emx2 to reverse the orientation of stereocilia, defined as "reversed" polarity. Then, how does *Emx2* change the interpretation between the intercellular and intracellular polarity signals?

The communication between polarity proteins from different regulatory levels is not well understood. Several examples show that cPCP proteins collaborate with the Par/Insc/LGN/Gαi complex to establish the planar polarity. For example, as mentioned above, the spindles within the pI cells need to be oriented correctly based on intercellular and intracellular polarity signaling during asymmetric division. The cPCP proteins are

required to establish the anterior-posterior axis of the spindles: fz and dsh are located at the posterior side and vangl and pk are concentrated at the anterior end (Besson et al., 2015). Then, cPCP proteins, fz and dsh guide the localization of Par complex to the posterior end of the cell, but restrict the Pins/Gαi (homologs of LGN/Gαi) complex to the anterior end. In addition to amplifying the intercellular polarity signals and localizing the spindle locations along the anterior-posterior axis, Pins/Gαi and cPCP components are required to generate the apical-basal axis of the spindle (Fig. 1.11B; (Morin & Bellaiche, 2011)). Mutation of the cPCP components, like fz, causes a reduction of the apical-basal tilt of spindles and their random orientation at the apical surface (Morin & Bellaiche, 2011; Segalen et al., 2010). Using Ptx to block the function of Gαi or mutation of Pins resulted in prolonged mitosis, tilted mitotic spindle movements along the apical-basal axis, but oriented spindle on the apical surface (Segalen et al., 2010; Woodard et al., 2010). These results indicate that the cPCP proteins are required for spindle alignment of dividing pI cells along anterior-posterior axis, while both Pins/Gαi and cPCP components are important for apical-basal orientation (Segalen et al., 2010). Only the collaboration between these two groups of proteins can ensure the proper axis of cell division to form the correct mechanosensory organ. How does cPCP proteins collaborate with the intracellular proteins? One hypothesis is fz/dsh and Gαi/Pins interact with NuMA/Dynein complex separately, which bind microtubules and orient the spindle (Morin & Bellaiche, 2011; Segalen et al., 2010). Asymmetrical division of SOP is a good example of interactions between intercellular and intracellular polarity pathways. It is most likely that cPCP pathway also interacts with intracellular Par/Insc/LGN/Gαi complex to orient stereocilia polarity in HCs, and such interactions are altered in the

presence of Emx2. Some of the possibilities where Emx2 could act are listed below and illustrated in Fig. 3.1.

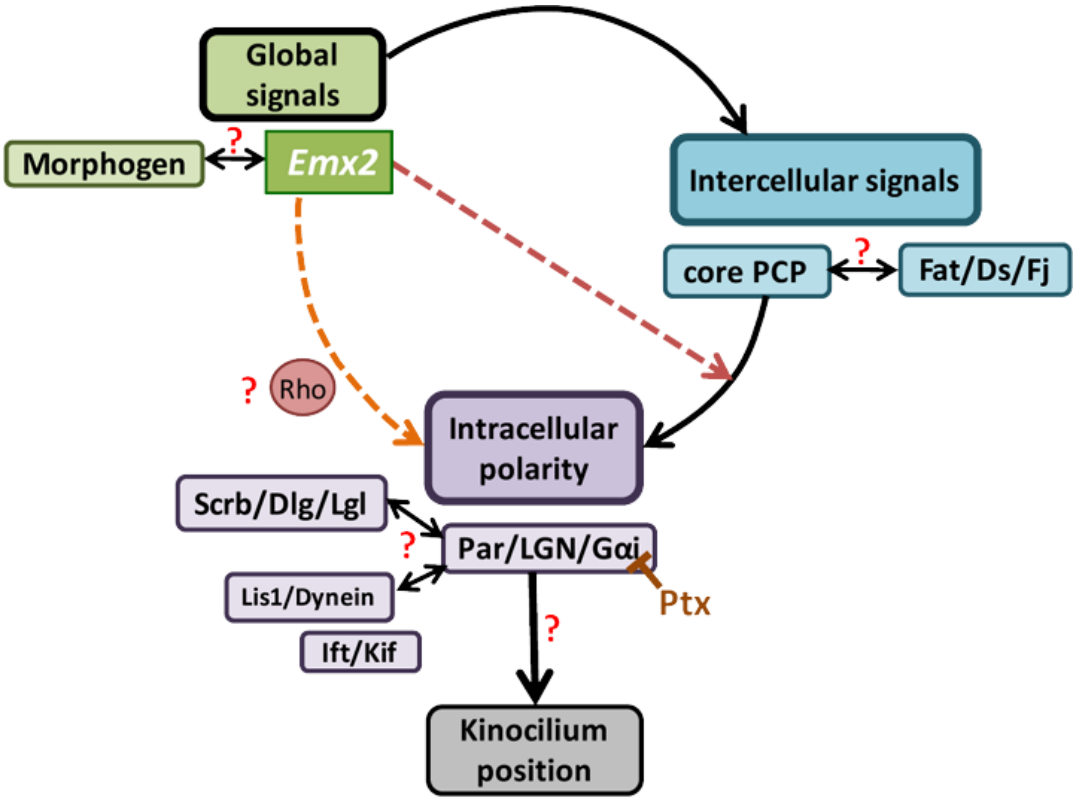

Figure 3.1. Potential signaling pathways of the stereocilia orientation establishment. The stereocilia polarity can be established by various signals. Global polarity signals instruct the formation of intercellular signals, which are amplified by intracellular polarity proteins and guide the kinocilium migration to its proper location (black arrows). Emx2, may function as a global polarity signal that regulate the interpretation between inter- and intracellular signals (dashed orange arrows). Alternatively, Emx2 could bypass the cPCP pathways and function independently to regulate stereocilia polarity (dashed red arrows). Question marks represent relationships that are not clear.

A. Direct interaction: G-protein dependent pathway

There could be a direct link between inter- and intracellular polarity through a G-protein system. Fz recruits vang to form a complex across cell boundary in response to Wnt in *Drosophila*. The cPCP complex located across the cell junction promotes the polarity establishment and coordinates the polarity between cells such that a trichome forms at the distal side where fz is expressed across the wing disc for example (Y. Yang & Mlodzik, 2015). To establish the polarity within a given cell, it has been proposed that fz, as a seven-transmembrane G-protein coupled receptor (GPCR), interacts with G-protein α subunit to instruct the planar polarization. For example, in *Drosophila* wing disc, the G-protein transduces fz signals to establish the trichome formation and orientation. Expression of Gαo, one of the Ptx sensitive G-protein, polarized at the proximal end of the wing cell opposite to fz. This relationship of fz and Gαo distributions is mutually dependent. Expression of hypomorphic allele of Gαo reduces fz localization, while overexpression of Gαo results in broader fz distribution and induces PCP defects such that multiple randomly oriented trichomes are formed in a given wing cell. In the ommatidia of *Drosophila,* overexpression of fz disrupts the cell shape and orientation. These phenotypes could be rescued by expression of Ptx that inhibited Gαi, suggesting that Gαi is required for the function of cPCP proteins in ommatidia orientation (Katanaev et al., 2005; Katanaev & Tomlinson, 2006). In addition, in zebrafish embryos, fz receives Wnt signaling and controls the intracellular calcium release (Slusarski, Corces, & Moon, 1997). This function is inhibited by Ptx expression in the embryos. Taken together these results, the G-proteins are likely to directly transduce the fz-dependent PCP signals from the membrane to downstream components (Katanaev et al., 2005).

The polarity establishment of the stereocilia is Ptx dependent and also utilizes G-proteins (Ezan et al., 2013; Tarchini et al., 2013). Similar to the *Drosophila*, Fz3/6 is asymmetrical distributed in sensory organs of the inner ear (Y. Wang et al., 2006). To establish intracellular polarity, Fz3/6 could interact with Gαi to guide the kinocilium to be polarized at the Fz3/6 side. This process establishes the "default" polarity in the non-Emx2-expressing sensory HCs. However, *Emx2* could activate transcription of other GPCRs to compete with Fz3/6 for binding to Gαi. Since it has been demonstrated that the G-protein activity with fz to Gαi binding is relative low in the *Drosophila* (Nichols, Floyd, Bruinsma, Narzinski, & Baranski, 2013), it is possible that a GPCR with higher activity to Gαi could easily displace the normal binding of Fz3/6 to Gαi. These GPCRs are distributed at the opposite end of the cell from Fz3/6, which lead to reverse polarization of Gαi and establish the "reversed" stereocilia polarity, as observed in cochlear HCs (Fig. 3.2).

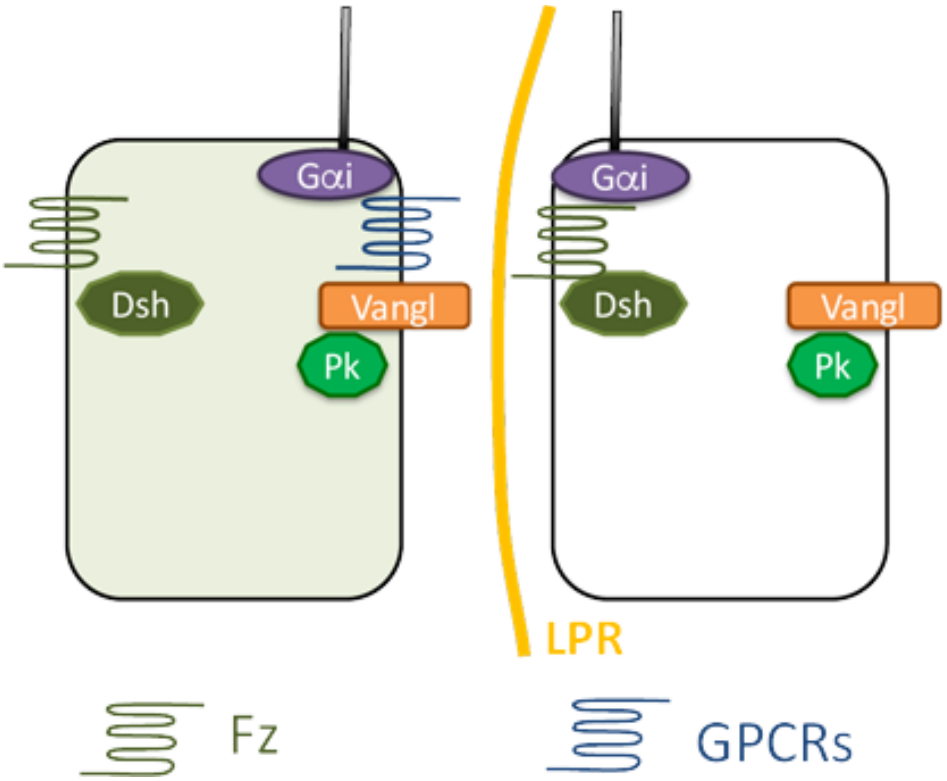

Figure 3.2. G-protein dependent pathway during the establishment of stereocilia orientation. Schematic for the formation of the LPR in the utricle. In the non-*Emx2* expressing cells (white), Gαi interacts with seven-transmembrane protein, Fz (cyan lines), to transduce the polarity signals that polarize the kinocilium at the opposite side of Pk2. However, in the presence of *Emx2* expression (green cells), other GPCRs (orange lines) accumulate on the Pk2 side that opposite to Fz location, and Gαi relocates the kinocilium towards the Pk2 end.

B. *Emx2* regulates the effectors of the cPCP proteins

Alternatively, Emx2 could alter downstream effectors of the cPCP pathway, even though it does not regulate cPCP proteins. Products of *inturned* and *fuzzy* are examples of downstream cPCP signaling. These cPCP effectors in *Drosophila* are known to regulate ciliogenesis and cilia polarity in vertebrates (Wallingford & Mitchell, 2011). Based on studies in *Drosophila* and *Xenopus*, Inturned is asymmetrically located in the cytoplasm close to Vangl/Pk and it is required for docking of basal bodies in the apical

surface such as multi-ciliated cells in frog epidermis (Park et al., 2008). In contrast, Fuzzy does not mediate basal body docking, but cargo trafficking to basal body within the cell and this process is important for ciliogenesis (Gray et al., 2009; Park et al., 2008). It is possible that *Emx2* affects cPCP effectors such as Inturned and Fuzzy, which lead to a switch in stereocilia orientation in HCs.

Another possibility is that Emx2 could be acting via the Scrb/Dlg/Lgl complex. As described in Chapter 1, Scrb (Scribble) is localized to septate junctions (analogous to tight junctions in vertebrates) where it interacts with Dlg (Discs-large) and Lgl (Lethal giant larvae) and form a complex to regulate apical-basal polarity in *Drosophila* epithelial cells (Bilder & Perrimon, 2000; Woods, Hough, Peel, Callaini, & Bryant, 1996). During stereocilia polarization, Scrb interacts genetically with Vangl2 since compound mutants missing one allele of these genes significantly increase the polarity defect in the cochlea (Montcouquiol et al., 2003; Montcouquiol et al., 2006). Scrb and Vangl are also known to interact physically (Montcouquiol et al., 2006). In addition, this complex collaborates with Par/Insc/LGN/Gαi complex to establish apical-basal polarity in other systems (Humbert et al., 2006) and this interaction may apply to stereocilia orientation. Dlg3 shares a similar distribution pattern as Par/Insc/LGN/Gαi complex in cochlear HCs, which could be a component that polarizes the Par/Insc/LGN/Gαi complex (Gegg et al., 2014). Knockout of *Dlg1* resulted in misorientation of cochlear HCs. Thus, the Scrb/Lgl/Dlg complex could receive the intercellular polarity information from cPCP proteins to regulate basal body polarization and docking through its interaction with the Par/Insc/LGN/Gαi complex. Thus, Scrb/Dlg/Lgl complex might interacts with both cPCP and Par/Insc/LGN/Gαi complexes, and the presence of *Emx2* might change the

distribution or function of the Scrb/Dlg/Lgl complex, leading to a switched distribution of Par/Insc/LGN/Gαi complex and reversed stereocilia orientation. Schematic graph of this hypothesis is shown in Fig. 3.3.

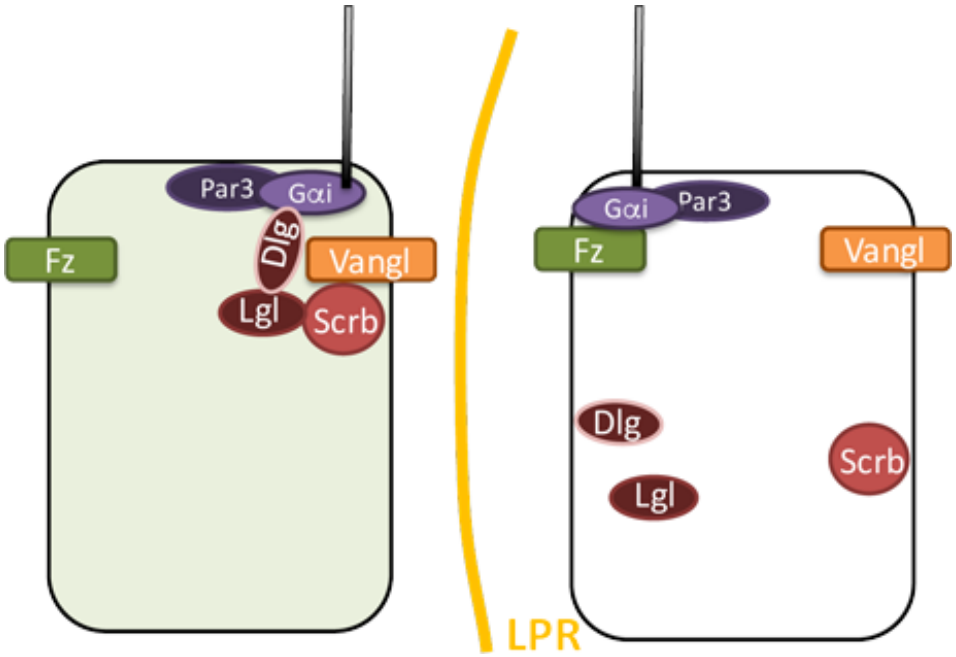

Figure 3.3. *Emx2* changed the Scrb/Dlg/Lgl complex localization. With *Emx2* expressing in the HCs (green), the relative localization within Scrb/Dlg/Lgl complex is changed, which leads to opposite recruitment of Par/Insc/LGN/Gαi complex, while the cPCP proteins maintained their localization.

C. *Emx2* regulates the orientation of microtubules

Furthermore, *Emx2* could invert polarity of stereocilia directly and not involve the cPCP pathway. Within each cell, subcellular structures and proteins are readout of global and intercellular polarity cues. To organize these proteins along an established polarity axis, orientation of microtubules is a key for the protein trafficking (van de Willige, Hoogenraad, & Akhmanova, 2016). Microtubules are oriented such that the plus-ends

are located towards the cell membrane, and the minus-ends are towards the centrosome (Jaffe & Hall, 2005). The NuMA is a known key regulator of spindle orientation. During cell division, NuMA binds to Insc/LGN/Gαi to direct the plus-end microtubules towards the cortical poles (di Pietro et al., 2016). In the *Drosophila* pI cells and S2 cell line, as well as zebrafish epiblast, both fz and dsh are able to recruit NuMA to posterior end of the cell and orient microtubules along the anterior-posterior axis (Segalen et al., 2010). Thus, NuMA guiding microtubules could be the readout of different polarity signals and establish the polarity of cellular organelles. Based on these results, it is possible that NuMA guides the plus-end of microtubules towards the Fz3/6 side in non-*Emx2* expressing HCs to establish the "default" polarity. However, the presence of *Emx2* effectors could directly switch the orientation of microtubule plus-ends within a HC without affecting the distribution of cPCP proteins. The reversed microtubule orientation then changes the Par/Insc/LGN/Gαi complex and NuMA localization and guides the kinocilium migration towards the opposite direction and forms the "reversed" polarity (Ezan et al., 2013).

A possible candidate that regulates the orientation of microtubules is Rho family of small GTPase, which is also regulated by cPCP components (Park et al., 2008). Rho GTPases are responsible for organizing microtubules cytoskeleton and governing cargo trafficking (Jaffe & Hall, 2005; Park et al., 2008). As effectors in polarity establishment (Y. Yang & Mlodzik, 2015), Rho GTPase could bind to intracellular polarity proteins and guide the asymmetric accumulation of the Par/Insc/LGN/Gαi complex (Arimura & Kaibuchi, 2005; Simoes Sde et al., 2010). Knockout two of the Rho family of GTPases, Rac1 and Cdc42, resultes in stereocilia misorientation (Grimsley-Myers et al., 2009;

Kirjavainen et al., 2015). Thus, Rho GTPases are important for establishing stereocilia polarity normally. Effectors of *Emx2* could regulate Rho GTPases directly and change the orientation of microtubules, thereby alter the distribution of Par/Insc/LGN/Gαi complex and kinocilium to the opposite pole of HCs. Schematic illustration of this hypothesis is illustrated in Fig. 3.4.

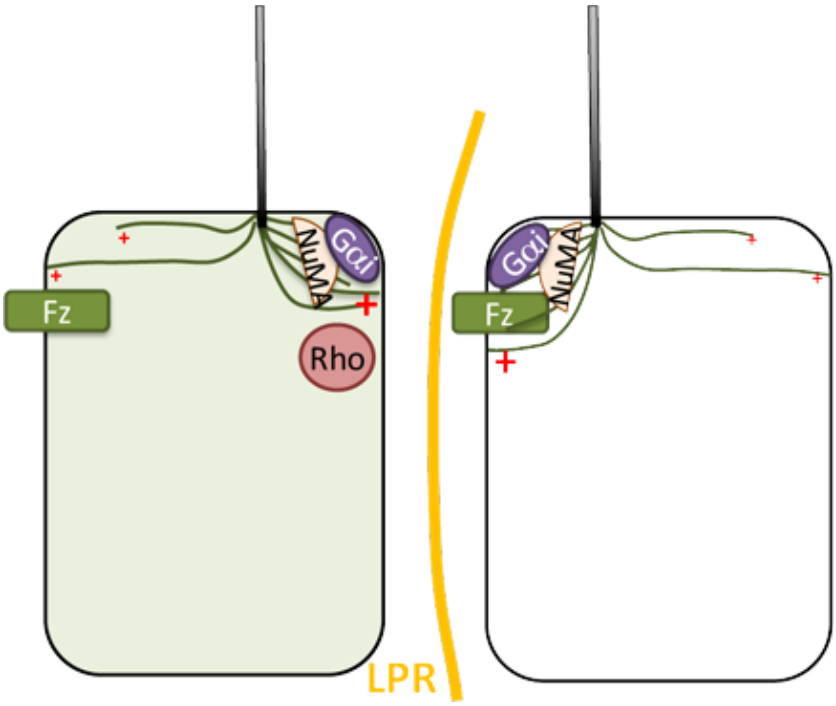

Figure 3.4. Independent regulation of microtubules orientation in the HCs. In establishing the "default" polarity, the orientation of microtubules in HCs is determined by cPCP proteins. Thus, the kinocilium is polarized towards the Fz end. However, in the presence of *Emx2*, the orientation of microtubules is switched, which results in reversed distribution of NuMA and Par/Insc/LGN/Gαi complex and consequently the kinocilium location is reversed.

VI. Other roles of Emx2

A. Role of *Emx2* in cell division

Par/Insc/LGN/Gαi complex is evolutionary conserved, involved in various polarity processes such as orienting spindles during cell division. During neuroblast division,

Par/Insc/LGN/Gαi complex at the cell cortex binds to Dynein/Dynactin complex associated with the microtubules, which then pulls the spindles attached at the minus-end of the microtubules towards one direction. Thus, the location of Par/Insc/LGN/Gαi complex at the cortex mediates symmetric or asymmetric cell division (Burns et al., 2012; Devenport, Oristian, Heller, & Fuchs, 2011; V. Lin et al., 2011; Morin & Bellaiche, 2011; Suzuki & Ohno, 2006). Notably, *Emx2* has been implicated to function in asymmetric and symmetric division of neuronal stem cell in the mouse as demonstrated in Chapter 1. *Emx2* is expressed in the telencephalon during development. Knockout mouse mutants of *Emx2* show a smaller cortex and the dentate gyrus of the hippocampus is missing (Cecchi, 2002). More cells are dividing perpendicular to the ventricular surface (symmetric division) in the *Emx2* expressing cortex compared to the null mutants, suggesting that *Emx2* expressing cells tend to divide symmetrically and maintain the progenitor fate (Heins et al., 2001). Introducing full length cDNA of *Emx2* into isolated embryonic telencephalon neuronal precursor cells promotes more proliferation, which indicates that the *Emx2* promotes symmetric cell divisions and maintains the "stemness" of neural progenitors. In contrast, *Emx2* appears to have opposite effects in adult neural stem cells. Loss of *Emx2* expression in cultures of adult neural stem cells, which normally express *Emx2*, promoted symmetric cell division. Significantly more secondary spheres with more total cell number are observed with *Emx2* loss-of-function cells than wildtype, whereas gain-of-*Emx2* function clones have much less total cell number than wildtype (R. Galli et al., 2002; Gangemi et al., 2001). Although the results from embryonic neuronal precursors and adult stem cells seem to be in conflict, this could be explained by the requirement of *Emx2* at different developmental times. Nevertheless,

these results suggest that *Emx2* is involved in regulation of spindle orientation during cell division, possibly through a similar Par/Insc/LGN/Gαi complex as proposed by mediating stereocilia polarity in HCs.

B. Role of *Emx2* in neuronal migration

During cortical neurogenesis, newly-formed neurons migrate beyond the older deeper neurons to settle in closer to the surface of the cortex. *Emx2* is expressed in the Cajal-Retzius cells of the marginal zone, which are essential for guiding the newborn neurons to radially migrate to the external layer. Loss of *Emx2* function affects radial neuronal migration (Cecchi, 2002; Mallamaci, Mercurio, et al., 2000). Interestingly, Par/Insc/LGN/Gαi complex is also involved in neuronal migration. Neuronal migration is a two-step process with extension of the leading axon followed by soma translocation. This process is coordinated by actin polymerization, cytoskeleton re-organization, and protein relocalization within the neuron. The Par complex is asymmetrically distributed in the migrating neurons, which relocated the centrosomes and provides the microtubule dynamics for neuronal migration. For example, Par6 regulates microtubule elongation, centrosome motility and cell body movements (Goldstein & Macara, 2007; Humbert et al., 2006; Ramahi & Solecki, 2014; Solecki, Govek, & Hatten, 2006). Thus, *Emx2* could also play a role in neuronal migration via the Par/Insc/LGN/Gαi complex.

C. Potential cytoplasmic function of *Emx2*

Another interesting function of *Emx2* stems from the study of olfactory neurons. *Emx2* is located not only in the nucleus of olfactory sensory neurons, but also in the in both axon bundles and terminals of olfactory sensory neurons (Nedelec et al., 2004). The

axonal localization of Emx2 directly interacts with regulator of mRNA translation, the mRNA cap-binding protein eukaryotic translation initiation factor 4E (eIF4E). This non-nucleus localization of Emx2 is proposed to be an evidence for on-site control of protein translation at the axon terminals in the olfactory sensory neurons. In addition to *Emx2,* several other homeodomain proteins such as Otx2 and Engrailed 2, have also been demonstrated to bind eIF4E at the olfactory neurons (Nedelec et al., 2004). These results indicate that Emx2 could function outside of the nucleus at the axonal terminal and may also regulate polarity proteins directly. Further experiments of co-immunoprecipitation of *Emx2* and polarity proteins, together with western blot of cytoplasmic *Emx2* of HCs are needed to examine whether Emx2 could function directly in mediating polarity.

Chapter 4: Future directions

I. Axon guidance

A. Rationale and Hypothesis

Stereocilia displacements of sensory HCs in response to sound in the form of vibrations, and changes in head positions and water pressure lead to neurotransmitter release. Released neurotransmitters are converted by the innervating neurons into action potentials, which propagate to the central nervous system. In the maculae, the innervating afferents are mutually exclusive across the LPR and the central projections of these neurons are also different. Neurons that innervate sensory HCs in LES of the utricle and IR of the saccule project to the cerebellum, whereas neurons that innervate the rest of maculae project to the brainstem (Maklad & Fritzsch, 2003; Maklad et al., 2010). In addition to the maculae, the afferents that innervate the neuromasts are also mutually segregated based on HC polarity. Whereas a single afferent neuron can innervate multiple neuromasts, it only innervates HCs sharing the same polarity (Faucherre et al., 2010; Faucherre et al., 2009; Lopez-Schier et al., 2004; Nagiel et al., 2008). This pattern of afferent organization has been suggested to provide the functional compartmentalization of the maculae and lateral line system (Faucherre et al., 2009; Maklad et al., 2010; Nagiel, Patel, Andor-Ardo, & Hudspeth, 2009). Since my results demonstrated that *Emx2* dictates the LPR formation in both maculae and neuromasts, it is possible that one or some of the downstream effectors of Emx2 regulate specific neuronal projection to the Emx2-positive HCs. The finding that olfactory neurons fail to target the

olfactory bulbs in the *Emx2* knockout mice supports the hypothesis that Emx2 functions in neuronal pathfinding (Pellegrini et al., 1996).

B. Proposed experiments

To test the hypothesis that *Emx2* dictates the innervation pattern of afferents in the maculae and neuromasts, I would like to propose several experiments in both mouse and zebrafish. I would like to conduct lipophilic dye tracing of neuronal trajectories in the gain- and loss-of Emx2 models that I have generated and collected in both mouse and fish. In mice, the lipophilic dye tracing of afferents in the maculae will be conducted according to methods previously described (Maklad & Fritzsch, 2003; Maklad et al., 2010). Filter paper soaked with lipophilic dye will be implanted into the cerebellum and brainstem to examine the retrograde-labeled afferents in the maculae. I will start with the *Emx2* null mutants and move into the $Sox2^{CreER};Rosa^{Emx2}$ and $Gfi1^{Cre};Rosa^{Emx2}$ gain-of-function models if the results from null mutants are promising.

In addition, I would like to use both the gain- and loss-of *emx2* function fish that I have generated to examine the neuronal innervation pattern in the neuromasts. I would like to inject small amount of *HuC:mem-tdTomato* plasmid into various *emx2* mutants crossed with *neuroD:GFP* line in order to label a single tdTomato positive neuron among all the GFP positive neurons to determine the innervation pattern and its relationship to HC polarity (Faucherre et al., 2009).

II. The relationship between Emx2 and the cPCP pathway

A. Rationale and Hypothesis

My results indicated that Emx2 does not mediate its effect via changing the distribution or expression of cPCP proteins. However, Emx2 could function independently or via cPCP effectors. How does cPCP pathway relate it polarity cues to the intracellular polarity pathway is not clear in the inner ear or other well studied systems.

B. Proposed experiments

To address whether Emx2 functions independently or via cPCP effectors, I would like to generate compound heterozygous mutants of *Emx2* and cPCP components such as Vangl2 and Fz. Specifically, I would like to use the $Vangl2^{lp/+}$ for this purpose (Deans et al., 2007). If *Emx2* functions independently of the cPCP pathway, then these compound heterozygous mutants should be normal. If the compound mutants show a phenotype that is not evident in either of the single mutant, it would suggest that Emx2 and the cPCP genetically interact. In principal, given the broad expression domain of *Vangl* and *Emx2*, I could also investigate possible phenotype in the brain and kidney of these compound mutants.

Similar experiments will be performed in zebrafish. I will use the *trilobite* mutants (Mirkovic et al., 2012) to breed with my loss- and gain-of-*emx2* function fish to explore whether the effects of *emx2* is conserved in vertebrates.

III. Screening for downstream targets of Emx2

A. Rationale and Hypothesis

Since *Emx2* encodes a transcription factor, identifying the downstream targets of Emx2 is essential for understanding the mechanism involved in mediating a switch in polarity. RNA-seq is an obvious choice. I have tried the RNA-seq approach by collecting maculae from $Gfi1^{Cre};Rosa^{Emx2/tdT}$ (gain-of-function) and $Gfi1^{Cre};Rosa^{tdT/+}$ (control). My first RNA-seq attempt was not successful. More attempts should be conducted in the future.

B. Proposed experiments

The failed first attempt of RNA-seq could be a technical issue. However, it could also be because the effects of *Emx2* in HCs are confounded by expression profiles from the entire maculae. Thus, for the next step, I would like to conduct single cell RNA-seq experiments. I will set up the same experiments of collecting maculae from $Gfi1^{Cre};Rosa^{Emx2/tdT}$ (gain-of-function) and $Gfi1^{Cre};Rosa^{tdT/+}$ (control) E15.5 embryos. In these macule, all the HCs will be tdTomato-positive and I will dissociate the cells with accutase and proceed to pick individual cells manually under a fluorescent microscope and processed them for RNA-seq. The time point of E15.5 was chosen because there should be enough HCs undergoing polarity establishment at this age. In the long-run, HCs with conditional loss-of *Emx2* function can be pursed for RNA-seq even though the target cell population is smaller than gain-of-function studies. I would like to collect single tdTomato-positive hair cells isolated from $Gfi1^{Cre};Emx2^{lox/+};Rosa^{tdT/+}$ (controls) $Gfi1^{Cre};Emx2^{lox/-};Rosa^{tdT/+}$ (loss-of-function) utricles and saccules. Then, RNA-seq will be performed on these two groups of hair cells.

IV. Functional significance of the LPR

A. Rationale and Hypothesis

What is the functional significance of the LPR? The *Emx2* knockout mice die at birth, which negate the option to study the behavioral consequence from lack of LPR in these mice. I have observed some vestibular phenotypes exhibited by the $Gfi1^{Cre/+};Rosa^{Emx2/+}$ gain-of-function mutants before their death around P20. However, it is difficult to address exclusively the loss of LPR in these mice because the stereocilia polarity is also reversed in all the cristae.

In addition to the $Gfi1^{Cre/+};Rosa^{Emx2/+}$ mice, I have also noticed swimming problems with the gain-of-function *emx2* zebrafish. However, for the same reasons stated for the mice, the stereocilia reversal is also present in the inner ear and the specific function of the LPR in neuromasts cannot be addressed easily. We will not be able to pinpoint the function of the LPR specifically using these mutants. The *emx2* null fish has a similar problem of losing LPR from both inner ear and lateral line. Oddly, the *emx2* null fish seem to swim fine before their demise at 10-12 dpf.

B. Proposed experiments

To address the specific function of LPR in maculae, conditional knock out of Emx2 mice should be generated. I had spent a lot of time in trying to generate the $Emx2^{lox/lox}$ using the embryonic stem cells provided by KOMP. Unfortunately, despite all my efforts, homozygous *Emx2-lox* mice are not viable (see Appendix II). Recently, we received another $Emx2^{lox/lox}$ mouse strain from Dennis O'Leary's lab at Salk. I am excited to be able to generate conditional knockout of *Emx2* using $Gfi1^{Cre}$ strain. In these conditional mutants, I will first address whether the polarity phenotype in the maculae is

recapitulated the *Emx2* nulls. If the LPR is indeed absent in the conditional mutants, I will conduct vestibular testing on these mice such as rotarod, forced swim test, open field tests and vestibular evoked potential. In addition, I will also investigate the cochlear phenotype in these mutants. I always think that the loss of outer HCs in the *Emx2* null mutants is due to an earlier requirement of *Emx2* in the organ of Corti development. The conditional knockout of *Emx2* only in the HCs of the cochlea will allow us to evaluate the requirement of *Emx2* in cochlear HC polarity.

V. Role of Emx2 in other ciliated cells

A. Rationale and Hypothesis

Many ciliated cells are polarized including cells in the node and Kupffer's vesicle, ependymal cells lining the brain ventricles, ciliated cells on epidermis of frogs. Notably, the cPCP pathway is required for cilia polarity in all of these cell types, similar to sensory HCs. Although Emx2 is not known to be expressed in ciliated cells other than sensory HCs, I asked whether there is a common machinery for mediating cilia polarity (i.e. basal body localization) among these ciliated cells and whether Emx2 is sufficient to switch the polarity as in sensory HCs.

B. Proposed experiments

To ask whether Emx2 is mediating a polarity switch via a machinery common to other ciliated cells, I would like to conduct experiments in Kupffer's vesicles and floor plate of zebrafish. First, I would like to confirm data in ZFIN that neither of these two tissues expresses *emx2*. Then, I would like to ectopic express *emx2* in zebrafish to investigate whether polarity is affected in these two tissues.

For the Kupffer's vesicle, I would like to inject *emx2* mRNA into the yolk of one-cell stage zebrafish embryos. Then, I will screen for any heart looping phenotype as a readout of left-right asymmetry defects from a possible perturbation of cilia polarity in the Kupffer's vesicle.

Floor plate cells in zebrafish contain a single cilium that is posteriorly-localized. For expression of *emx2* specifically in the floor plate, I will inject *UAS:emx2-GFP* into one-cell stage zebrafish embryo with a Gal4 promoter specifically expressed in the floor plate, *shh:Gal4*. The position of the cilium in reference to the cell boundary will be revealed using ccd2d2a and ZO-1 antibodies, respectively.

Similar experiments can be attempted in mice, though more time consuming. I can drive *Emx2* expression in the ependymal cells using $GFAP^{Cre}$. The ventricular region will be processed with antibodies to γ-tubulin and β-catenin to identify cilia localization and cell boundary of the ependymal cells.

Appendix I

Expression of *emx2* in the *trilobite* mutant larvae

To test if the expression of *emx2* is disturbed in the *vangl2* mutant, *trilobite,* I stained *trilobite* mutants at 3dpf with anti-Emx2 antibody. Larvae were processed for anti-emx2 staining, phalloidin to determine bundle orientation, and anti-parvalbumin to label each HC. In the littermate controls, HCs are polarized half and half in opposite direction along the dorsal-ventral, or anterior-posterior, respectively. The expression of emx2 within these neuromasts are preferentially aligned on one side of the neuromasts (Fig A.1A-A"). In the *trilobite* mutant, the stereocilia are randomly oriented, consistent with published data (Mirkovic et al., 2012). Emx2 are normally expressed in half of the HCs pointing in the same direction within a given neuromast. However, the emx2-expressing cells are no longer aligned at one side but randomly distributed within the neuromast (Fig. A.1B-B"). Thus, these results indicate that it is not the expression of emx2 but the alignment of emx2-expressing cells are disrupted by the *vangl* mutation.

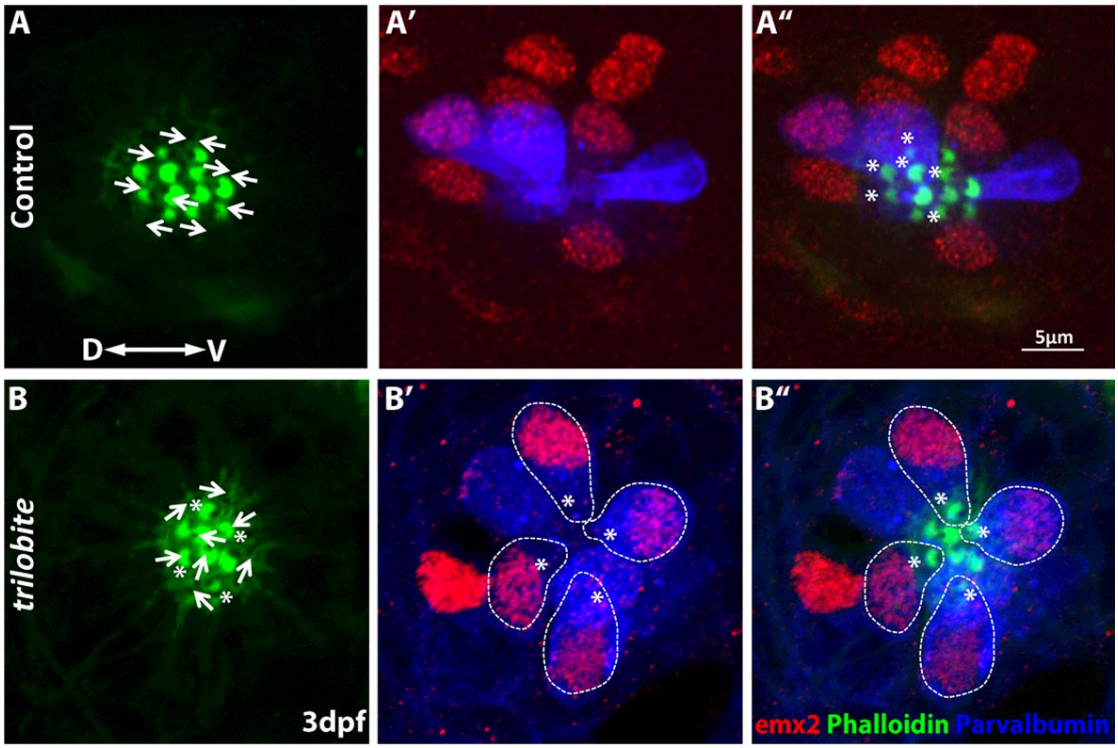

Figure A.1. emx2-expressing cells are randomly distributed in the neuromast of *trilobite* mutant. (A-A") In the control neuromast, HCs are aligned along dorsal-ventral axis. The emx2-expressing cells are facing ventral, which are aligned mostly in relative dorsal side of a D-V oriented neuromast (n=10, 3 experiments, 6 fishes). (B-B") Compared to the littermate controls (A-A"), HCs are randomly oriented in the *trilobite* mutants (B), and emx2-expressing cells (dashed-line circled) are no longer preferentially located to one side of the neuromast (n=20, 3 experiments, 5 fishes). Arrows indicate the orientation of HCs. Asterisks are marking the emx2-expressing cells. Arrowhead represents the expression of emx2 in non-HC.

Appendix II

Generation of *Emx2 lox* mice.

Given that the *Emx2* null mice die right after birth due to lack of the urogenital system, I wanted to generate conditional knockout mice for further studies of *Emx2* function specifically in the ear. There are several questions raised by my results shown in Chapter 2. First, what is the specific requirement of *Emx2* in the HCs and what is the role of Emx2 in supporting cells since *Emx2* is expressed in both cell types? Second, what is the functional significance of the LPR in the maculae as I have pointed out in Chapter 4. To answer these questions, tissue- and cell-specific knockout mutant of *Emx2* mice are needed.

We obtained the $Emx2^{lox/+}$ embryonic stem cells from KOMP (Fig. A.2). A targeted cassette containing *lacZ* as a reporter and neomycin as a drug selector was inserted from Exon1 to Exon3 of *Emx2*. After flipping out the *lacZ* and Neomycin in between the two FRT sites with flp, I obtained the $Emx2^{lox/+}$ mice. However, homozygous $Emx2^{lox/lox}$ is not viable and I was never able to obtain any embryos that are homozygous, even as early as E7.5. These results suggest a potential lethal effect caused by loxP insertions into introns of Exon2. In addition, I had bred $Emx2^{lox/+}$ mice with a ubiquitous cre strain, β-$actin^{Cre/+}$mice to determine if the recombination by cre was correct. However, no successful recombination has been identified thus far. Thus, there could be deleterious effects resulting from cre recombination, which will need further exploration.

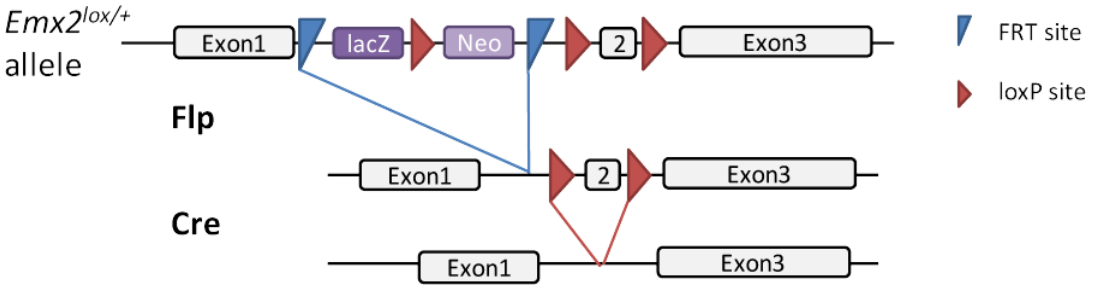

Figure A.2. Schematic of *Emx2*$^{lox/+}$ mice and the breeding strategy. A reporter cassette was inserted in the introns of *Emx2* to generate *Emx2*$^{lox/+}$ mice. The sequence between two FRT sites (blue tringle) was removed first. Then, with specific Cre recombinase, the sequence between the two remaining loxP sites (red tringle) was removed. Thus, the Exon2 can be deleted in a tissue-specific manner.

Bibliography

Ambegaonkar, A. A., Pan, G., Mani, M., Feng, Y., & Irvine, K. D. (2012). Propagation of Dachsous-Fat planar cell polarity. *Curr Biol, 22*(14), 1302-1308. doi:10.1016/j.cub.2012.05.049

Andreeva, A., Lee, J., Lohia, M., Wu, X., Macara, I. G., & Lu, X. (2014). PTK7-Src signaling at epithelial cell contacts mediates spatial organization of actomyosin and planar cell polarity. *Dev Cell, 29*(1), 20-33. doi:10.1016/j.devcel.2014.02.008

Arimura, N., & Kaibuchi, K. (2005). Key regulators in neuronal polarity. *Neuron, 48*(6), 881-884. doi:10.1016/j.neuron.2005.11.007

Arnold, K., Sarkar, A., Yram, M. A., Polo, J. M., Bronson, R., Sengupta, S., . . . Hochedlinger, K. (2011). Sox2(+) adult stem and progenitor cells are important for tissue regeneration and survival of mice. *Cell Stem Cell, 9*(4), 317-329. doi:10.1016/j.stem.2011.09.001

Ayukawa, T., Akiyama, M., Mummery-Widmer, J. L., Stoeger, T., Sasaki, J., Knoblich, J. A., . . . Yamazaki, M. (2014). Dachsous-dependent asymmetric localization of spiny-legs determines planar cell polarity orientation in Drosophila. *Cell Rep, 8*(2), 610-621. doi:10.1016/j.celrep.2014.06.009

Backman, M., Machon, O., Mygland, L., van den Bout, C. J., Zhong, W., Taketo, M. M., & Krauss, S. (2005). Effects of canonical Wnt signaling on dorso-ventral specification of the mouse telencephalon. *Dev Biol, 279*(1), 155-168. doi:10.1016/j.ydbio.2004.12.010

Bayly, R., & Axelrod, J. D. (2011). Pointing in the right direction: new developments in the field of planar cell polarity. *Nat Rev Genet, 12*(6), 385-391. doi:10.1038/nrg2956

Beauchemin, M., Del Rio-Tsonis, K., Tsonis, P. A., Tremblay, M., & Savard, P. (1998). Graded expression of Emx-2 in the adult newt limb and its corresponding regeneration blastema. *J Mol Biol, 279*(3), 501-511.

Bell, E., Ensini, M., Gulisano, M., & Lumsden, A. (2001). Dynamic domains of gene expression in the early avian forebrain. *Dev Biol, 236*(1), 76-88. doi:10.1006/dbio.2001.0301

Bellaiche, Y., Radovic, A., Woods, D. F., Hough, C. D., Parmentier, M. L., O'Kane, C. J., . . . Schweisguth, F. (2001). The Partner of Inscuteable/Discs-large complex is required to establish planar polarity during asymmetric cell division in Drosophila. *Cell, 106*(3), 355-366.

Berger, M. F., Badis, G., Gehrke, A. R., Talukder, S., Philippakis, A. A., Pena-Castillo, L., . . . Hughes, T. R. (2008). Variation in homeodomain DNA binding revealed by high-resolution analysis of sequence preferences. *Cell, 133*(7), 1266-1276. doi:10.1016/j.cell.2008.05.024

Bergstralh, D. T., Lovegrove, H. E., & St Johnston, D. (2013). Discs large links spindle orientation to apical-basal polarity in Drosophila epithelia. *Curr Biol, 23*(17), 1707-1712. doi:10.1016/j.cub.2013.07.017

Bertet, C., & Lecuit, T. (2009). Planar polarity and short-range polarization in Drosophila embryos. *Semin Cell Dev Biol, 20*(8), 1006-1013. doi:10.1016/j.semcdb.2009.05.004

Besson, C., Bernard, F., Corson, F., Rouault, H., Reynaud, E., Keder, A., . . . Schweisguth, F. (2015). Planar Cell Polarity Breaks the Symmetry of PAR Protein Distribution prior to Mitosis in Drosophila Sensory Organ Precursor Cells. *Curr Biol, 25*(8), 1104-1110. doi:10.1016/j.cub.2015.02.073

Bilder, D., & Perrimon, N. (2000). Localization of apical epithelial determinants by the basolateral PDZ protein Scribble. *Nature, 403*(6770), 676-680. doi:10.1038/35001108

Bishop, K. M., Garel, S., Nakagawa, Y., Rubenstein, J. L., & O'Leary, D. D. (2003). Emx1 and Emx2 cooperate to regulate cortical size, lamination, neuronal differentiation, development of cortical efferents, and thalamocortical pathfinding. *J Comp Neurol, 457*(4), 345-360. doi:10.1002/cne.10549

Bok, J., Chang, W., & Wu, D. K. (2007). Patterning and morphogenesis of the vertebrate inner ear. *Int J Dev Biol, 51*(6-7), 521-533. doi:10.1387/ijdb.072381jb

Bok, J., Zenczak, C., Hwang, C. H., & Wu, D. K. (2013). Auditory ganglion source of Sonic hedgehog regulates timing of cell cycle exit and differentiation of mammalian cochlear hair cells. *Proc Natl Acad Sci U S A, 110*(34), 13869-13874. doi:10.1073/pnas.1222341110

Borovina, A., Superina, S., Voskas, D., & Ciruna, B. (2010). Vangl2 directs the posterior tilting and asymmetric localization of motile primary cilia. *Nat Cell Biol, 12*(4), 407-412. doi:10.1038/ncb2042

Boutin, C., Labedan, P., Dimidschstein, J., Richard, F., Cremer, H., Andre, P., . . . Tissir, F. (2014). A dual role for planar cell polarity genes in ciliated cells. *Proc Natl Acad Sci U S A, 111*(30), E3129-3138. doi:10.1073/pnas.1404988111

Briata, P., Di Blas, E., Gulisano, M., Mallamaci, A., Iannone, R., Boncinelli, E., & Corte, G. (1996). EMX1 homeoprotein is expressed in cell nuclei of the developing cerebral cortex and in the axons of the olfactory sensory neurons. *Mech Dev, 57*(2), 169-180.

Brittle, A., Thomas, C., & Strutt, D. (2012). Planar polarity specification through asymmetric subcellular localization of Fat and Dachsous. *Curr Biol, 22*(10), 907-914. doi:10.1016/j.cub.2012.03.053

Brittle, A. L., Repiso, A., Casal, J., Lawrence, P. A., & Strutt, D. (2010). Four-jointed modulates growth and planar polarity by reducing the affinity of dachsous for fat. *Curr Biol, 20*(9), 803-810. doi:10.1016/j.cub.2010.03.056

Burns, J. C., On, D., Baker, W., Collado, M. S., & Corwin, J. T. (2012). Over half the hair cells in the mouse utricle first appear after birth, with significant numbers

originating from early postnatal mitotic production in peripheral and striolar growth zones. *J Assoc Res Otolaryngol, 13*(5), 609-627. doi:10.1007/s10162-012-0337-0

Caddy, J., Wilanowski, T., Darido, C., Dworkin, S., Ting, S. B., Zhao, Q., . . . Jane, S. M. (2010). Epidermal wound repair is regulated by the planar cell polarity signaling pathway. *Dev Cell, 19*(1), 138-147. doi:10.1016/j.devcel.2010.06.008

Campos-Ortega, J. A., & Hartenstein, V. (1985). The embryonic development of Drosophila melanogaster.

Carbonetti, N. H. (2010). Pertussis toxin and adenylate cyclase toxin: key virulence factors of Bordetella pertussis and cell biology tools. *Future Microbiology, 5*(3), 455-469.

Cardenas-Rodriguez, M., & Badano, J. L. (2009). Ciliary biology: understanding the cellular and genetic basis of human ciliopathies. *Am J Med Genet C Semin Med Genet, 151C*(4), 263-280. doi:10.1002/ajmg.c.30227

Cecchi, C. (2002). Emx2: a gene responsible for cortical development, regionalization and area specification. *Gene, 291*(1-2), 1-9.

Cecchi, C., & Boncinelli, E. (2000). Emx homeogenes and mouse brain development. *Trends Neurosci, 23*(8), 347-352.

Chitnis, A. B., Nogare, D. D., & Matsuda, M. (2012). Building the posterior lateral line system in zebrafish. *Dev Neurobiol, 72*(3), 234-255. doi:10.1002/dneu.20962

Copley, C. O., Duncan, J. S., Liu, C., Cheng, H., & Deans, M. R. (2013). Postnatal refinement of auditory hair cell planar polarity deficits occurs in the absence of Vangl2. *J Neurosci, 33*(35), 14001-14016. doi:10.1523/JNEUROSCI.1307-13.2013

Dabdoub, A., Donohue, M. J., Brennan, A., Wolf, V., Montcouquiol, M., Sassoon, D. A., . . . Kelley, M. W. (2003). Wnt signaling mediates reorientation of outer hair cell stereociliary bundles in the mammalian cochlea. *Development, 130*(11), 2375-2384. doi:10.1242/dev.00448

Dalton, D., Chadwick, R., & McGinnis, W. (1989). Expression and embryonic function of empty spiracles: a Drosophila homeo box gene with two patterning functions on the anterior-posterior axis of the embryo. *Genes Dev, 3*(12A), 1940-1956.

Dawe, H. R., Farr, H., & Gull, K. (2007). Centriole/basal body morphogenesis and migration during ciliogenesis in animal cells. *J Cell Sci, 120*(Pt 1), 7-15. doi:10.1242/jcs.03305

Deans, M. R. (2013). A balance of form and function: planar polarity and development of the vestibular maculae. *Semin Cell Dev Biol, 24*(5), 490-498. doi:10.1016/j.semcdb.2013.03.001

Deans, M. R., Antic, D., Suyama, K., Scott, M. P., Axelrod, J. D., & Goodrich, L. V. (2007). Asymmetric distribution of prickle-like 2 reveals an early underlying polarization of vestibular sensory epithelia in the inner ear. *J Neurosci, 27*(12), 3139-3147. doi:10.1523/JNEUROSCI.5151-06.2007

Denman-Johnson, K., & Forge, A. (1999). Establishment of hair bundle polarity and orientation in the developing vestibular system of the mouse. *J Neurocytol, 28*(10-11), 821-835.

Desai, S. S., Zeh, C., & Lysakowski, A. (2005). Comparative morphology of rodent vestibular periphery. I. Saccular and utricular maculae. *J Neurophysiol, 93*(1), 251-266. doi:10.1152/jn.00746.2003

Devenport, D. (2016). Tissue morphodynamics: Translating planar polarity cues into polarized cell behaviors. *Semin Cell Dev Biol, 55*, 99-110. doi:10.1016/j.semcdb.2016.03.012

Devenport, D., Oristian, D., Heller, E., & Fuchs, E. (2011). Mitotic internalization of planar cell polarity proteins preserves tissue polarity. *Nat Cell Biol, 13*(8), 893-902. doi:10.1038/ncb2284

di Pietro, F., Echard, A., & Morin, X. (2016). Regulation of mitotic spindle orientation: an integrated view. *EMBO Rep, 17*(8), 1106-1130. doi:10.15252/embr.201642292

Doherty, D., Chudley, A. E., Coghlan, G., Ishak, G. E., Innes, A. M., Lemire, E. G., . . . Zelinski, T. (2012). GPSM2 mutations cause the brain malformations and hearing loss in Chudley-McCullough syndrome. *Am J Hum Genet, 90*(6), 1088-1093. doi:10.1016/j.ajhg.2012.04.008

Duckert, L. G., & Rubel, E. W. (1993). Morphological correlates of functional recovery in the chicken inner ear after gentamycin treatment. *J Comp Neurol, 331*(1), 75-96. doi:10.1002/cne.903310105

Eatock, R. A., & Songer, J. E. (2011). Vestibular hair cells and afferents: two channels for head motion signals. *Annu Rev Neurosci, 34*, 501-534. doi:10.1146/annurev-neuro-061010-113710

Essner, J. J., Amack, J. D., Nyholm, M. K., Harris, E. B., & Yost, H. J. (2005). Kupffer's vesicle is a ciliated organ of asymmetry in the zebrafish embryo that initiates left-right development of the brain, heart and gut. *Development, 132*(6), 1247-1260. doi:10.1242/dev.01663

Etienne-Manneville, S. (2004). Cdc42--the centre of polarity. *J Cell Sci, 117*(Pt 8), 1291-1300. doi:10.1242/jcs.01115

Ezan, J., Lasvaux, L., Gezer, A., Novakovic, A., May-Simera, H., Belotti, E., . . . Montcouquiol, M. (2013). Primary cilium migration depends on G-protein signalling control of subapical cytoskeleton. *Nat Cell Biol, 15*(9), 1107-1115. doi:10.1038/ncb2819

Faucherre, A., Baudoin, J. P., Pujol-Marti, J., & Lopez-Schier, H. (2010). Multispectral four-dimensional imaging reveals that evoked activity modulates peripheral arborization and the selection of plane-polarized targets by sensory neurons. *Development, 137*(10), 1635-1643. doi:10.1242/dev.047316

Faucherre, A., Pujol-Marti, J., Kawakami, K., & Lopez-Schier, H. (2009). Afferent neurons of the zebrafish lateral line are strict selectors of hair-cell orientation. *PLoS One, 4*(2), e4477. doi:10.1371/journal.pone.0004477

Galli, R., Fiocco, R., De Filippis, L., Muzio, L., Gritti, A., Mercurio, S., . . . Vescovi, A. L. (2002). Emx2 regulates the proliferation of stem cells of the adult mammalian central nervous system. *Development, 129*(7), 1633-1644.

Galli, R., Fiocco, R., Filippis, L. D., Muzio, L., Gritti, A., Mercurio, S., . . . Vescovi, A. L. (2002). Emx2 regulates the proliferation of stem cells of the adult mammalian central nervous system. *Development, 129*, 1633-1644.

Gangemi, R. M., Daga, A., Marubbi, D., Rosatto, N., Capra, M. C., & Corte, G. (2001). Emx2 in adult neural precursor cells. *Mech Dev, 109*(2), 323-329.

Gangemi, R. M., Daga, A., Muzio, L., Marubbi, D., Cocozza, S., Perera, M., . . . Corte, G. (2006). Effects of Emx2 inactivation on the gene expression profile of neural precursors. *Eur J Neurosci, 23*(2), 325-334. doi:10.1111/j.1460-9568.2005.04559.x

Gao, B., Song, H., Bishop, K., Elliot, G., Garrett, L., English, M. A., . . . Yang, Y. (2011). Wnt signaling gradients establish planar cell polarity by inducing Vangl2 phosphorylation through Ror2. *Dev Cell, 20*(2), 163-176. doi:10.1016/j.devcel.2011.01.001

Gegg, M., Böttcher, A., Burtscher, n., Hasenoeder, S., Campenhout, C. V., Aichler, M., . . . Lickert, H. (2014). Flattop regulates basal body docking and positioning in mono- and multiciliated cells. *eLife*. doi:10.7554/eLife.03842.001

10.7554/eLife.03842.002

Ghysen, A., & Dambly-Chaudiere, C. (2007). The lateral line microcosmos. *Genes Dev, 21*(17), 2118-2130. doi:10.1101/gad.1568407

Giese, A. P., Ezan, J., Wang, L., Lasvaux, L., Lembo, F., Mazzocco, C., . . . Montcouquiol, M. (2012). Gipc1 has a dual role in Vangl2 trafficking and hair bundle integrity in the inner ear. *Development, 139*(20), 3775-3785. doi:10.1242/dev.074229

Gohla, A., Klement, K., Piekorz, R. P., Pexa, K., vom Dahl, S., Spicher, K., . . . Nurnberg, B. (2007). An obligatory requirement for the heterotrimeric G protein Gi3 in the antiautophagic action of insulin in the liver. *Proc Natl Acad Sci U S A, 104*(8), 3003-3008. doi:10.1073/pnas.0611434104

Goldstein, B., & Macara, I. G. (2007). The PAR proteins: fundamental players in animal cell polarization. *Dev Cell, 13*(5), 609-622. doi:10.1016/j.devcel.2007.10.007

Goodrich, L. V., & Strutt, D. (2011). Principles of planar polarity in animal development. *Development, 138*(10), 1877-1892. doi:10.1242/dev.054080

Goodyear, R., Killick, R., Legan, P. K., & Richardson, G. P. (1996). Distribution of beta-tectorin mRNA in the early posthatch and developing avian inner ear. *Hear Res, 96*(1-2), 167-178.

Gray, R. S., Abitua, P. B., Wlodarczyk, B. J., Szabo-Rogers, H. L., Blanchard, O., Lee, I., . . . Finnell, R. H. (2009). The planar cell polarity effector Fuz is essential for targeted membrane trafficking, ciliogenesis and mouse embryonic development. *Nat Cell Biol, 11*(10), 1225-1232. doi:10.1038/ncb1966

Gray, R. S., Roszko, I., & Solnica-Krezel, L. (2011). Planar cell polarity: coordinating morphogenetic cell behaviors with embryonic polarity. *Dev Cell, 21*(1), 120-133. doi:10.1016/j.devcel.2011.06.011

Green, J. L., Inoue, T., & Sternberg, P. W. (2008). Opposing Wnt pathways orient cell polarity during organogenesis. *Cell, 134*(4), 646-656. doi:10.1016/j.cell.2008.06.026

Grifoni, D., Froldi, F., & Pession, A. (2013). Connecting epithelial polarity, proliferation and cancer in Drosophila: the many faces of lgl loss of function. *Int J Dev Biol, 57*(9-10), 677-687. doi:10.1387/ijdb.130285dg

Grimsley-Myers, C. M., Sipe, C. W., Geleoc, G. S., & Lu, X. (2009). The small GTPase Rac1 regulates auditory hair cell morphogenesis. *J Neurosci, 29*(50), 15859-15869. doi:10.1523/JNEUROSCI.3998-09.2009

Gubb, D., Green, C., Huen, D., Coulson, D., Johnson, G., Tree, D., . . . Roote, J. (1999). The balance between isoforms of the prickle LIM domain protein is critical for planar polarity in Drosophila imaginal discs. *Genes Dev, 13*(17), 2315-2327.

Guirao, B., Meunier, A., Mortaud, S., Aguilar, A., Corsi, J. M., Strehl, L., . . . Spassky, N. (2010). Coupling between hydrodynamic forces and planar cell polarity orients mammalian motile cilia. *Nat Cell Biol, 12*(4), 341-350. doi:10.1038/ncb2040

Guo, J., Yang, Z., Song, W., Chen, Q., Wang, F., Zhang, Q., & Zhu, X. (2006). Nudel contributes to microtubule anchoring at the mother centriole and is involved in both dynein-dependent and -independent centrosomal protein assembly. *Mol Biol Cell, 17*(2), 680-689. doi:10.1091/mbc.E05-04-0360

Haffter, P., Granato, M., Brand, M., Mullins, M. C., Hammerschmidt, M., Kane, D. A., . . . Nusslein-Volhard, C. (1996). The identification of genes with unique and essential functions in the development of the zebrafish, Danio rerio. *Development, 123*, 1-36.

Hale, R., Brittle, A. L., Fisher, K. H., Monk, N. A., & Strutt, D. (2015). Cellular interpretation of the long-range gradient of Four-jointed activity in the Drosophila wing. *eLife, 4*. doi:10.7554/eLife.05789

Hammond, K. L., & Whitfield, T. T. (2006). The developing lamprey ear closely resembles the zebrafish otic vesicle: otx1 expression can account for all major patterning differences. *Development, 133*(7), 1347-1357. doi:10.1242/dev.02306

Hartmann, B., Hirth, F., Walldorf, U., & Reichert, H. (2000). Expression, regulation and function of the homeobox gene empty spiracles in brain and ventral nerve cord development of Drosophila. *Mech Dev, 90*(2), 143-153. doi:10.1016/s0925-4773(99)00237-3

Harumoto, T., Ito, M., Shimada, Y., Kobayashi, T. J., Ueda, H. R., Lu, B., & Uemura, T. (2010). Atypical cadherins Dachsous and Fat control dynamics of noncentrosomal microtubules in planar cell polarity. *Dev Cell, 19*(3), 389-401. doi:10.1016/j.devcel.2010.08.004

Hebert, J. M., & McConnell, S. K. (2000). Targeting of cre to the Foxg1 (BF-1) locus mediates loxP recombination in the telencephalon and other developing head structures. *Dev Biol, 222*(2), 296-306. doi:10.1006/dbio.2000.9732

Heins, N., Cremisi, F., Malatesta, P., Gangemi, R. M., Corte, G., Price, J., . . . Gotz, M. (2001). Emx2 promotes symmetric cell divisions and a multipotential fate in precursors from the cerebral cortex. *Mol Cell Neurosci, 18*(5), 485-502. doi:10.1006/mcne.2001.1046

Hirokawa, N., Tanaka, Y., Okada, Y., & Takeda, S. (2006). Nodal flow and the generation of left-right asymmetry. *Cell, 125*(1), 33-45. doi:10.1016/j.cell.2006.03.002

Holley, M., Rhodes, C., Kneebone, A., Herde, M. K., Fleming, M., & Steel, K. P. (2010). Emx2 and early hair cell development in the mouse inner ear. *Dev Biol, 340*(2), 547-556. doi:10.1016/j.ydbio.2010.02.004

Hudspeth, A. J., & Corey, D. P. (1977). Sensitivity, polarity, and conductance change in the response of vertebrate hair cells to controlled mechanical stimuli. *Proc Natl Acad Sci U S A, 74*(6), 2407-2411.

Humbert, P. O., Dow, L. E., & Russell, S. M. (2006). The Scribble and Par complexes in polarity and migration: friends or foes? *Trends Cell Biol, 16*(12), 622-630. doi:10.1016/j.tcb.2006.10.005

Huss, D., Navaluri, R., Faulkner, K. F., & Dickman, J. D. (2010). Development of otolith receptors in Japanese quail. *Dev Neurobiol, 70*(6), 436-455. doi:10.1002/dneu.20787

Iler, N., Rowitch, D. H., Echelard, Y., McMahon, A. P., & Abate-Shen, C. (1995). A single homeodomain binding site restricts spatial expression of Wnt-1 in the developing brain. *Mech Dev, 53*(1), 87-96.

Jaffe, A. B., & Hall, A. (2005). Rho GTPases: biochemistry and biology. *Annu Rev Cell Dev Biol, 21*, 247-269. doi:10.1146/annurev.cellbio.21.020604.150721

Jenny, A. (2010). Planar Cell Polarity Signaling in the Drosophila Eye. *Curr Top Dev Biol, 93*, 189-227. doi:10.1016/B978-0-12-385044-7.00007-2

10.1016/S0070-2153(10)93007-X

Jenny, A., Reynolds-Kenneally, J., Das, G., Burnett, M., & Mlodzik, M. (2005). Diego and Prickle regulate Frizzled planar cell polarity signalling by competing for Dishevelled binding. *Nat Cell Biol, 7*(7), 691-697. doi:10.1038/ncb1271

Jones, C., Qian, D., Kim, S. M., Li, S., Ren, D., Knapp, L., . . . Chen, P. (2014). Ankrd6 is a mammalian functional homolog of Drosophila planar cell polarity gene diego and regulates coordinated cellular orientation in the mouse inner ear. *Dev Biol, 395*(1), 62-72. doi:10.1016/j.ydbio.2014.08.029

Jones, C., Roper, V. C., Foucher, I., Qian, D., Banizs, B., Petit, C., . . . Chen, P. (2008). Ciliary proteins link basal body polarization to planar cell polarity regulation. *Nat Genet, 40*(1), 69-77. doi:10.1038/ng.2007.54

Jurgens, G., Wieschaus, E., Nussleinvolhard, C., & Kluding, H. (1984). Mutations Affecting the Pattern of the Larval Cuticle in Drosophila-Melanogaster .2. Zygotic Loci on the 3rd Chromosome. *Wilhelm Rouxs Archives of Developmental Biology, 193*(5), 283-295.

Katada, T. (2012). The inhibitory G protein G(i) identified as pertussis toxin-catalyzed ADP-ribosylation. *Biol Pharm Bull, 35*(12), 2103-2111.

Katanaev, V. L., Ponzielli, R., Semeriva, M., & Tomlinson, A. (2005). Trimeric G protein-dependent frizzled signaling in Drosophila. *Cell, 120*(1), 111-122. doi:10.1016/j.cell.2004.11.014

Katanaev, V. L., & Tomlinson, A. (2006). Multiple roles of a trimeric G protein in Drosophila cell polarization. *Cell Cycle, 5*(21), 2464-2472. doi:10.4161/cc.5.21.3410

Kawahara, A., & Dawid, I. B. (2002). Developmental expression of zebrafish emx1 during early embryogenesis. *Gene Expr Patterns, 2*(3-4), 201-206. doi:10.1016/s1567-133x(02)00062-5

Kibar, Z., Vogan, K. J., Groulx, N., Justice, M. J., Underhill, D. A., & Gros, P. (2001). Ltap, a mammalian homolog of Drosophila Strabismus/Van Gogh, is altered in the mouse neural tube mutant Loop-tail. *Nat Genet, 28*(3), 251-255. doi:10.1038/90081

Kiernan, A. E., Steel, K. P., & Fekete, D. M. (2002). Development of the mouse inner ear.

Kimura, J., Suda, Y., Kurokawa, D., Hossain, Z. M., Nakamura, M., Takahashi, M., . . . Aizawa, S. (2005). Emx2 and Pax6 function in cooperation with Otx2 and Otx1 to develop caudal forebrain primordium that includes future archipallium. *J Neurosci, 25*(21), 5097-5108. doi:10.1523/JNEUROSCI.0239-05.2005

Kindt, K. S., Finch, G., & Nicolson, T. (2012). Kinocilia mediate mechanosensitivity in developing zebrafish hair cells. *Dev Cell, 23*(2), 329-341. doi:10.1016/j.devcel.2012.05.022

Kirjavainen, A., Laos, M., Anttonen, T., & Pirvola, U. (2015). The Rho GTPase Cdc42 regulates hair cell planar polarity and cellular patterning in the developing cochlea. *Biol Open, 4*(4), 516-526. doi:10.1242/bio.20149753

Kramer-Zucker, A. G., Olale, F., Haycraft, C. J., Yoder, B. K., Schier, A. F., & Drummond, I. A. (2005). Cilia-driven fluid flow in the zebrafish pronephros, brain and Kupffer's vesicle is required for normal organogenesis. *Development, 132*(8), 1907-1921. doi:10.1242/dev.01772

Kusaka, M., Katoh-Fukui, Y., Ogawa, H., Miyabayashi, K., Baba, T., Shima, Y., . . . Morohashi, K. (2010). Abnormal epithelial cell polarity and ectopic epidermal growth factor receptor (EGFR) expression induced in Emx2 KO embryonic gonads. *Endocrinology, 151*(12), 5893-5904. doi:10.1210/en.2010-0915

Kwan, K. M., Fujimoto, E., Grabher, C., Mangum, B. D., Hardy, M. E., Campbell, D. S., . . . Chien, C. B. (2007). The Tol2kit: a multisite gateway-based construction kit

for Tol2 transposon transgenesis constructs. *Dev Dyn, 236*(11), 3088-3099. doi:10.1002/dvdy.21343

Lamouille, S., Xu, J., & Derynck, R. (2014). Molecular mechanisms of epithelial-mesenchymal transition. *Nat Rev Mol Cell Biol, 15*(3), 178-196. doi:10.1038/nrm3758

Lancaster, M. A., & Knoblich, J. A. (2012). Spindle orientation in mammalian cerebral cortical development. *Curr Opin Neurobiol, 22*(5), 737-746. doi:10.1016/j.conb.2012.04.003

Lawrence, P. A., Struhl, G., & Casal, J. (2007). Planar cell polarity: one or two pathways? *Nat Rev Genet, 8*(7), 555-563. doi:10.1038/nrg2125

Lee, H., & Adler, P. N. (2004). The grainy head transcription factor is essential for the function of the frizzled pathway in the Drosophila wing. *Mechanisms of Development, 121*(1), 37-49. doi:10.1016/j.mod.2003.11.002

Lee, J., Andreeva, A., Sipe, C. W., Liu, L., Cheng, A., & Lu, X. (2012). PTK7 regulates myosin II activity to orient planar polarity in the mammalian auditory epithelium. *Curr Biol, 22*(11), 956-966. doi:10.1016/j.cub.2012.03.068

Li, A., Xue, J., & Peterson, E. H. (2008). Architecture of the mouse utricle: macular organization and hair bundle heights. *J Neurophysiol, 99*(2), 718-733. doi:10.1152/jn.00831.2007

Lin, V., Golub, J. S., Nguyen, T. B., Hume, C. R., Oesterle, E. C., & Stone, J. S. (2011). Inhibition of Notch activity promotes nonmitotic regeneration of hair cells in the adult mouse utricles. *J Neurosci, 31*(43), 15329-15339. doi:10.1523/JNEUROSCI.2057-11.2011

Lin, Y. Y., & Gubb, D. (2009). Molecular dissection of Drosophila Prickle isoforms distinguishes their essential and overlapping roles in planar cell polarity. *Dev Biol, 325*(2), 386-399. doi:10.1016/j.ydbio.2008.10.042

Liu, S., Gao, X., Qin, Y., Liu, W., Huang, T., Ma, J., . . . Chen, Z. J. (2015). Nonsense mutation of EMX2 is potential causative for uterus didelphysis: first molecular explanation for isolated incomplete mullerian fusion. *Fertil Steril, 103*(3), 769-774 e762. doi:10.1016/j.fertnstert.2014.11.030

Lopez-Bendito, G., Chan, C. H., Mallamaci, A., Parnavelas, J., & Molnar, Z. (2002). Role of Emx2 in the development of the reciprocal connectivity between cortex and thalamus. *J Comp Neurol, 451*(2), 153-169. doi:10.1002/cne.10345

Lopez-Schier, H., Starr, C. J., Kappler, J. A., Kollmar, R., & Hudspeth, A. J. (2004). Directional cell migration establishes the axes of planar polarity in the posterior lateral-line organ of the zebrafish. *Dev Cell, 7*(3), 401-412. doi:10.1016/j.devcel.2004.07.018

Lu, X., Borchers, A. G. M., Jolicoeur, C., Rayburn, H., Baker, J. C., & Tessier-Lavigne, M. (2004). PTK7/CCK-4 is a novel regulator of planar cell polarity in vertebrates. *Nature, 430*(6995), 93-98. doi:10.1038/nature02555

Lu, X., & Sipe, C. W. (2016). Developmental regulation of planar cell polarity and hair-bundle morphogenesis in auditory hair cells: lessons from human and mouse genetics. *Wiley Interdiscip Rev Dev Biol, 5*(1), 85-101. doi:10.1002/wdev.202

Lundberg, Y. W., Zhao, X., & Yamoah, E. N. (2006). Assembly of the otoconia complex to the macular sensory epithelium of the vestibule. *Brain Res, 1091*(1), 47-57. doi:10.1016/j.brainres.2006.02.083

Lysakowski, A., Gaboyard-Niay, S., Calin-Jageman, I., Chatlani, S., Price, S. D., & Eatock, R. A. (2011). Molecular microdomains in a sensory terminal, the vestibular calyx ending. *J Neurosci, 31*(27), 10101-10114. doi:10.1523/JNEUROSCI.0521-11.2011

Madisen, L., Zwingman, T. A., Sunkin, S. M., Oh, S. W., Zariwala, H. A., Gu, H., . . . Zeng, H. (2010). A robust and high-throughput Cre reporting and characterization system for the whole mouse brain. *Nat Neurosci, 13*(1), 133-140. doi:10.1038/nn.2467

Maklad, A., & Fritzsch, B. (2003). Partial segregation of posterior crista and saccular fibers to the nodulus and uvula of the cerebellum in mice, and its development. *Brain Res Dev Brain Res, 140*(2), 223-236. doi:10.1016/s0165-3806(02)00609-0

Maklad, A., Kamel, S., Wong, E., & Fritzsch, B. (2010). Development and organization of polarity-specific segregation of primary vestibular afferent fibers in mice. *Cell Tissue Res, 340*(2), 303-321. doi:10.1007/s00441-010-0944-1

Mallamaci, A., Iannone, R., Briata, P., Pintonello, L., Mercurio, S., Boncinelli, E., & Corte, G. (1998). EMX2 protein in the developing mouse brain and olfactory area. *Mech Dev, 77*(2), 165-172.

Mallamaci, A., Mercurio, S., Muzio, L., Cecchi, C., Pardini, C. L., Gruss, P., & Boncinelli, E. (2000). The lack of Emx2 causes impairment of Reelin signaling and defects of neuronal migration in the developing cerebral cortex. *J Neurosci, 20*(3), 1109-1118.

Mallamaci, A., Muzio, L., Chan, C. H., Parnavelas, J., & Boncinelli, E. (2000). Area identity shifts in the early cerebral cortex of Emx2-/- mutant mice. *Nat Neurosci, 3*(7), 679-686. doi:10.1038/76630

Marin, O., & Rubenstein, J. L. (2003). Cell migration in the forebrain. *Annu Rev Neurosci, 26*, 441-483. doi:10.1146/annurev.neuro.26.041002.131058

Matis, M., & Axelrod, J. D. (2013). Regulation of PCP by the Fat signaling pathway. *Genes Dev, 27*(20), 2207-2220. doi:10.1101/gad.228098.113

Maung, S. M., & Jenny, A. (2011). Planar cell polarity in Drosophila. *Organogenesis, 7*(3), 165-179. doi:10.4161/org.7.3.18143

May, L. A., Kramarenko, II, Brandon, C. S., Voelkel-Johnson, C., Roy, S., Truong, K., . . . Cunningham, L. L. (2013). Inner ear supporting cells protect hair cells by secreting HSP70. *J Clin Invest, 123*(8), 3577-3587. doi:10.1172/JCI68480

May-Simera, H., & Kelley, M. W. (2012). Planar cell polarity in the inner ear. *Curr Top Dev Biol, 101*, 111-140. doi:10.1016/B978-0-12-394592-1.00006-5

May-Simera, H. L., Kai, M., Hernandez, V., Osborn, D. P., Tada, M., & Beales, P. L. (2010). Bbs8, together with the planar cell polarity protein Vangl2, is required to establish left-right asymmetry in zebrafish. *Dev Biol, 345*(2), 215-225. doi:10.1016/j.ydbio.2010.07.013

May-Simera, H. L., Ross, A., Rix, S., Forge, A., Beales, P. L., & Jagger, D. J. (2009). Patterns of expression of Bardet-Biedl syndrome proteins in the mammalian cochlea suggest noncentrosomal functions. *J Comp Neurol, 514*(2), 174-188. doi:10.1002/cne.22001

Meng, X., & Wolfe, S. A. (2006). Identifying DNA sequences recognized by a transcription factor using a bactrial one-hybrid system. *Nat Protoc, 1*(1), 30-45.

Merkel, M., Sagner, A., Gruber, F. S., Etournay, R., Blasse, C., Myers, E., . . . Julicher, F. (2014). The balance of prickle/spiny-legs isoforms controls the amount of coupling between core and fat PCP systems. *Curr Biol, 24*(18), 2111-2123. doi:10.1016/j.cub.2014.08.005

Mirkovic, I., Pylawka, S., & Hudspeth, A. J. (2012). Rearrangements between differentiating hair cells coordinate planar polarity and the establishment of mirror symmetry in lateral-line neuromasts. *Biol Open, 1*(5), 498-505. doi:10.1242/bio.2012570

Mirzadeh, Z., Han, Y. G., Soriano-Navarro, M., Garcia-Verdugo, J. M., & Alvarez-Buylla, A. (2010). Cilia organize ependymal planar polarity. *J Neurosci, 30*(7), 2600-2610. doi:10.1523/JNEUROSCI.3744-09.2010

Miyamoto, N., Yoshida, M., Kuratani, S., Matsuo, I., & Aizawa, S. (1997). Defects of urogenital development in mice lacking Emx2. *Development, 124*(9), 1653-1664.

Montcouquiol, M., Rachel, R. A., Lanford, P. J., Copeland, N. G., Jenkins, N. A., & Kelley, M. W. (2003). Identification of Vangl2 and Scrb1 as planar polarity genes in mammals. *Nature, 423*(6936), 173-177. doi:10.1038/nature01618

Montcouquiol, M., Sans, N., Huss, D., Kach, J., Dickman, J. D., Forge, A., . . . Kelley, M. W. (2006). Asymmetric localization of Vangl2 and Fz3 indicate novel mechanisms for planar cell polarity in mammals. *J Neurosci, 26*(19), 5265-5275. doi:10.1523/JNEUROSCI.4680-05.2006

Morin, X., & Bellaiche, Y. (2011). Mitotic spindle orientation in asymmetric and symmetric cell divisions during animal development. *Dev Cell, 21*(1), 102-119. doi:10.1016/j.devcel.2011.06.012

Morita, T., Nitta, H., Kiyama, Y., Mori, H., & Mishina, M. (1995). Differential expression of two zebrafish emx homeoprotein mRNAs in the developing brain. *Neurosci Lett, 198*(2), 131-134.

Morsli, H., Choo, D., Ryan, A., Johnson, R., & Wu, D. K. (1998). Development of the mouse inner ear and origin of its sensory organs. *J Neurosci, 18*(9), 3327–3335.

Muzio, L., Soria, J. M., Pannese, M., Piccolo, S., & Mallamaci, A. (2005). A mutually stimulating loop involving emx2 and canonical wnt signalling specifically

promotes expansion of occipital cortex and hippocampus. *Cereb Cortex, 15*(12), 2021-2028. doi:10.1093/cercor/bhi077

Muzumdar, M. D., Tasic, B., Miyamichi, K., Li, L., & Luo, L. (2007). A global double-fluorescent Cre reporter mouse. *Genesis, 45*(9), 593-605. doi:10.1002/dvg.20335

Nagiel, A., Andor-Ardo, D., & Hudspeth, A. J. (2008). Specificity of afferent synapses onto plane-polarized hair cells in the posterior lateral line of the zebrafish. *J Neurosci, 28*(34), 8442-8453. doi:10.1523/JNEUROSCI.2425-08.2008

Nagiel, A., Patel, S. H., Andor-Ardo, D., & Hudspeth, A. J. (2009). Activity-independent specification of synaptic targets in the posterior lateral line of the larval zebrafish. *Proc Natl Acad Sci U S A, 106*(51), 21948-21953. doi:10.1073/pnas.0912082106

Nedelec, S., Foucher, I., Brunet, I., Bouillot, C., Prochiantz, A., & Trembleau, A. (2004). Emx2 homeodomain transcription factor interacts with eukaryotic translation initiation factor 4E (eIF4E) in the axons of olfactory sensory neurons. *Proc Natl Acad Sci U S A, 101*(29), 10815-10820. doi:10.1073/pnas.0403824101

Nichols, A. S., Floyd, D. H., Bruinsma, S. P., Narzinski, K., & Baranski, T. J. (2013). Frizzled receptors signal through G proteins. *Cell Signal, 25*(6), 1468-1475. doi:10.1016/j.cellsig.2013.03.009

Noonan, F. C., Mutch, D. G., Ann Mallon, M., & Goodfellow, P. J. (2001). Characterization of the homeodomain gene EMX2: sequence conservation, expression analysis, and a search for mutations in endometrial cancers. *Genomics, 76*(1-3), 37-44. doi:10.1006/geno.2001.6590

Norris, D. P., & Grimes, D. T. (2012). Mouse models of ciliopathies: the state of the art. *Dis Model Mech, 5*(3), 299-312. doi:10.1242/dmm.009340

Obholzer, N., Wolfson, S., Trapani, J. G., Mo, W., Nechiporuk, A., Busch-Nentwich, E., . . . Nicolson, T. (2008). Vesicular glutamate transporter 3 is required for synaptic transmission in zebrafish hair cells. *J Neurosci, 28*(9), 2110-2118. doi:10.1523/JNEUROSCI.5230-07.2008

Olofsson, J., Sharp, K. A., Matis, M., Cho, B., & Axelrod, J. D. (2014). Prickle/spiny-legs isoforms control the polarity of the apical microtubule network in planar cell polarity. *Development, 141*(14), 2866-2874. doi:10.1242/dev.105932

Pannese, M., Lupo, G., Kablar, B., Boncinelli, E., Barsacchi, G., & Vignali, R. (1998). The Xenopus Emx genes identify presumptive dorsal telencephalon and are induced by head organizer signals. *Mechanisms of Development, 73*(1), 73-83. doi:Doi 10.1016/S0925-4773(98)00034-3

Park, T. J., Haigo, S. L., & Wallingford, J. B. (2006). Ciliogenesis defects in embryos lacking inturned or fuzzy function are associated with failure of planar cell polarity and Hedgehog signaling. *Nat Genet, 38*(3), 303-311. doi:10.1038/ng1753

Park, T. J., Mitchell, B. J., Abitua, P. B., Kintner, C., & Wallingford, J. B. (2008). Dishevelled controls apical docking and planar polarization of basal bodies in ciliated epithelial cells. *Nat Genet, 40*(7), 871-879. doi:10.1038/ng.104

Pellegrini, M., Mansouri, A., Simeone, A., Boncinelli, E., & Gruss, P. (1996). Dentate gyrus formation requires Emx2. *Development, 122*(12), 3893-3898.

Piard, J., Mignot, B., Arbez-Gindre, F., Aubert, D., Morel, Y., Roze, V., . . . Van Maldergem, L. (2014). Severe sex differentiation disorder in a boy with a 3.8 Mb 10q25.3-q26.12 microdeletion encompassing EMX2. *Am J Med Genet A, 164A*(10), 2618-2622. doi:10.1002/ajmg.a.36662

Piotrowski, T., & Baker, C. V. (2014). The development of lateral line placodes: taking a broader view. *Dev Biol, 389*(1), 68-81. doi:10.1016/j.ydbio.2014.02.016

Postiglione, M. P., Juschke, C., Xie, Y., Haas, G. A., Charalambous, C., & Knoblich, J. A. (2011). Mouse inscuteable induces apical-basal spindle orientation to facilitate intermediate progenitor generation in the developing neocortex. *Neuron, 72*(2), 269-284. doi:10.1016/j.neuron.2011.09.022

Pujol-Marti, J., Faucherre, A., Aziz-Bose, R., Asgharsharghi, A., Colombelli, J., Trapani, J. G., & Lopez-Schier, H. (2014). Converging axons collectively initiate and maintain synaptic selectivity in a constantly remodeling sensory organ. *Curr Biol, 24*(24), 2968-2974. doi:10.1016/j.cub.2014.11.012

Pujol-Marti, J., & Lopez-Schier, H. (2013). Developmental and architectural principles of the lateral-line neural map. *Front Neural Circuits, 7*, 47. doi:10.3389/fncir.2013.00047

Qian, D., Jones, C., Rzadzinska, A., Mark, S., Zhang, X., Steel, K. P., . . . Chen, P. (2007). Wnt5a functions in planar cell polarity regulation in mice. *Dev Biol, 306*(1), 121-133. doi:10.1016/j.ydbio.2007.03.011

Ramahi, J. S., & Solecki, D. J. (2014). The PAR polarity complex and cerebellar granule neuron migration. *Adv Exp Med Biol, 800*, 113-131. doi:10.1007/978-94-007-7687-6_7

Rau, A., Legan, P. K., & Richardson, G. P. (1999). Tectorin mRNA expression is spatially and temporally restricted during mouse inner ear development. *J Comp Neurol, 405*(2), 271-280.

Rhodes, C. R., Parkinson, N., Tsai, H., Brooker, D., Mansell, S., Spurr, N., . . . Brown, S. D. (2003). The homeobox gene Emx2 underlies middle ear and inner ear defects in the deaf mouse mutant pardon. *J Neurocytol, 32*(9), 1143-1154. doi:10.1023/B:NEUR.0000021908.98337.91

Rivera, C., Simonson, S. J., Yamben, I. F., Shatadal, S., Nguyen, M. M., Beurg, M., . . . Griep, A. E. (2013). Requirement for Dlgh-1 in planar cell polarity and skeletogenesis during vertebrate development. *PLoS One, 8*(1), e54410. doi:10.1371/journal.pone.0054410

Romero-Carvajal, A., Navajas Acedo, J., Jiang, L., Kozlovskaja-Gumbriene, A., Alexander, R., Li, H., & Piotrowski, T. (2015). Regeneration of Sensory Hair Cells Requires Localized Interactions between the Notch and Wnt Pathways. *Dev Cell, 34*(3), 267-282. doi:10.1016/j.devcel.2015.05.025

Rouse, G. W., & Pickles, J. O. (1991). Paired development of hair cells in neuromasts of the teleost lateral line. *Proc Biol Sci, 246*(1316), 123-128. doi:10.1098/rspb.1991.0133

Saburi, S., Hester, I., Fischer, E., Pontoglio, M., Eremina, V., Gessler, M., . . . McNeill, H. (2008). Loss of Fat4 disrupts PCP signaling and oriented cell division and leads to cystic kidney disease. *Nat Genet, 40*(8), 1010-1015. doi:10.1038/ng.179

Saburi, S., Hester, I., Goodrich, L., & McNeill, H. (2012). Functional interactions between Fat family cadherins in tissue morphogenesis and planar polarity. *Development, 139*(10), 1806-1820. doi:10.1242/dev.077461

Savory, J. G., Mansfield, M., Rijli, F. M., & Lohnes, D. (2011). Cdx mediates neural tube closure through transcriptional regulation of the planar cell polarity gene Ptk7. *Development, 138*(7), 1361-1370. doi:10.1242/dev.056622

Schindler, A. J., & Sherwood, D. R. (2013). Morphogenesis of the caenorhabditis elegans vulva. *Wiley Interdiscip Rev Dev Biol, 2*(1), 75-95. doi:10.1002/wdev.87

Segalen, M., & Bellaiche, Y. (2009). Cell division orientation and planar cell polarity pathways. *Semin Cell Dev Biol, 20*(8), 972-977. doi:10.1016/j.semcdb.2009.03.018

Segalen, M., Johnston, C. A., Martin, C. A., Dumortier, J. G., Prehoda, K. E., David, N. B., . . . Bellaiche, Y. (2010). The Fz-Dsh planar cell polarity pathway induces oriented cell division via Mud/NuMA in Drosophila and zebrafish. *Dev Cell, 19*(5), 740-752. doi:10.1016/j.devcel.2010.10.004

Shnitsar, I., & Borchers, A. (2008). PTK7 recruits dsh to regulate neural crest migration. *Development, 135*(24), 4015-4024. doi:10.1242/dev.023556

Shotwell, S. L., Jacobs, R., & Hudspeth, A. J. (1981). Directional sensitivity of individual vertebrate hair cells to controlled deflection of their hair bundles. *Ann N Y Acad Sci, 374*, 1-10.

Siller, K. H., & Doe, C. Q. (2009). Spindle orientation during asymmetric cell division. *Nat Cell Biol, 11*(4), 365-374. doi:10.1038/ncb0409-365

Silverman, M. A., & Leroux, M. R. (2009). Intraflagellar transport and the generation of dynamic, structurally and functionally diverse cilia. *Trends Cell Biol, 19*(7), 306-316. doi:10.1016/j.tcb.2009.04.002

Simeone, A., Gulisano, M., Acampora, D., Stornaiuolo, A., Rambaldi, M., & Boncinelli, E. (1992). Two vertebrate homeobox genes related to the Drosophila empty spiracles gene are expressed in the embryonic cerebral cortex. *EMBO J, 11*(7), 2541-2550.

Simmons, D. D., Tong, B., Schrader, A. D., & Hornak, A. J. (2010). Oncomodulin identifies different hair cell types in the mammalian inner ear. *J Comp Neurol, 518*(18), 3785-3802. doi:10.1002/cne.22424

Simoes Sde, M., Blankenship, J. T., Weitz, O., Farrell, D. L., Tamada, M., Fernandez-Gonzalez, R., & Zallen, J. A. (2010). Rho-kinase directs Bazooka/Par-3 planar

polarity during Drosophila axis elongation. *Dev Cell, 19*(3), 377-388. doi:10.1016/j.devcel.2010.08.011

Sipe, C. W., Liu, L., Lee, J., Grimsley-Myers, C., & Lu, X. (2013). Lis1 mediates planar polarity of auditory hair cells through regulation of microtubule organization. *Development, 140*(8), 1785-1795. doi:10.1242/dev.089763

Sipe, C. W., & Lu, X. (2011). Kif3a regulates planar polarization of auditory hair cells through both ciliary and non-ciliary mechanisms. *Development, 138*(16), 3441-3449. doi:10.1242/dev.065961

Slusarski, D. C., Corces, V. G., & Moon, R. T. (1997). Interaction of Wnt and a Frizzled homologue triggers G-protein-linked phosphatidylinositol signalling. *Nature, 390*(6658), 410-413. doi:10.1038/37138

Solecki, D. J., Govek, E. E., & Hatten, M. E. (2006). mPar6 alpha controls neuronal migration. *J Neurosci, 26*(42), 10624-10625. doi:10.1523/JNEUROSCI.4060-06.2006

Song, H., Hu, J., Chen, W., Elliott, G., Andre, P., Gao, B., & Yang, Y. (2010). Planar cell polarity breaks bilateral symmetry by controlling ciliary positioning. *Nature, 466*(7304), 378-382. doi:10.1038/nature09129

Song, M. R., Shirasaki, R., Cai, C. L., Ruiz, E. C., Evans, S. M., Lee, S. K., & Pfaff, S. L. (2006). T-Box transcription factor Tbx20 regulates a genetic program for cranial motor neuron cell body migration. *Development, 133*(24), 4945-4955. doi:10.1242/dev.02694

Strigini, M., & Cohen, S. M. (1999). Formation of morphogen gradients in the Drosophila wing. *Semin Cell Dev Biol, 10*(3), 335-344. doi:10.1006/scdb.1999.0293

Strutt, D. (2003). Frizzled signalling and cell polarisation in Drosophila and vertebrates. *Development, 130*(19), 4501-4513. doi:10.1242/dev.00695

Strutt, D. I. (2001). Asymmetric localization of frizzled and the establishment of cell polarity in the Drosophila wing. *Mol Cell, 7*(2), 367-375.

Strutt, D. I., Weber, U., & Mlodzik, M. (1997). The role of RhoA in tissue polarity and Frizzled signalling. *Nature, 87*(6630), 292-295. doi:10.1038/387292a0

Suda, Y., Hossain, Z. M., Kobayashi, C., Hatano, O., Yoshida, M., Matsuo, I., & Aizawa, S. (2001). Emx2 directs the development of diencephalon in cooperation with Otx2. *Development, 128*(13), 2433-2450.

Suzuki, A., & Ohno, S. (2006). The PAR-aPKC system: lessons in polarity. *J Cell Sci, 119*(Pt 6), 979-987. doi:10.1242/jcs.02898

Tarchini, B., Jolicoeur, C., & Cayouette, M. (2013). A molecular blueprint at the apical surface establishes planar asymmetry in cochlear hair cells. *Dev Cell, 27*(1), 88-102. doi:10.1016/j.devcel.2013.09.011

Tasic, B., Hippenmeyer, S., Wang, C., Gamboa, M., Zong, H., Chen-Tsai, Y., & Luo, L. (2011). Site-specific integrase-mediated transgenesis in mice via pronuclear

injection. *Proc Natl Acad Sci U S A, 108*(19), 7902-7907. doi:10.1073/pnas.1019507108

Taylor, H. S. (2015). The role of EMX2 in uterine development. *Fertil Steril, 103*(3), 633-634. doi:10.1016/j.fertnstert.2015.01.009

Theil, T., Aydin, S., Koch, S., Grotewold, L., & Ruther, U. (2002). Wnt and Bmp signalling cooperatively regulate graded Emx2 expression in the dorsal telencephalon. *Development, 129*(13), 3045-3054.

Tilney, L. G., Tilney, M. S., & DeRosier, D. J. (1992). Actin filaments, stereocilia, and hair cells: how cells count and measure. *Annu Rev Cell Biol, 8*, 257-274. doi:10.1146/annurev.cb.08.110192.001353

Tissir, F., & Goffinet, A. M. (2010). Planar cell polarity signaling in neural development. *Curr Opin Neurobiol, 20*(5), 572-577. doi:10.1016/j.conb.2010.05.006

Tissir, F., & Goffinet, A. M. (2013). Shaping the nervous system: role of the core planar cell polarity genes. *Nat Rev Neurosci, 14*(8), 525-535. doi:10.1038/nrn3525

Tissir, F., Qu, Y., Montcouquiol, M., Zhou, L., Komatsu, K., Shi, D., . . . Goffinet, A. M. (2010). Lack of cadherins Celsr2 and Celsr3 impairs ependymal ciliogenesis, leading to fatal hydrocephalus. *Nat Neurosci, 13*(6), 700-707. doi:10.1038/nn.2555

Tree, D. R. P., Shulman, J. M., Raphae¨l Rousset, Scott, M. P., Gubb, D., & Axelrod, J. D. (2002). Prickle Mediates Feedback Amplification to Generate Asymmetric

Planar Cell Polarity Signaling. *Cell, 109*, 371-381.

van de Willige, D., Hoogenraad, C. C., & Akhmanova, A. (2016). Microtubule plus-end tracking proteins in neuronal development. *Cell Mol Life Sci, 73*(10), 2053-2077. doi:10.1007/s00018-016-2168-3

Varshney, G. K., Pei, W., LaFave, M. C., Idol, J., Xu, L., Gallardo, V., . . . Burgess, S. M. (2015). High-throughput gene targeting and phenotyping in zebrafish using CRISPR/Cas9. *Genome Res, 25*(7), 1030-1042. doi:10.1101/gr.186379.114

Vichas, A., & Zallen, J. A. (2011). Translating cell polarity into tissue elongation. *Semin Cell Dev Biol, 22*(8), 858-864. doi:10.1016/j.semcdb.2011.09.013

Vladar, E. K., Bayly, R. D., Sangoram, A. M., Scott, M. P., & Axelrod, J. D. (2012). Microtubules enable the planar cell polarity of airway cilia. *Curr Biol, 22*(23), 2203-2212. doi:10.1016/j.cub.2012.09.046

Walldorf, U., & Gehring, W. J. (1992). Empty spiracles,a gap gene containing a homeobox involved in Drosophila head development. *EMBO J, 11*(6), 2247-2259.

Wallingford, J. B. (2010). Planar cell polarity signaling, cilia and polarized ciliary beating. *Curr Opin Cell Biol, 22*(5), 597-604. doi:10.1016/j.ceb.2010.07.011

Wallingford, J. B. (2012). Planar cell polarity and the developmental control of cell behavior in vertebrate embryos. *Annu Rev Cell Dev Biol, 28*, 627-653. doi:10.1146/annurev-cellbio-092910-154208

Wallingford, J. B., & Mitchell, B. (2011). Strange as it may seem: the many links between Wnt signaling, planar cell polarity, and cilia. *Genes Dev, 25*(3), 201-213. doi:10.1101/gad.2008011

Wang, J., Hamblet, N. S., Mark, S., Dickinson, M. E., Brinkman, B. C., Segil, N., . . . Wynshaw-Boris, A. (2006). Dishevelled genes mediate a conserved mammalian PCP pathway to regulate convergent extension during neurulation. *Development, 133*(9), 1767-1778. doi:10.1242/dev.02347

Wang, J., Mark, S., Zhang, X., Qian, D., Yoo, S. J., Radde-Gallwitz, K., . . . Chen, P. (2005). Regulation of polarized extension and planar cell polarity in the cochlea by the vertebrate PCP pathway. *Nat Genet, 37*(9), 980-985. doi:10.1038/ng1622

Wang, Y., Guo, N., & Nathans, J. (2006). The role of Frizzled3 and Frizzled6 in neural tube closure and in the planar polarity of inner-ear sensory hair cells. *J Neurosci, 26*(8), 2147-2156. doi:10.1523/JNEUROSCI.4698-05.2005

Wang, Y., & Nathans, J. (2007). Tissue/planar cell polarity in vertebrates: new insights and new questions. *Development, 134*(4), 647-658. doi:10.1242/dev.02772

Wehner, P., Shnitsar, I., Urlaub, H., & Borchers, A. (2011). RACK1 is a novel interaction partner of PTK7 that is required for neural tube closure. *Development, 138*(7), 1321-1327. doi:10.1242/dev.056291

Wong, L. L., & Adler, P. N. (1993). Tissue polarity genes of Drosophila regulate the subcellular location for prehair initiation in pupal wing cells. *J Cell Biol, 123*(1), 209-221.

Woodard, G. E., Huang, N. N., Cho, H., Miki, T., Tall, G. G., & Kehrl, J. H. (2010). Ric-8A and Gi alpha recruit LGN, NuMA, and dynein to the cell cortex to help orient the mitotic spindle. *Mol Cell Biol, 30*(14), 3519-3530. doi:10.1128/MCB.00394-10

Woods, D. F., Hough, C., Peel, D., Callaini, G., & Bryant, P. J. (1996). Dlg protein is required for junction structure, cell polarity, and proliferation control in Drosophila epithelia. *J Cell Biol, 134*(6), 1469–1482.

Wu, D. K., & Kelley, M. W. (2012). Molecular mechanisms of inner ear development. *Cold Spring Harb Perspect Biol, 4*(8), a008409. doi:10.1101/cshperspect.a008409

Wu, J., Roman, A. C., Carvajal-Gonzalez, J. M., & Mlodzik, M. (2013). Wg and Wnt4 provide long-range directional input to planar cell polarity orientation in Drosophila. *Nat Cell Biol, 15*(9), 1045-1055. doi:10.1038/ncb2806

Yang, C. H., Axelrod, J. D., & Simon, M. A. (2002). Regulation of Frizzled by fat-like cadherins during planar polarity signaling in the Drosophila compound eye. *Cell, 108*(5), 675-688.

Yang, H., Gan, J., Xie, X., Deng, M., Feng, L., Chen, X., . . . Gan, L. (2010). Gfi1-Cre knock-in mouse line: A tool for inner ear hair cell-specific gene deletion. *Genesis, 48*(6), 400-406. doi:10.1002/dvg.20632

Yang, Y., & Mlodzik, M. (2015). Wnt-Frizzled/planar cell polarity signaling: cellular orientation by facing the wind (Wnt). *Annu Rev Cell Dev Biol, 31*, 623-646. doi:10.1146/annurev-cellbio-100814-125315

Yariz, K. O., Walsh, T., Akay, H., Duman, D., Akkaynak, A. C., King, M. C., & Tekin, M. (2012). A truncating mutation in GPSM2 is associated with recessive non-syndromic hearing loss. *Clin Genet, 81*(3), 289-293. doi:10.1111/j.1399-0004.2011.01654.x

Yin, H., Copley, C. O., Goodrich, L. V., & Deans, M. R. (2012). Comparison of phenotypes between different vangl2 mutants demonstrates dominant effects of the Looptail mutation during hair cell development. *PLoS One, 7*(2), e31988. doi:10.1371/journal.pone.0031988

Yoshida, M., Suda, Y., Matsuo, I., Miyamoto, N., Takeda, N., Kuratani, S., & Aizawa, S. (1997). Emx1 and Emx2 functions in development of dorsal telencephalon. *Development, 124*(101-111).

Zallen, J. A. (2007). Planar polarity and tissue morphogenesis. *Cell, 129*(6), 1051-1063. doi:10.1016/j.cell.2007.05.050

Zallen, J. A., & Wieschaus, E. (2004). Patterned gene expression directs bipolar planar polarity in Drosophila. *Dev Cell, 6*(3), 343-355.

Zecca, M., & Struhl, G. (2010). A feed-forward circuit linking wingless, fat-dachsous signaling, and the warts-hippo pathway to Drosophila wing growth. *PLoS Biol, 8*(6), e1000386. doi:10.1371/journal.pbio.1000386

Zigman, M., Cayouette, M., Charalambous, C., Schleiffer, A., Hoeller, O., Dunican, D., . . . Knoblich, J. A. (2005). Mammalian inscuteable regulates spindle orientation and cell fate in the developing retina. *Neuron, 48*(4), 539-545. doi:10.1016/j.neuron.2005.09.030